Ion channel control of phasic insulin secretion.

Jing, Xingjun

2007

ION CHANNEL CONTROL OF PHASIC INSULIN SECRETION

Xingjun Jing, M.D.

LUND
UNIVERSITY

ACADEMIC DISSERTATION

With approval of the Medical Faculty of Lund University to be defended on the 21st of December 2007
at 9:15 in the Clinical Research Center (CRC) Lecture Hall
Malmö University Hospital
Malmö
Sweden

Faculty opponent:
Prof. Åke Sjöholm
Department of Clinical Science and Education, Södersjukhuset,
Karolinska Institute,
Sweden

Department of Clinical Sciences, Malmö
Lund University
Sweden

ISSN 1652-8220
ISBN 978-91-85897-51-3
Lund University, Faculty of Medicine Doctoral Dissertation Series 2007:173

Printed by Media-Tryck, Lund University, Lund, Sweden

Organisation
LUND UNIVERSITY
Clinical Research Center
UMAS, Ingång 72, Hus 91, Plan 11

Document name
DOCTORAL DISSERTATION

Date of issue
2007-12-21

Author(s)
Xingjun Jing

Sponsoring organization

Title and subtitle
Ion channel control of phasic insulin secretion

Abstract:

Glucose-stimulated insulin secretion exhibits a biphasic pattern. The mechanism underling biphasic insulin secretion is not fully understood, but consensus exists that an elevation in $[Ca^{2+}]_i$ is required for both first- and second-phase insulin secretion. The molecular identity of the pancreatic β-cell L-type Ca^{2+} channel has not been established and it has variably been reported to be $Ca_V1.2$ (α_{1C}) or $Ca_V1.3$ (α_{1D}). Though the cellular background to the two phases of release remains unknown, it has been suggested to reflect the sequential release of distinct pools of granules, which vary with regard to release competence. This thesis investigated the role of different ion channels in insulin secretion.

β-cell-selective ablation of the $Ca_V1.2$ gene($\beta Ca_V1.2^{-/-}$ mouse) decreased the whole-cell Ca^{2+} current by only ~45%, but almost abolished first-phase insulin secretion and resulted in systemic glucose intolerance. High-resolution capacitance measurements of exocytosis in single β-cells revealed that the loss of first-phase insulin secretion in the $\beta Ca_V1.2^{-/-}$ mouse was associated with the disappearance of a rapid component of exocytosis reflecting fusion of secretory granules physically attached to the $Ca_V1.2$ channel.

A 20% reduction in glucose-evoked insulin secretion was observed in $Ca_V2.3$-knockout ($Ca_V2.3^{-/-}$) islets, close to the 17% inhibition by the R-type blocker SNX482. Genetic or pharmacological $Ca_V2.3$ ablation strongly suppressed second-phase secretion *in vitro*, as well as *in vivo*, whereas first-phase secretion was unaffected. Suppression of the second phase coincided with an 18% reduction in oscillatory Ca^{2+} signaling and a 25% reduction in granule recruitment after completion of the initial exocytotic burst in single $Ca_V2.3^{-/-}$ β-cells.

Intracellular ClC-3 chloride channels have been implicated in the process of making insulin granules release-competent, a process referred to as *priming*. Analysis of insulin secretion *in vivo* and *in vitro* as well as capacitance measurements revealed that the secretory response of ClC-3 deficient β-cells was reduced, but not abolished. The presence of ClC-3 in insulin granules was detected in a high-purification fraction of LDCVs obtained by phogrin-GFP labelling.

In conclusion: (1) $Ca_V1.2$ Ca^{2+} channels are required for first-phase insulin release and maintenance of systemic glucose tolerance. (2) $Ca_V2.3$ Ca^{2+} channels play an important role in second-phase insulin release. (3) ClC-3 chloride channels facilitate insulin secretion by enhancing properly acidification of insulin granules needed for granule priming.

Key words
Diabetes, phasic insulin secretion, pancreatic β-cells, exocytosis, Ca_V channel, ClC chloride channel

Classification system and/or index terms (if any)

Supplementary bibliographical information

Language
English

ISSN and key title:
1652-8220

ISBN
978-91-85897-51-3

Recipient's notes

Number of pages
108

Price

Security classification

Table of contents

Original papers

This thesis is the summary of the following studies, referred to in the text by Roman numerals:

Ⅰ. Schulla V., Renström E., Feil R., Feil S., Franklin I., Gjinovci A., **Jing XJ**., Laux D., Lundquist I., Magnuson MA., Obermuller S., Olofsson CS., Salehi A., Wendt A., Klugbauer N., Wollheim CB., Rorsman P. and Hofmann F. (2003)
Impaired insulin secretion and glucose tolerance in β-cell-selective $Ca_V1.2$ Ca^{2+} channel null mice. The EMBO journal Vol. 22 No. 15 pp.3844-3854, 2003

Ⅱ. **Jing XJ.**, Li DQ., Olofsson C., Salehi A., Surve V., Caballero J., Ivarsson R., Lundquist I, Pereverzev A., Schneider T., Rorsman P. and Renström E. (2005)
$Ca_V2.3$ calcium channels control second-phase insulin release. J Clin Invest. 2005 Jan;115(1):146-54

Ⅲ. Renström E., Li DQ., Maritzen T., Salehi A., Breiderhoff T., Eliasson L., **Jing XJ.**, Lundquist I., Olofsson CS., Zdebik AA., Jentsch TJ, Rorsman P. (2007)
Supression of sulfonylurea- and glucose-induced insulin secretion in vitro and in vivo in mice lacking the chloride transport protein ClC-3. *Manuscript*

Abbreviations

ADP	adenosine diphosphate
ATP	adenosine triphosphate
$[Ca^{2+}]_i$	intracellular calcium concentration
cAMP	cyclic adenosine monophosphate
CFTR	cystic fibrosis transmembrane conductance regulator
CPT-1	carnitine palmitoyl transferase 1
DHP	dihydropyridine
ER	endoplasmic reticulum
GABA	γ-aminobutyric acid
GAD	glutamic acid decarboxylase
GLUT	glucose transporter
GSK3	glycogen synthase kinase 3
IGT	impaired glucose tolerance
IRP	the immediately releasable pool
IRS	insulin receptor substrate
K_{ATP} channel	ATP-sensitive potassium channel
LDCVs	large dense core vesicles
RP	the reserve pool
RRP	the readily releasable pool
SLMVs	synaptic-like micro vesicles
SNARE	soluble N-ethylmaleimide-sensitive fusion protein attachment receptor
SNAP-25	synaptosomal-associated protein of 25 kDa
SUR1	sulfonylurea receptor protein 1
TCA cycle	tricarboxylic acid cycle
TGN	the *trans*-Golgi network
VAMP	vesicle-associated membrane protein
V-ATPase	the vacuolar-type ATPase
VGCCs	voltage-gated calcium channels

Introduction

Diabetes

Diabetes mellitus is a metabolic disorder of multiple aetiology. It is characterized by chronic hyperglycaemia with disturbances of carbohydrate, fat and protein metabolism resulting from defects in insulin secretion, or insulin action, or both. Diabetes mellitus may present with characteristic symptoms such as thirst, polyuria, blurring of vision, and weight loss. The effects of diabetes mellitus include long–term damage, dysfunction and failure of various organs, for example, renal failure, vascular disease (including coronary artery disease), vision damage. Currently, diabetes mellitus is considered to be manifest when the plasma glucose concentration exceeds 7.0 mM during fasting and/or 11.1 mM 2 hours after a 75 g oral glucose challenge, according to the criteria set by the World Health Organization (WHO 2006). Typically, patients with diabetes mellitus can be divided into two main forms: Type 1 and type 2.

Type 1 diabetes mellitus is characterized by loss of the insulin-producing β-cells of the islets of Langerhans of the pancreas leading to an absolute deficiency of insulin. The patients with type 1 diabetes usually present disease early in life. Sensitivity to insulin is usually normal, especially in the early stages. The most common cause of β-cell loss leading to type 1 diabetes is autoimmune destruction, accompanied by autoantibodies directed against insulin and islet cell proteins (Atkinson and Maclaren 1994; Rother 2007). The autoantibodies include those to insulin (Palmer, Asplin et al. 1983), glutamic acid decarboxylase (GAD) (Baekkeskov, Aanstoot et al. 1990) and the tyrosine phosphatase IA-2 (Atkinson and Maclaren 1993; Bonifacio, Lampasona et al. 1995). Type 1 diabetes is distinguished by virtually no levels of circulating insulin and the patients rely on life-long daily insulin medication for survival.

Type 2 diabetes mellitus is due to a combination of defective insulin secretion and insulin resistance. Insulin resistance is defined as reduced responsiveness in insulin target cells (such as muscle cells, adipocytes, liver cells) so that higher insulin concentrations are required to achieve euglycemia with a given glucose load (Trout, Homko et al. 2007). There are numerous theories as to the exact cause and mechanism for this resistance, but central obesity is known to predispose individuals for insulin resistance (Eberhart, C. et al. 2004), possibly due to its increased secretion of adipokines (e.g, TNF-α) that decrease insulin sensitivity by inducing lipolysis and down-regulates IRS-1 and the insulin-sensitive glucose transporter (GLUT)-4 (Fasshauer and Paschke 2003; Zhao and Chen 2007). Other factors include aging and family history. The patients with type 2 diabetes are often older and over-weight and can usually control their hyperglycemia with diet, exercise and oral anti-diabetic drugs. In late-stage cases, insulin replacement therapy is normally required.

Although the precise mechanisms of type 2 diabetes are uncertain, it has been suggested that the final common pathway responsible for the development of type 2 diabetes is the failure of the pancreatic beta-cell to compensate for insulin resistance (Cavaghan, Ehrmann et al. 2000). Type 2 diabetes may go unnoticed for years in a patient before diagnosis, as visible symptoms are typically mild or non-existent. However, severe long-term complications can result from unnoticed type 2 diabetes as mentioned above.

Regulation of blood glucose

Glucose constitutes the major energy supplier for most tissues. Normally, the blood-glucose level (≈5 mM in healthy individuals) is balanced within a very narrow range by the uptake of glucose into the peripheral tissue and the entry of the glucose into the bloodstream. Insulin and glucagon are the major hormones regulating the blood glucose concentration (Figure 1).

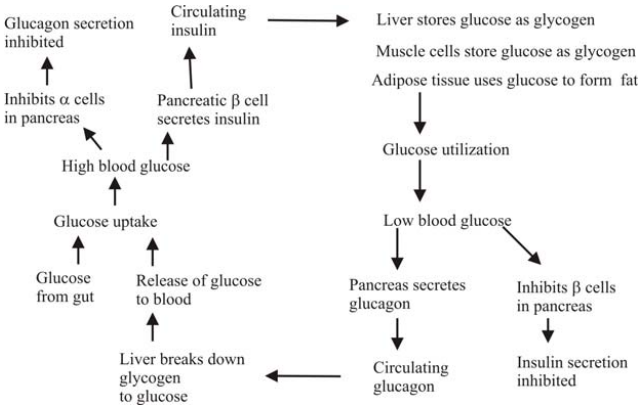

Figure 1: *Regulation of blood glucose concentration by insulin and glucagon.*

The body's sole glucose-lowing hormone insulin is produced and secreted by pancreatic β-cells. When levels of blood sugar rise, whether as a result of glycogen conversion or from digestion of a meal, insulin secretion is initiated. Insulin causes the liver to convert more glucose into glycogen by glycogenesis, and force body cells (primarily muscle and fat tissue cells) to take up glucose from the blood, thus decreasing blood sugar levels. A defect in insulin secretion, insulin action, or both, results initially in impaired glucose tolerance (IGT) and causes temporary hyperglycemia. Eventually, most cases of IGT will progress toward overt diabetes mellitus, a condition where the blood glucose level exceeds the reabsorption threshold of the kidneys and glucose is excreted in the urine.

Binding of insulin to its receptor leads to the activation of the insulin receptor. Activation of the insulin receptor evokes the phosphorylation of insulin receptor substrate (IRS). IRS in turn interacts with signaling molecules, which results in the activation of a variety of signaling pathways. Insulin promotes glucose storage as glycogen by the inactivation of glycogen synthase kinase 3 (GSK3) which break-down the glycogen synthase. In addition to promoting glucose storage, insulin inhibits the production and release of glucose by the liver by blocking gluconeogenesis and glycogenolysis (Saltiel and Kahn 2001). Insulin directly controls the activities of a set of metabolic enzymes by phosphorylation and dephosphorylation events and also regulates the expression of genes encoding hepatic enzymes involved in gluconeogenesis (Schmoll, Walker et al. 2000; Barthel, Schmoll et al. 2001). A key action of insulin is to stimulate glucose uptake into cells by inducing translocation of the glucose transporter, GLUT4, from intracellular storage to the plasma membrane. PI 3-kinase and AKT are known to play a role in GLUT4 translocation (Lizcano and Alessi 2002).

Glucagon, which is produced and secreted by pancreatic α-cell, opposes insulin by increasing glucose appearance in the circulation (Kruger., Martin et al. 2006). If the blood glucose level

falls to lower levels (as in very heavy exercise or lack of food for extended periods), the α-cells of the pancreas release glucagon. The hormone increases the blood glucose by acting on liver cells, which convert glycogen storage into glucose by glycogenolysis. The glucose is released into the bloodstream, thereby increasing blood sugar levels.

Except for insulin and glucagon, there are also several other factors influencing blood sugar levels. The 'stress' hormones such as adrenaline affect blood sugar by inhibiting insulin secretion and stimulating glucagon secretion. The effect of cortisol on blood sugar level appears to include both impaired insulin-dependent glucose uptake in the periphery and enhanced gluconeogenesis in the liver (Andrews and Walker 1999). Elevated cortisol levels can lead to central obesity which is known to predispose individuals for insulin resistance as mentioned above.

Insulin secretion

Insulin is a small molecule, with a molecular weight of 5808 Daltons. It is composed of two chains held together by disulfide bonds. Insulin is synthesized in significant quantities only in β-cells in the pancreas. In the assembly of insulin, the messenger RNA transcript is translated into the inactive precursor preproinsulin. Preproinsulin contains an amino-terminal signal sequence that is required for the precursor hormone to pass through the membrane into the endoplasmic reticulum (ER). Upon entering the ER, the preproinsulin signal sequence, now useless, is proteolytically removed to form proinsulin. Once the post-translational formation of three vital disulfide bonds occurs, specific peptidases cleave proinsulin to form insulin and C-peptide. This causes condensation of insulin in the immature granules.The final product of the biosynthesis is mature insulin packaged and stored in secretory granules, which accumulate in the cytoplasm until release is triggered.

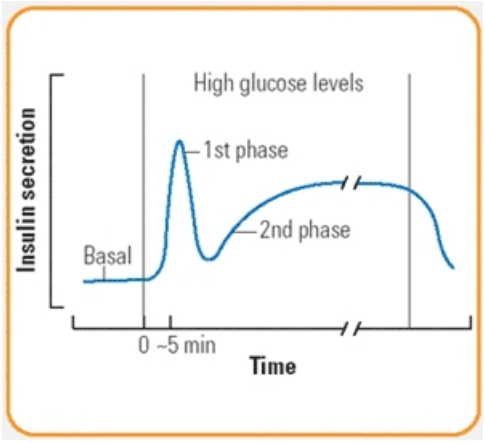

Figure 2: *Biphasic insulin secretion. The rapid first phase is followed by a sustained second phase. (Reproduced with permission from Williams G & Pickup JC, eds. Handbook of Diabetes, 2nd ed: Blackwell Science, Oxford, 1999, 30)*

Insulin secretion in response to a glucose challenge exhibits a typical biphasic manner (Figure 2). In *in vitro* experiments, the exposure of β-cells to glucose results in an immediate increase in insulin secretion (first-phase insulin secretion), followed by a decrease to basal rates. If exposure to glucose is prolonged, a slower, second- or late-phase insulin secretion is observed

(Curry, Bennett et al. 1968; Straub and Sharp 2002). In non-diabetic animals and humans, the infusion of glucose elicits an insulin secretory response that follows the same biphasic pattern as seen in vitro. Within minutes of ingestion of a glucose load, the plasma insulin concentration peaks within 5 to 7 min. This early phase of insulin release lasts no more than 10 to 15 min and is followed by a more sustained secretion lasting several hours, until the stimulus is removed or the plasma glucose concentration has returned to baseline values (Del Prato 2003).

Stimulus-secretion coupling

Pancreatic β-cells are electrically active (Dean and Matthews 1968) and use this property to couple elevation of blood glucose to stimulation of insulin secretion. At substimulatory glucose concentrations (< 7 mmol/l), the membrane potential of the beta cell is negative (–70 mV). In mouse β-cells, electrical activity is generated at glucose concentration ≥7 mmol/l (Renstrom, Eliasson et al. 1997). The steps that link changes in glucose levels to insulin secretion are well characterized (Langin 2001). Glucose enters the β-cell via the glucose transporter 2 (GLUT2) by facilitated diffusion across the plasma membrane, ensuring that the extracellular and intracellular glucose concentrations are rapidly equilibrated (Meglasson and Matschinsky 1986). Following its entry into the β-cell, glucose is phosphorylated by glucokinase to generate *glucose-6-phosphate*. This rate-limiting enzymatic step constitutes a *glucose sensor*, since it allows rapid and precise adjustments to be made in response to changes in extracellular glucose levels. Glucose-6-phosphate is further metabolised to produce pyruvate that is oxidised to generate acetyl-CoA. Acetyl-CoA in turn enters the citric acid cycle for adenosine triphosphate (ATP) synthesis (Schuit, Huypens et al. 2001). Following the production of ATP at the expense of adenosine diphosphate (ADP), the resultant increase in the ATP/ADP ratio leads to a decrease in K^+ conductance of the plasma membrane by closure of the ATP-sensitive potassium channel (K_{ATP} channel) (Ashcroft and Rorsman 1989; Seino, Iwanaga et al. 2000). The K_{ATP} channels are composed of two different subunits, the inward rectifier K^+-channel $Kir_{6.2}$ subunit and the sulfonylurea receptor subuinit SUR1, assembled at 4:4 stoichiometry (Inagaki, Gonoi et al. 1995; Ashcroft and Gribble 1998). Both subunits are necessary to constitute a functional K_{ATP} channel. The maintenance of the β-cell resting membrane potential at about –70 mV depends on properly functioning K^+-channels. The closure of K^+-channel suppresses efflux of K^+ ions, leading to progressive depolarization of the plasma membrane. When the β-cell reaches the threshold potential (~ -50 mV) electrical activity is initiated leading to the opening of voltage-dependent calcium channels and influx of Ca^{2+} down the electrochemical gradient. The resultant increase in intracellular calcium concentration $[Ca^{2+}]_i$ triggers exocytosis of insulin containing secretory granules (Ashcroft and Rorsman 1989; Lang 1999; Rorsman and Renstrom 2003). This stimulus-secretion mechanism described above is referred to as the K_{ATP} channel-dependent or triggering pathway of glucose-stimulated insulin release (Henquin 2000; Straub and Sharp 2002). This triggering pathway of glucose-stimulated insulin release is essential for proper stimulation of the first phase of insulin release.

Besides the triggering pathway mentioned above, glucose can also produce signals that amplify the action of $[Ca^{2+}]_i$ on the exocytosis process, a process called amplifying or K_{ATP} channel-independent pathway. The amplifying pathway was first demonstrated in 1992 by two independently groups (Gembal, Gilon et al. 1992; Sato, Aizawa et al. 1992). They found that when K_{ATP} channel are kept open by diazoxide combined with high K^+ to stimulate Ca^{2+}-influx or when K_{ATP} channel are completely closed by maximally effective concentration of

sulfonylreas, glucose is still able to increase insulin secretion independently of further associated changes in membrane potential or $[Ca^{2+}]_i$. The amplifying pathway operates to augment the β-cell secretory response induced by the triggering signals. Thus, the amplifying pathway does not initiate the insulin release on its own and secretion must first be stimulated by the triggering pathway. This ensures that insulin secretion is not augmented under low glucose concentration. It is accepted that during the second phase of insulin release the K_{ATP} channel-independent pathways determine the secretory response (Taguchi, Aizawa et al. 1995; Aizawa, Komatsu et al. 1998).

The mechanisms underlying the amplifying pathway of glucose-stimulated insulin release are incompletely elucidated. It is generally accepted that they require metabolism of the sugar. Several potential mechanisms have been suggested, as will be discussed in the following.

Metabolic coupling factors:

1. *Malonyl-CoA*. Glucose induces an increase in the amount of mitochondrial citrate, which is exported to the cytosol, cytosolic citrate, and cytosolic malonyl-CoA. Malonyl-CoA is also a potent inhibitor of carnitine palmitoyl transferase 1 (CPT-1) (Chen, Ogawa et al. 1994). The inhibition of CPT-1 blocks transport of long-chain acyl-CoA into mitochondria (McGarry, Mannaerts et al. 1977) resulting in accumulation of long-chain acyl-CoA in cytosol. These and other potential signalling molecules are presumed responsible for the second phase of insulin release (Corkey, Glennon et al. 1989; Prentki, Vischer et al. 1992; Chen, Ogawa et al. 1994; Brun, Roche et al. 1996).
2. *Glutamate*. Glycolysis converts glucose to pyruvate, which enters the mitochondrion and the tricarboxylic-acid (TCA) cycle. Glutamate is then formed from α-ketoglutarate by the glutamate dehydrogenase. It is proposed that in the cytosol, glutamate sensitizes the secretory machinery to Ca^{2+} perhaps by an action on the insulin-containing granules (Maechler and Wollheim 1999; Maechler and Wollheim 2000; Rubi, Ishihara et al. 2001).
3. *ATP*. Glucose induces concentration-dependent increases in the ATP:ADP and GTP:GDP ratios. Insulin secretion is inversely correlated with ADP and GDP levels and is positively correlated with the ATP:ADP and GTP:GDP ratios up to 20-mM glucose (Detimary, Van den Berghe et al. 1996; Detimary, Dejonghe et al. 1998; Sato and Henquin 1998; Henquin 2000).
4. *cAMP*. Another potentiator of insulin secretion is cyclic AMP (cAMP). The cAMP is unable to stimulate insulin secretion on its own. However, upon a simultaneous increase in $[Ca^{2+}]_i$, cAMP augments insulin secretion. This augmentation has been proposed to involve increased conductance of L-type Ca^{2+} channels via activation of protein kinase A as well as a cAMP-mediated direct effect on the exocytotic machinery (Ammala, Ashcroft et al. 1993; Renstrom, Eliasson et al. 1997).
5. *NADPH*. NADPH is a potential mitochondrial signalling molecule derived from glucose metabolism. Metabolizable insulin secretagogues increase the NADPH-to-NADP ratio in rodent islets (Ashcroft and Christie 1979). NADPH is taken up into the granules and stimulates insulin secretion in toadfish (Watkins and Moore 1977). Inhibition of NADPH formation reduces glucose-stimulated insulin secretion in rats (Ammon and Steinke 1972). Effects of NADPH on exocytosis are proposed to be mediated by the redox proteins glutaredoxin (GRX) and thioredoxin (TRX) (Ivarsson, Quintens et al. 2005).

Granule pools with different release properties:

In the mouse β-cell, the total granule number has been estimated morphometrically to approximately 13 000 (Dean 1973), but not all of these are released upon stimulation. As the

triggering pathway and amplifying pathways result in exocytosis of the insulin-containing granules, an understanding of granule pools, status, and function is essential. It is known that the number of insulin-containing granules in the endocrine pancreas is in large excess over the number required to handle the nutrient load of a single meal. Typically, only a small percentage of the granules and therefore of the total insulin content of the β-cell is secreted in response to a high glucose stimulus (Rorsman, Eliasson et al. 2000; Bratanova-Tochkova, Cheng et al. 2002). In many cells exhibiting regulated exocytosis, the granules are present in distinct functional pools depending on their release-competence (Proks, Eliasson et al. 1996; Neher 1998; Voets, Neher et al. 1999). Those granules that can undergo exocytosis immediately upon stimulation are referred to as the readily releasable pool (RRP) while those granules that need to undergo further modification before secretion belong to the reserve pool (RP). A subpool of RRP, the immediately releasable pool (IRP), is situated in the close vicinity of the Ca^{2+} channels (Voets, Neher et al. 1999; Barg, Eliasson et al. 2002). Both RRP and IRP granules are connected to the plasma membrane (docked) via trans-SNARE (soluble N-ethylmaleimide-sensitive fusion protein [NSF]-attachment protein [SNAP] receptor) complexes, therefore they only require a rise in $[Ca^{2+}]_i$ for exocytosis. In order for transition of reserve pool granules to readily releasable pool granules, granules need to be mobilized and/or primed prior to fusion with the plasma membrane. The priming process involves a series of ATP-, Ca^{2+}-, and temperature-dependent reactions to become release-competent (Bittner and Holz 1992; Parsons, Coorssen et al. 1995; Renstrom, Eliasson et al. 1996; Eliasson, Renstrom et al. 1997). In rat pancreatic islets, glucose-stimulated ATP turnover mediated by calcium influx plays a role in the amplifying pathway of insulin secretion (Sweet and Gilbert 2006). The process of exocytosis of the secretory granules in β-cell is supposed to recruite many proteins. In order to permit fusion of the granule with the plasma membrane, SNARE-complexes assemble during the priming process (Lin and Scheller 2000; Bruns and Jahn 2002). The SNARE proteins consist of VAMP (vesicle-associated membrane protein, also known as synaptobrevin), syntaxin 1, and SNAP-25 (synaptosomal-associated protein of 25 kDa). The formation of trans-SNARE complexes brings the vesicular membrane in close contact with the plasma membrane (Lang 1999).

A growing body of evidence shows that the release of RRP granules account for the first phase of insulin secretion, whereas subsequent replenishment of the readily releasable pool by priming of previously nonreleasable granules from reserve pool is required for second-phase insulin secretion (Daniel, Noda et al. 1999; Rorsman, Eliasson et al. 2000; Barg, Eliasson et al. 2002; Olofsson, Gopel et al. 2002). The release of RRP granules is independent of ATP, whereas the release of RP granules is correlated with an increase in the ATP/ADP ratio in β-cells. The refilling of the RRP by mobilization of granules originally residing in a much larger reserve pool is a time- and energy-dependent process (Gembal, Detimary et al. 1993; Eliasson, Renstrom et al. 1997). The actin-based molecular motor Myosin 5a has been demonstrated to be involved in the transport of insulin granules during second phase of insulin secretion (Ivarsson, Jing et al. 2005).

As already alluded to, secretion of insulin from pancreatic β-cell is achieved by Ca^{2+}-dependent regulated exocytosis (Wollheim and Sharp 1981; Jones, Stutchfield et al. 1985; Prentki and Matschinsky 1987; Ashcroft and Rorsman 1989; Ammala, Ashcroft et al. 1993). The increase in $[Ca^{2+}]_i$ resulting from Ca^{2+} influx through voltage-gated Ca^{2+}-channels in the plasma membrane is sensed by the Ca^{2+} sensor proteins synaptotagmins. Synaptotagmins are situated on the secretory granules and interact with the SNARE proteins to form a stable four-helical complex which is suggested to pull the granular and plasma membrane together (Sutton, Fasshauer et al. 1998; Rorsman and Renstrom 2003).

Voltage-gated calcium channels

Voltage-gated calcium channels (VGCCs) or voltage-dependent calcium channels (VDCCs) are Ca^{2+}-conducting pores in the plasma membrane of electrically excitable cells. They open in response to membrane depolarization and allow calcium influx from the extracellular space. The resulting increase in the intracellular free calcium concentration triggers, or modulates, a variety of important physiological processes such as contraction, secretion, neurotransmission, and gene expression (Catterall 2000). The malfunction of calcium channels, resulting from their mutation, altered expression, and impairment by autoantibodies, leads to a series of clinical syndromes, referred to as calcium channelopathies or calcium channel diseases (Waxman 2001; Flink and Atchison 2003; Rizzuto and Pozzan 2003).

The calcium channels are complex proteins composed of four or five distinct subunits, which are encoded by multiple genes. The largest subunit, α_1 subunit of 190-250kDa incorporates the conduction pore, the voltage sensor and gating apparatus, and the known sites of channel regulation by second messengers, drugs, and toxins (Hockerman, Peterson et al. 1997). The α_1 subunit of voltage-gated calcium channels is composed of four homologous domains (I-IV) with six transmembrane segments (S1-S6) in each. The S4 segment serves as the voltage sensor. The pore loop between transmembrane segments S5 and S6 in each domain determines ion conductance and selectivity (Dirksen, Nakai et al. 1997). The synaptic protein interaction (SYNPRINT) sites in the intracellular loop Ⅱ-Ⅲ (L Ⅱ-Ⅲ) of $\alpha_{1B,}$ α_{1A}, α_{1C} and α_{1D} subunits of N-type, P/Q-type and L-type Ca^{2+} channels bind to syntaxin, SNAP-25, and synaptotagmin (Catterall 1999). No such interaction has been demonstrated for the R-type $Ca_V2.3$ channels. An intracellular β subunit and a transmembrane, disulphide-linked $\alpha_2\delta$ subunit complex are components of most types of calcium channels (Takahashi, Seagar et al. 1987). A γ subunit has also been found in skeletal muscle calcium channels and related subunits are expressed in heart and brain (Hofmann, Biel et al. 1994; Catterall, Striessnig et al. 2003).

Since the first recordings of Ca^{2+} currents in cardiac myocytes (Reuter 1967), it has become apparent that there are multiple types of Ca^{2+} currents as defined by physiological and pharmacological criteria (Tsien, Lipscombe et al. 1988; Bean 1989; Llinas, Sugimori et al. 1992; Ellinor, Zhang et al. 1993; Zhang, Randall et al. 1993). Calcium currents recorded in different cell types have diverse physiological and pharmacological properties, and an alphabetical nomenclature has evolved for the distinct classes of calcium currents. L-type calcium currents require a strong depolarisation for activation, are long-lasting (Nowycky, Fox et al. 1985), and are blocked by the organic L-type calcium channel antagonists, including dihydropyridines (DHP), phenylalkylamines, and benzothiazepines (Reuter 1983). They are the main calcium currents recorded in muscle and endocrine cells. N-type, P/Q-type, and R-type calcium currents also require strong depolarisation for activation (Randall and Tsien 1995). They are relatively unaffected by L-type calcium channel antagonist drugs but are blocked by specific polypeptide toxins from snail and spider venoms. P/Q-type calcium currents are blocked by ω-agatoxin IVA from funnel web spider venom. N-type calcium currents are blocked by ω-conotoxin GVIA and related cone snail toxins. R-type calcium currents are blocked by the synthetic peptide toxin SNX-482 derived from tarantula venom. T-type calcium currents are activated by weak depolarisation and are transient. They are resistant to both organic antagonists and to the snake and spider toxins used to define the N-

and P/Q-type calcium currents (Nowycky, Fox et al. 1985; Miljanich and Ramachandran 1995; Newcomb, Szoke et al. 1998).

Mammalian α_1 subunits are encoded by at least ten distinct genes that can be grouped in three subfamilies. In 2000, a rational nomenclature was adopted (Ertel, Campbell et al. 2000) based on the well-defined potassium channel nomenclature. Calcium channels were named using the chemical symbol of the principal permeating ion (Ca) with the principal physiological regulator (voltage) indicated as a subscript (Ca_V). The numerical identifier corresponds to the Ca_V channel α_1 subunit gene subfamily (1 to 3 at present) and the order of discovery of the α_1 subunit within that subfamily (1 through *n*). According to this nomenclature, the Ca_V1 subfamily ($Ca_V1.1$–$Ca_V1.4$) includes α_{1S}, α_{1C}, α_{1D}, and α_{1F}, which mediate L-type Ca^{2+} currents. The Ca_V2 subfamily ($Ca_V2.1$–$Ca_V2.3$) includes α_{1A}, α_{1B}, and α_{1E}, which mediate P/Q-type, N-type, and R-type Ca^{2+} currents, respectively. The Ca_V3 subfamily ($Ca_V3.1$–$Ca_V3.3$) includes α_{1G}, α_{1H}, and α_{1I}, which mediate T-type Ca^{2+} currents (Table 1).

Table 1: *Types of Ca_V channels.*

Channel	Current	α_1 subunit	I or A*	Localization
$Ca_V1.1$	L	α_{1S}	I: nifedipine, isradipine A: BayK8644	Skeletal muscle
$Ca_V1.2$	L	α_{1C}	I: nifedipine, isradipine A: BayK8644	Brain, heart, endocrine tissue
$Ca_V1.3$	L	α_{1D}	I: nifedipine, isradipine A: BayK8644	Brain, heart, endocrine tissue, cochlear hair cells
$Ca_V1.4$	L	α_{1F}	I: nifedipine, isradipine A: BayK8644	Retina
$Ca_V2.1$	P/Q	α_{1A}	I: ω-agatoxin IVA	Brain
$Ca_V2.2$	N	α_{1B}	I: ω-conotoxin-GVIA	Neurones, endocrine tissue
$Ca_V2.3$	R	α_{1E}	I: SNX-482	Neurones, endocrine tissue
$Ca_V3.1$	T	α_{1G}		Neurones, heart, endocrine tissue
$Ca_V3.2$	T	α_{1H}		Neurones, heart, endocrine tissue
$Ca_V3.3$	T	α_{1I}		Neurones, heart, endocrine tissue

*I: inhibitor; A: activator.

Pancreatic β-cells are electrically excitable and sensitive to glucose. In response to blood glucose, these cells secrete insulin and thus play a unique role in glucose homeostasis. β-cell Ca_V channels take a center stage in this process. Voltage-gated calcium currents were first recorded in rat pancreatic β-cell in 1985 (Satin and Cook 1985). Soon, whole-cell Ca_V currents were visualized in a variety of β-cells, including insulin-secreting cell lines and islet β-cells from different species (Yang and Berggren 2006). There is now considerable consensus that the L-type Ca_V current is the major Ca_V current subtype in the mouse β-cell. The presence of both $Ca_V1.2$ and $Ca_V1.3$ has been reported (Wiser, Trus et al. 1999; Yang,

Larsson et al. 1999; Barg, Huang et al. 2001; Liu, Hilliard et al. 2004). The distinct contribution of $Ca_V1.2$ and $Ca_V1.3$ subtypes to insulin exocytosis has not been thoroughly studied in different species and remains controversial. It has been demonstrated that L-type calcium channels are co-localized with insulin-containing granules (Bokvist, Eliasson et al. 1995). The loop between domain Ⅱ and Ⅲ of Ca_V channel α_1 subunit is responsible for channel interaction with the insulin granule (Wiser, Trus et al. 1999; Barg, Huang et al. 2001). The involvement of $Ca_V2.1$ channels in glucose-stimulated insulin secretion from rat β-cells has been demonstrated by electrophysiological and pharmacological means (Ligon, Boyd et al. 1998). The role of $Ca_V2.2$ channels in insulin exocytosis is controversial. Davalli et al. showed that the $Ca_V2.2$ channel had no effect on glucose-dependent insulin secretion in human islets (Davalli, Biancardi et al. 1996). However, others demonstrated that an appreciable inhibition occurred by the $Ca_V2.2$ channel blocker ω-conotoxin GVIA in the RINm5F rat insulinoma cell line, and reduced secretagogue-induced insulin release from the same cells (Sher, Giovannini et al. 2003). Experimental evidence has demonstrated that Ca^{2+} entry through $Ca_V2.3$ channels regulates insulin secretion from both the pancreatic β-cell line INS-1 and primary mouse β-cells (Vajna, Klockner et al. 2001; Pereverzev, Mikhna et al. 2002; Pereverzev, Vajna et al. 2002). Experimental evidence suggests that Ca_V3 channels are likely to be players in the β-cell stimulus-secretion coupling, the Ca_V3 channel blocker $NiCl_2$ dose-dependently inhibits insulin secretion from INS-1 cells (Bhattacharjee, Whitehurst et al. 1997).

In addition to the ion channels residing in the plasma membrane, intracellular ion channels are also supposed to play a role in insulin secretion. Barg et al. reported that granular Cl^- uptake is important not only for the stimulation of exocytosis by sulfonylureas, but also for Ca^{2+}-induced β-cell exocytosis in general. Inhibition of Cl^- fluxes across membranes of β-cell granules impaired their luminal acidification and their priming for exocytosis (Barg, Huang et al. 2001).

Granule acidification

The compartmentalization of membrane-bound compartments with unique microenvironments enables eukaryotic cells to perform a myriad of reactions simultaneously with precision and speed. The compartments of the highly dynamic eukaryotic endomembrane system are acidified to varying degrees. Acidified organelles in cells include the Golgi complex, endosomes, lysosomes, secretory granules, and synaptic vesicles. In most cells, the pH of these organelles ranges from 4.5 to 6.5. The pH encountered by internalized ligands decreases gradually along the endocytic pathway. Early endosomes have a pH of approximately 6.2–6.3 (Yamashiro and Maxfield 1987). The pH of sorting endosomes is lower than that of early endosomes (~6.0, and possibly as low as 5.4 in some cells) (van Renswoude, Bridges et al. 1982; Sipe and Murphy 1987; Yamashiro and Maxfield 1987). Late endosomes are more acidic, with a measured pH of between 5.0 and 5.8 (Tycko and Maxfield 1982; Tycko, Keith et al. 1983; Yamashiro and Maxfield 1987). Lysosomes are the most acidic cellular compartment, with pHs between 4.6 and 5.3 measured in mammalian cells (Ohkuma and Poole 1978; Tycko and Maxfield 1982; Yamashiro and Maxfield 1987). In the biosynthetic pathway, pHs of organelles decreases gradually. ER pH is between 7.1 and 7.4, similar to the pH of cytoplasm (Kim, Johannes et al. 1998; Wu, Grabe et al. 2001). The *trans*-Golgi network (TGN) pH is between 5.9 and 6.3 (Seksek, Biwersi et al. 1995; Miesenbock, De Angelis et al. 1998). The pH of immature secretory granules measured in live cells is about 6.3, and decreases to 5.0–5.6 in mature secretory granules (Urbe, Dittie et al.

1997; Miesenbock, De Angelis et al. 1998; Blackmore, Varro et al. 2001; Wu, Grabe et al. 2001). The maintenance of an acidic pH milieu within a subset of these organelles is key to the optimal performance of the sorting and processing events that normally occur within these compartments. Organelle acidification is implicated in protein degradation, release of ligands from receptors, and proteolytic processing of precursor proteins into mature products, and provides a driving force for the accumulation of hormones or transmitters into secretory vesicles, synaptic vesicles, or synaptic-like microvesicles (Mellman, Fuchs et al. 1986; Stevens and Forgac 1997). However, in addition to these functions, acidification appears to regulate the molecular mechanism of membrane traffic through some compartments, as the sorting and transport of many proteins are less efficient when acidification is disrupted (Nishi and Forgac 2002).

Steady-state organelle pH is regulated and maintained by a balance between the rates of intralumenal protonpumping, counterion conductance, and intrinsic proton leak. As protons are pumped into compartments against their concentration gradients by the vacuolar-type ATPase (V-ATPase), the ability of this electrogenic pump to function further is theoretically limited by the accumulation of a positive membrane potential. In mammalian cells, passive ion flow through anion channels neutralizes this potential and allows acidification to continue (Glickman, Croen et al. 1983; Xie, Stone et al. 1983; Arai, Pink et al. 1989). In addition, the extent of intrinsic membrane permeability to protons also contributes to the steady-state pH (Futai, Oka et al. 1998; Grabe and Oster 2001). Proton concentration plays a fundamental role in the organelle acidification processes. The alpha and omega for increasing the proton concentration in organelle lumen is the action of a primary electrogenic proton pump, the V-ATPase. V-ATPases appear to be integral components of nearly all organelles which pumps proton from cytosol to organelle lumen. V-ATPases have also been identified in the plasma membrane of cells, like renal intercalated cells, osteoclasts and macrophages, where they are important in acid secretion, bone degradation and control of cytoplasmic pH, respectively (Brisseau, Grinstein et al. 1996; Li, Chen et al. 1999; Brown and Breton 2000). In all cases, they carry out ATP-dependent proton transport from the cytoplasmic compartment to the opposite side of the membrane (which might be either the lumen of an intracellular compartment or the extracellular space).

Due to its electrogenic nature, proton pumping by the V-ATPase can be limited by the generation of a transmembrane voltage across the organelle membrane. In mammalian cells, passive anion flow through a chloride channel neutralizes this potential to allow acidification to continue. The existence of a high Cl^- permeability in endosomes is well established, and Cl^- influx is thought to sustain the rapid acidification of endosomes. The secretagogue thyrotropin was shown to induce acidification of secretory granules in parafollicular cells by increasing chloride conductance of the granular membrane (Barasch, Gershon et al. 1988). Evidence for the role of Cl^- conductance in regulating organelle pH comes from studies of ClC chloride channel family members. Mutations in the ClC-5 chloride channel lead to Dent's disease, which is characterized by the defect in endosomal acidification resulting in an inability to reabsorb low-molecular-weight proteins and albumin in the kidney (Devuyst 2004). The ClC-3 chloride channel has been suggested to play a role in lysosome acidification (Li, Wang et al. 2002) and in endosomal acidification (Hara-Chikuma, Yang et al. 2005).

Other ion fluxes may also modulate acidification. In the Golgi complex, passive efflux of K^+ normally neutralizes the inward pumping of H^+ by the V-ATPase, thereby facilitates the acidification (Schapiro and Grinstein 2000). Inhibition of acidification by Na^+, K^+-ATPase in early endosomes but not in later endocytic compartments has been proposed to explain the

difference in pH between these organelles (Cain, Sipe et al. 1989; Fuchs, Schmid et al. 1989). However, the most important ion fluxes in terms of pH regulation are probably those involving chloride (Cl^-) ions.

Chloride channels

Anion channels are protein pores in biological membranes that allow the passive diffusion of negatively charged ions along their electrochemical gradient. Chloride ions (Cl^-) are the most abundant anion in mammals. Cl^- channels reside both in the plasma membrane and in intracellular organelle membranes. Their functions range from ion homeostasis to cell volume regulation, transepithelial transport and regulation of electrical excitability. Three molecularly distinct Cl^- channel families are well established:

1. CFTR(cystic fibrosis transmembrane conductance regulator) is known to be an ABC transport protein with a tandem repeat of a transmembrane domain of six putative transmembrane helices (TMD) and a nucleotide binding fold (NBF), linked by a regulator domain containing numerous phosphorylation sites (Riordan, Rommens et al. 1989). CFTR is now known to be a voltage-independent anion channel, which requires the presence of hydrolyzable nucleoside triphosphates for efficient activity (Tabcharani, Low et al. 1990). CFTR is expressed in the apical membrane of various epithelia, most prominently in those of the intestine, airways, secretory glands, bile ducts, and epididymis. CFTR is crucial for a number of transepithelial transport processes. This is readily evident from the pathophysiology of cystic fibrosis (CF) patients, which show severe impairments of epithelial salt and fluid secretion as well as reabsorption (Quinton 1990).
2. Ligand-gated chloride channels include γ-aminobutyric acid (GABA) and glycine receptors. GABA and glycine binding to their receptors opens intrinsic anion channels that belong to the ligand-gated ion channel superfamily. They have a common structure in which five subunits form an ion channel. Each subunit consists of 4 putative transmembrane domains. Both GABA and glycine receptors are predominantly expressed in central nervous system. They play an inhibitory role by hyperpolarizing the neuron and thereby inhibiting neuronal activity (Betz 1990).
3. In mammals, the ClC gene family of chloride channels has nine members that may function in the plasma membrane or in intracellular compartments. ClC channels are dimers in which each monomer has one pore (double-barreled channels). The crystal structure reveals that the bacterial ClC protein is composed of 18 helices, most of which do not cross the membrane entirely (Dutzler, Campbell et al. 2002). Most of the ClC channels that have been possible to test in heterologous expression systems show voltage-dependent gating.

- ClC-1 is predominantly expressed in the skeletal muscle. ClC-1 contributes 70–80% to the resting membrane conductance of muscle, ensuring its electrical stability. Mutations in ClC-1 lead to myotonia.
- ClC-2 is a broadly expressed Cl^- channel that can be activated by hyperpolarization, cell swelling, and extracellular acidification. The testicular and retinal degeneration resulting from its disruption in mice may suggest a role in transepithelial transport.
- The two renal ClC-K channels (ClC-Ka and ClC-Kb) function (in a heteromeric complex with barttin) in transepithelial transport across different nephron segments. Dysfunction of ClC-Kb leads to Bartter's syndrome in humans and renal diabetes insipidus in mice. In addition, both ClC-Ka/barttin and ClC-Kb/barttin are important for inner ear K^+ secretion. Accordingly, human mutations in barttin lead to a variant of Bartter's syndrome associated with deafness.

- ClC-3 through ClC-7 are intracellular chloride channels. ClC-3 is present in endosome and synaptic vesicles. ClC-3 is shown to be expressed in many tissues, including brain, kidney, liver, skeletal muscle, heart, adrenal gland, and pancreas. ClC-3 is involved in acidification of endosomes and synaptic vesicles.
- The function of ClC-4 remains largely uninvestigated.
- ClC-5 is predominantly expressed in kidney but is also present in liver, brain, testis, and intestine. ClC-5 is present in endosomes involved in endocytosis.
- ClC-6 is an intracellular channel of unknown function.
- ClC-7 is highly expressed in osteoclasts. ClC-7 may provide the electrical shunt that is necessary for the efficient pumping of H^+-ATPase during the resorption of lacuna of osteoclasts (Jentsch, Stein et al. 2002).

Aims

General aims

The mechanisms underling biphasic insulin secretion remains incompletely understood, but loss of first phase insulin secretion is a characteristic of early type 2 diabetes mellitus. In this thesis I have investigated the involvement of ion channels in phasic insulin release.

The specific aims were to:

1. Determine the molecular identity of the L-type Ca_V channel in the pancreatic β-cell, as well as to pin-point its effect on phasic insulin secretion.
2. Study the effects of the R-type $Ca_V2.3$ channel-resposible for the major non-L-type Ca^{2+} current in the β-cell-on phasic insulin release.
3. Evaluate the role of intracellular ClC-3 chloride channels in the insulin release machinery.

Methodology

Conditional Gene Knockouts using Cre recombinase

To generate β-cell-specific gene knockout, the Cre-loxP system was employed. The Cre recombinase of the P1 bacteriophage belongs to the integrase family of site-specific recombinases. It is a 38 kD protein that catalyzes the recombination between two of its recognition sites, called *loxP* (Hamilton and Abremski 1984). This is a 34 bp consensus sequence, consisting of a core spacer sequence of 8 bp and two 13 bp palindromic flanking sequences. An important feature of the Cre/*loxP* system is that it is functional in mammalian cells. The usual procedure requires generation of 2 independent varieties of transgenic mice.
The first is generated by homologous recombination to insert *LoxP* sites into the gene of interest in a manner in which function of the gene is not impaired. In this transgenic mouse, the gene of interest is flanked by two *loxP* sites (hence the term *floxed*). A second line of transgenic mice is generated by random chromosomal insertion of a transgene expressing Cre recombinase under the control of a tissue-specific promoter. Double transgenic animals resulting from matings of these original transgenic lines will carry null alleles of the gene of interest only in those cells that have expressed Cre. Hence, the target gene remains active in all cells and tissues which do not express Cre (Figure 3).

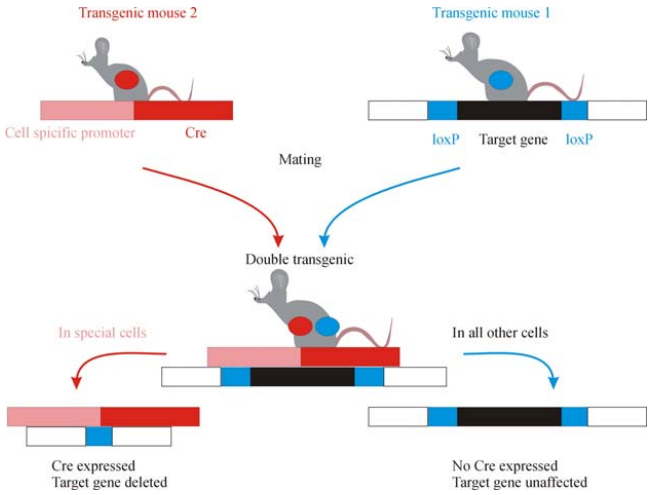

***Figure** 3: A conditional gene knockout strategy using Cre-LoxP system.*

In this thesis, Cre recombinase expression is under the control of insulin promoter such that gene knockout will take place only in insulin-expressing cells.

In vivo glucose challenge

The experiments started in the morning at 9:00 a.m. in non-fasted mice. Glucose challenge was performed without anaesthesia by intraperitoneal injection of 2.0 g glucose (equivalent to 11.1 mmol)/kg body weight. Blood samples were drawn into tubes coated with heparin at baseline and 3, 8 min after glucose load. Insulin and glucose concentrations in the blood

sample were detected by radioimmunoassay (RIA) and the glucose oxidase method, respectively.

In situ pancreatic perfusion

Experiments were performed in the morning at 10:00 a.m. in non-fasted mice. Anesthesia was given by intraperitoneal injection of midazolam (Hofmann-La Roche AG; 0.4 mg/25 g body weight) and fentanyl (Janssen Pharmaceuticals Inc.; 0.02 mg/25 g body weight). The mice were kept on a heating pad during the entire experiment. After opening the abdominal cavity and ligating the renal, hepatic, and splenic arteries, the aorta was tied off above the level of the pancreatic artery. The pancreas was perfused with modified Krebs-Ringer HEPES buffer preheated to 37°C (1 ml/min) via a silicone catheter placed in the aorta. The basal glucose concentrations were 1 mM (paper Ⅰ) and 3.3 mM (paper Ⅱ). The perfusate was collected via a silicone catheter from the portal vein at 30- or 60-second intervals, as indicated, in 2.5-ml Eppendorf tubes containing 25 μl Trasylol. Insulin and glucose concentrations in the effluent medium were detected by RIA and the glucose oxidase method, respectively.

Islet isolation and insulin release measurement

Islets were isolated from mouse by injection of a collagenase solution into the bile-pancreatic duct of the mouse directly after being killed by cervical dislocation. The distended pancreas was excised and the digestion was performed in a water-bath at 37 °C for 30 min. Islets were hand-picked and counted under a microscope. Freshly isolated islets were preincubated for 30 min at 37 °C in Krebs—Ringer bicarbonate buffer (KRB), pH 7.4, supplemented with 10 mM Hepes, 0.1% bovine serum albumin and 1 mM glucose. Each incubation vial contained 10 islets in 1.0 ml (30-40 islets in 1.5 ml) buffer solution and was gassed with 96% O_2/5% CO_2 to obtain constant pH and oxygenation. After preincubation the buffer was changed to a medium containing the agents to be tested. The islets were then incubated for 60 min at 37℃ in an incubation box (30 cycles/min). Immediately after incubation, aliquots of the medium were removed for assay of insulin. Alternatively, aliquots of the medium were frozen for subsequent assay of insulin. Insulin secretion from islets was measured by RIA or the enzyme-liked-immunoabsorbent assay (ELISA).

Western blot analysis

Approximately 900 islets of control and $\beta Ca_V1.2^{-/-}$ mice were cultured in RPMI 1640 for 48 h at 37°C. Thereafter, the islets were homogenized after one freeze-thaw cycle in a hypotonic buffer (20 mM K_2HPO_4/KH_2PO_4 pH 7.2, 1 mM EDTA) containing protease inhibitors [1 mM benzamidine, 0.1 mM PMSF and Protease Inhibitor Cocktail (1:500; Sigma)]. The homogenates (40 mg protein) were separated on an 11% SDS-PAGE (lower crosslinking with 0.2% bis-acrylamide). Peptides were blotted on a PVDF membrane (Millipore) and probed with a $Ca_V1.2$-(Chemicon) and a panCa_V-specific antibody (Calbiochem). Equal loading of the slots was ascertained using a monoclonal β-actin antibody (Abcam). Antibodies were visualized by the ECL system (NEN).

The patch-clamp technique

The patch-clamp technique was invented by Sakmann and Neher in the 70's (Neher, Sakmann et al. 1978). Patch-clamp is a versatile technique and its various configurations enables the experimenter to 1) study ion channels at different levels, either whole-cell currents (activity of all ion channels added up) or currents flowing through individual ion channels; 2) easily manipulate the fluid on the extracellular or the intracellular side of the membrane during a recording.

The most straight-forward patch clamp configuration (in terms of physical manipulation) is the *cell-attached patch* mode, which is where every patch clamp experiment starts. This configuration is attained when a high-resistance seal is formed between glass pipette and the plasma membrane. This enables allowing measurements of currents passing through single ion channels situated within the "patched" piece of the membrane as well as recordings of single granule release events. This configuration leaves the cell intact, and is therefore the most "physiological" configuration to study single channels.

To gain electrical access to the ion channels in the entire cell membrane, the membrane under the pipette tip in cell-attached patch mode has to either be ruptured by gentle suction (*the standard whole-cell configuration*) or perforated by pore-forming agent such as nystatin or amphotericin B (*perforated-patch whole-cell configuration*). In the standard whole-cell configuration, the pipette solution makes direct contact with the cytoplasm. The standard whole-cell configuration permits control of the intracellular milieu via wash-in of the pipette solution. The ionic composition of the cytosol can thus be controlled and various membrane-impermeable compounds, including large molecules such as antibodies, can be applied via the patch-pipette by inclusion in the pipette solution dialyzing the cell interior. This configuration disrupts cell metabolism and effects of a metabolite added to the cell interior can thus be investigated without much conversion into down-steam products. However, the disruption of cell metabolism is a non-physiological situation and washout of cytoplasmic enzymes is disadvantageous if metabolic pathways are to be studied (Hamill, Marty et al. 1981). To avoid wash-out of intracellular factors and proteins, one can use a perforated-patch whole-cell configuration. Instead of making one hole into the cell as in standard whole-cell, pore-forming agents such as amphotericin B make small perforations in the membrane so that only small molecules such as ions can pass through. The pores establish electrical contact between pipette solution and the cell interior while intact cell metabolism is maintained and therefore perforated-patch whole-cell configuration is a more "physiological" (Horn and Marty 1988). In this thesis, whole-cell Ca^{2+} currents were measured in intact cells using the perforated-patch whole-cell approach.

Cell capacitance measurements

Capacitance measurements provide an electrophysiological single-cell assay to study secretion, which is a development of the patch-clamp technique. High-resolution capacitance measurements monitor the changes of cell surface area that arise when secretory granules fuse with the plasma membrane. Biological membranes act as electrical capacitors. The relationship between the cell surface area (A) and membrane capacitance (C) is given by the equation

$C = \varepsilon * A/d$

where ε is the specific membrane capacitance and d is the membrane thickness. An increase in membrane capacitance can thus be considered as an indicator of exocytosis. The granules in β-cells have spherical geometry with diameters of 300 nm. Assuming a specific membrane capacitance of 9 fF/μm^2 (Gentet, Stuart et al. 2000), the fusion of one β-cell granule corresponds to an increase in membrane capacitance of 3 fF. In the voltage clamp mode (holding the membrane voltage at a set level), the exocytosis can be evoked by single or repetitive depolarizations from the resting potential (-70 mV) to 0 mV. Capacitance measurements have several advantages over traditional biochemical assays of secretions. For instance, exocytosis can be monitored in a single cell, making the study of release kinetics available. Although capacitance measurements are a powerful assay to monitor secretion, it has disadvantages. Capacitance measurements record the cell surface area at a given moment. This means that the change in capacitance reflects the net result of exo- and endocytosis occurring in the cell. Therefore it has to be ascertained that endocytosis does not contaminated the capacitance recordings.

In this thesis, cell membrane capacitance measurements were performed using the standard whole-cell configuration.

Measuement of intracellular Ca^{2+} concentration

Currently the most popular method for measuring $[Ca^{2+}]_i$ in mammalian cells is by microfluorimetry which involves measurement of the fluorescence of an indicator. Fluorescence is a luminescence in which the molecular absorption of a photon triggers the emission of another photon with a longer wavelength. For some indicators, the free and the ion-bound form of the fluorophore have different excitation and emission spectras. One such indicator is fura-2, which can be used for ratiometric monitoring $[Ca^{2+}]_i$. The fluorescence excitation spectrum of fura-2 shifts to the lower wavelength upon Ca^{2+} binding (Figure 4).

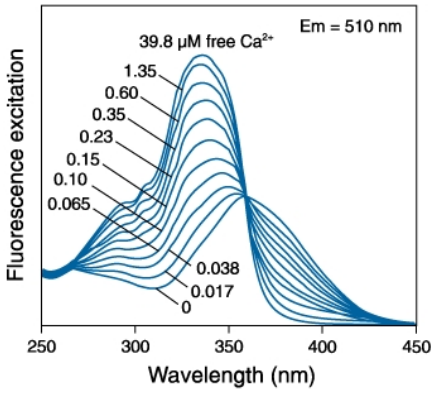

Figure 4: *Fluorescence excitation spectra of fura-2 in solutions containing 0–39.8 μM free Ca^{2+}. (Reproduced with permission from invitrogen^{TM})*

The excitation source alternates between two different excitation wavelengths that are characteristic of the probe. The emission intensity caused by either excitation wavelength is measured at the longer emission wavelength and the ratio of these intensities is calculated.

Ratiometric measurements have the advantage of eliminating variance between experiments due to differences in dye loading, variations in tissue thickness, irreversible destruction of the fluorophore, (photobleaching) or instrumental instability such as alterations of the illumination source.

In this thesis, fura-2 AM was used. Fura-2-AM is the membrane-permeant acetoxymethyl ester derivative of fura-2 and can be easily loaded into cells by incubation. Fura-2 AM itself does not bind Ca^{2+}, but it is readily hydrolyzed to active fura-2 by endogenous esterases once the dye is inside the cells. The deesterification results in fura-2 being trapped inside the cell. The measurements were carried out using a microfluorimetry system (D104, PTI, Monmouth Junction, N.J., USA). The fluorophore was excited alternately at 350 nm and 380 nm and emitted light was collected at 510 nm. The $[Ca^{2+}]_i$ was calculated using the equation as described previously (Grynkiewicz, Poenie et al. 1985; Olofsson, Gopel et al. 2002).

Subcellular fractionation

Cells contain a variety of organelles. Each type of organelles in a cell has a specific density and based on that density you can separate a certain type of organelle from the others. This is usually accomplished by differential centrifugation, a method to separate the components of cells on the basis of their size and density. The fractions obtained from differential centrifugation correspond to enriched, but still not pure, organelle preparations. A greater degree of purification can be achieved by density-gradient centrifugation, in which organelles are separated by sedimentation through a gradient of a dense substance, such as sucrose. In velocity centrifugation, the starting material is layered on top of the sucrose gradient. Particles of different sizes sediment through the gradient at different rates, move as discrete bands. Following centrifugation, the collection of individual fractions of the gradient provides sufficient resolution to separate organelles of similar size, such as mitochondria, lysosomes, and peroxisomes (Graham and Rickwood 1997).

Results and Discussion

Impaired insulin secretion and glucose tolerance in β cell-selective $Ca_V1.2$ Ca^{2+} channel null mice (paper Ⅰ)

We investigated the role of the L-type $Ca_V1.2$ Ca^{2+} channel for insulin secretion by combining a targeted gene knockout approach with time-resolved insulin release assays and high-resolution single-cell capacitance measurements of exocytosis. β-cell-specific inactivation of the $Ca_V1.2$ gene was achieved using *Cre-loxP* system under the control of the insulin 2 promoter.

$Ca_V1.2$ Ca^{2+} channel is the only L-type Ca^{2+} channel in β cell

Whole-cell Ca^{2+} currents were reduced in β-cells from $\beta Ca_V1.2^{-/-}$ mice by ~55% in perforated-patch whole cell Ca^{2+}-current measurements. The consequences of ablating $Ca_V1.2$ on the β-cell Ca^{2+} current were similar to those obtained using isradipine. Isradipine blocked the Ca^{2+} current to the same extent at all voltages and the integrated current (expressed as total charge movement) observed at -10 mV was reduced by 53±6% (n = 9).

Impaired first-phase insulin secretion in $\beta Ca_V1.2^{-/-}$ mice

The pattern of single-cell exocytosis elicited by a train of ten 500 ms depolarizations was analysed carefully. Exocytosis of β-cells from $\beta Ca_V1.2^{-/-}$ mice in response to the initial depolarizations was markedly reduced whereas that elicited later during the train was not affected (Figure 5).

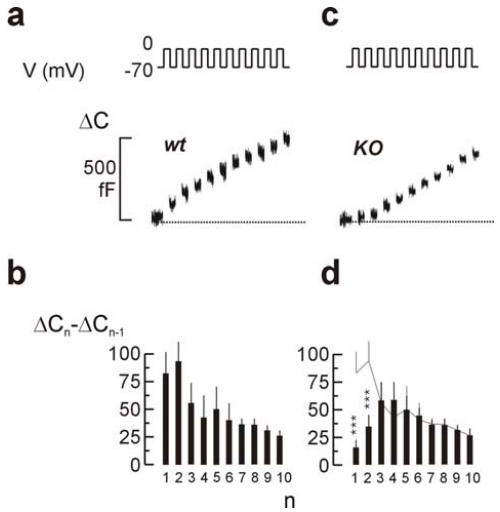

***Figure 5**: Loss of rapid exocytosis in $\beta Ca_V1.2^{-/-}$ β- cells. (A) Increase in cell capacitance (ΔC, lower) elicited by a train of ten 500 ms depolarizations from -70 to 0 mV (V, upper). The dotted line indicates the pre-stimulatory level. (B) Increment in cell capacitance by each depolarization (ΔC_n- ΔC_{n-1}) displayed against pulse number (n). (C and D) The same as in (A and B) but using a β-cell obtained from a $\beta Ca_V1.2^{-/-}$ mouse.*

The acute effects of applying the L-type Ca^{2+} channel antagonist isradipine were by and large identical to those resulting from $Ca_V1.2$ disruption. SNX482, which reduced the Ca^{2+} current by ~25%, affected late exocytosis but had no significant effect on the response to the first depolarization. The $\beta Ca_V1.2^{-/-}$ mice exhibited a slight hyperglycemia under basal and fasted (6 h) conditions. An intraperitoneal glucose challenge (2g/kg body weight) in fed mice revealed an impaired glucose tolerance in $\beta Ca_V1.2^{-/-}$ mice. This correlated with a slight reduction of basal plasma insulin levels and marked reduction of glucose-induced first-phase insulin secretion (measured 3 min after the glucose challenge) in the $\beta Ca_V1.2^{-/-}$ mice. *In situ* pancreatic perfusion reveals blunted first-phase insulin secretion in pancreata from $\beta Ca_V1.2^{-/-}$ mice (Figure 6).

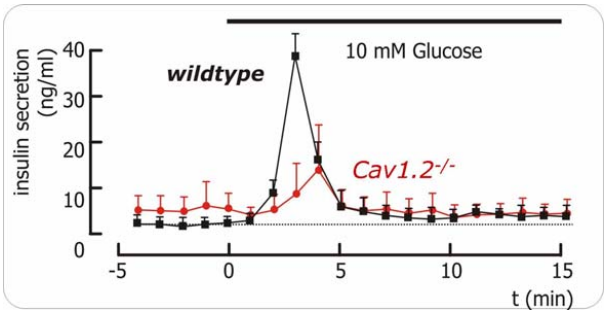

***Figure 6**: Blunted first-phase insulin secretion in $\beta Ca_V1.2^{-/-}$ pancreata. Insulin release from in situ perfused pancreatic glands from control (black squares) and $\beta Ca_V1.2^{-/-}$ mice (red circles) before and after elevating glucose from 1 to 10 mM (black horizontal bar). The dotted horizontal line corresponds to the pre-stimulatory rate of insulin release in control mice.*

In vitro insulin secretion assays using isolated islets demonstrated that basal insulin secretion in islets from $\beta Ca_V1.2^{-/-}$ mice was unaffected, but glucose-induced insulin secretion was much lower than in the control mice and comparable to that seen after blockage of the Ca^{2+} channels with nifedipine (2.7-fold enhancement).

$Ca_V2.3$ calcium channels control second-phase insulin release (paper Ⅱ)

In paper Ⅱ we have investigated the role of $Ca_V2.3$ calcium channels on insulin secretion by performing in vivo glucose tolerance tests, dynamic measurements of phasic insulin secretion in situ, static pancreatic hormone–release experiments in isolated islets, as well as single cell recordings of whole-cell Ca^{2+} currents and exocytosis and ratiometric measurements of the cytoplasmic Ca^{2+} concentration in WT and $Ca_V2.3^{-/-}$ islets.

Effects of $Ca_V2.3$ calcium channels on whole cell Ca^{2+} currents in β cell

We studied the functional consequences of ablation of the $Ca_V2.3$ gene using perforated-patch whole cell Ca^{2+}-current measurements. β-cells from $Ca_V2.3^{-/-}$ mice exhibited a selective loss of a high voltage Ca^{2+} current component, and current amplitudes at voltages below –10 mV were not affected. At –10 mV, the reduction averaged approximately 23%. The R-type Ca^{2+} channel blocker SNX482 (100 nM) had no effect on voltage-gated Ca^{2+} currents in $Ca_V2.3^{-/-}$

mice, whereas the L-type inhibitor isradipine (2 μM) significantly reduced Ca^{2+} influx approximately 60% at potentials more positive than or equal to –30 mV.

$Ca_V2.3$ gene ablation alter the intracellular Ca^{2+} homeostasis

Resting $[Ca^{2+}]_i$ measured at 5 mM glucose was identical in islets from $Ca_V2.3^{-/-}$ and WT mice. After elevation of glucose to 10 mM, in $Ca_V2.3^{-/-}$ islets, the glucose-evoked initial peak in $[Ca^{2+}]_i$ occurred later than in WT islets (227 ± 15 versus 204 ± 33 seconds in $Ca_V2.3^{-/-}$ and WT islets, respectively). This initial amplitude was almost unaffected (7% decrease), but the time-averaged $[Ca^{2+}]_i$ during the subsequent oscillatory phase was 17% lower than in WT islets ($P < 0.01$). In addition, the oscillatory activity was 29% slower in the $Ca_V2.3^{-/-}$ islets (1.8 ± 0.1 versus 2.5 ± 0.2 bursts/minute in $Ca_V2.3^{-/-}$ and WT islets, respectively).

Effects of $Ca_V2.3$ gene ablation on insulin secretion

We used cell capacitance measurements to study the kinetics of depolarization-evoked exocytosis in single β-cells from control and $Ca_V2.3^{-/-}$ mice. Exocytosis was elicited by trains of 10 500-ms voltage clamp depolarisations. In β-cells from $Ca_V2.3^{-/-}$ mice, the increase in cell capacitance during the train was 21% suppressed than the exocytotic response evoked by the same stimulus in WT β-cells. Interestingly, exocytosis in response to the initial depolarisations was not affected whereas that elicited later during the train was entirely responsible for the overall reduction (Figure 7).

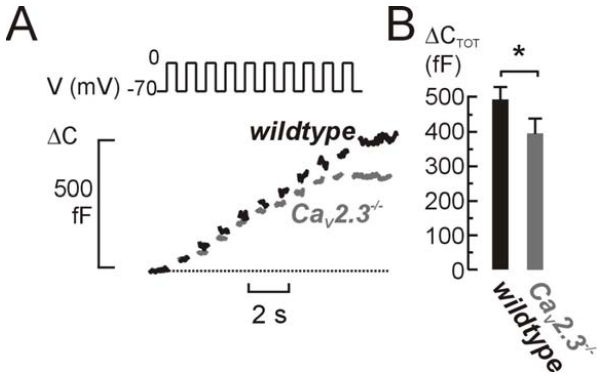

Figure 7: *Effects of $Ca_V2.3$ ablation on single-cell exocytosis in islet cells. (A) Exocytosis evoked by trains of 10 depolarizations (V) and monitored as increases in cell capacitance (ΔC) in WT $Ca_V2.3^{+/+}$ (black) and $Ca_V2.3^{-/-}$ (gray) β-cells. (B) Average total increase in capacitance evoked by the trains (ΔC_{TOT}).*

To determine the consequences of the $Ca_V2.3$ deficiency on glucose homeostasis and insulin release, serum insulin and glucose concentrations were measured in $Ca_V2.3^{-/-}$ mice and WT mice after an intraperitoneal glucose challenge (2 g/kg body weight). In $Ca_V2.3^{-/-}$ mice, basal glucose levels were elevated by 17% compared with WT ($P < 0.05$ versus WT; $n = 9$), and the plasma glucose concentrations measured 3 and 8 minutes after challenge were also elevated approximately 15% ($P < 0.05$ for values at 8 minutes versus WT). Basal plasma insulin levels did not differ between the $Ca_V2.3^{-/-}$ and WT strains. In $Ca_V2.3^{-/-}$ mice, the glucose-induced increase in circulating insulin was similar to that in WT mice 3 minutes after challenge, but after 8 minutes it was limited to less than 10% ($P < 0.05$ versus WT).

To investigate whether the reduced insulin secretion in $Ca_V2.3^{-/-}$ mice depends on systemic factors or reflects processes within the islets, insulin secretion from isolated islets was studied. In $Ca_V2.3^{-/-}$ islets, glucose-stimulated insulin release was reduced approximately 25% compared with WT. The effects of isradipine on glucose-stimulated insulin release were comparable in WT (66% reduction) and in $Ca_V2.3^{-/-}$ islets (68% suppression). Insulin secretion elicited by stimulation with high extracellular K^+ (50 mM) resulted in a 75% enhancement of release relative to that observed in the presence of glucose alone in WT islets. A similar relative stimulation was observed in $Ca_V2.3^{-/-}$ islets (96%), but in absolute terms, the response in the latter type of islets was reduced 13% compared with WT islets.

To assess the role of $Ca_V2.3$ in dynamic insulin release, we performed *in situ* pancreatic perfusions with fractionated sampling. In $Ca_V2.3^{-/-}$ pancreata, the peak in first-phase insulin secretion was only slightly reduced (19%) and measured 7.1 ± 2.1 ng/ml (NS; n = 4). More importantly, second-phase insulin release was markedly suppressed and averaged 9.4 ± 2.7 ng/ml, representing a 46% reduction compared with WT ($P < 0.05$) (Figure 8).

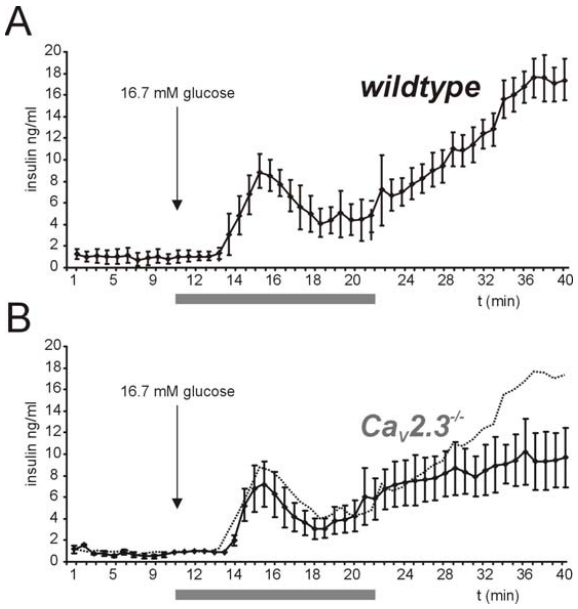

Figure 8: *Dynamics of insulin release measured by in situ pancreatic perfusion.*

Effects of $Ca_V2.3$ gene ablation on glucagon secretion

We also found that $Ca_V2.3$ ablation affects glucagon secretion. In isolated islets, the ability of glucose to suppress glucagon secretion is severely impaired. In the in vivo glucose challenge test, 3-minute values for plasma glucagon were stimulated approximately 15% in $Ca_V2.3^{-/-}$ mice, whereas in WT they were reduced approximately 20%.

Immunostaining against insulin and glucagon performed on $Ca_V2.3^{-/-}$ isltet cells revealed that 75% and 9% of the cells could readily be characterized as β- and α-cells, respectively, 16% of the 210 cells coexpressed insulin and glucagon.

Discussion papers Ⅰ&Ⅱ

Glucose-induced insulin secretion follows a biphasic time-course. A transient first phase lasting 5-10 min is followed by a sustained second phase. It has been suggested to reflect the sequential release of distinct pools of granules, which vary with regard to release competence. Insulin is secreted from pancreatic β-cells in response to an elevation of cytoplasmic Ca^{2+} resulting from enhanced Ca^{2+} influx through voltage-gated Ca^{2+} channels. Mouse β-cells express several types of voltage-gated Ca^{2+} channel (L-, R- and possibly P/Q-type). We have investigated the role of the L-type $Ca_V1.2$ Ca^{2+} channel and the R-type $Ca_V2.3$ Ca^{2+} channels for insulin secretion.

Mouse pancreatic β-cells contain dihydropyridine-sensitive L-type Ca^{2+} channels and glucose-induced insulin secretion is almost abolished by pharmacological inhibitors of L-type Ca^{2+} channels such as nifedipine. Previous studies have argued that $Ca_V1.3$ (α_{1D}) or $Ca_V1.2$ (α_{1C}) might be of importance in insulin release (Yang, Larsson et al. 1999; Barg, Huang et al. 2001). The present data that the entire DHP-sensitive Ca^{2+} current is lost following inactivation of the $Ca_V1.2$ gene reinforces previous immunochemical and electrophysiological data that $Ca_V1.2$ is the only L-type Ca^{2+} channel variety expressed in mouse β-cells. Previous studies have demonstrated that $Ca_V1.2$ Ca^{2+} channels functionally associate with insulin granules in the β-cells, and that the loop connecting the second and third homologous domains physically tethers the channel to components of the exocytotic core complex (Wiser, Trus et al. 1999). The close connection between the secretory granules and the Ca^{2+} channel was further supported by experiments using the synprint peptide (Barg, Huang et al. 2001). Our data reveals that $Ca_V1.2$ Ca^{2+} channels are required for first-phase insulin secretion and rapid exocytosis in pancreatic β cells. We propose that in $\beta Ca_V1.2^{-/-}$ mice, the $Ca_V1.2$/granule complex is disrupted, leading to selective suppression of fast exocytosis.

A significant fraction (~50%) of the whole-cell Ca^{2+} current is resistant to nifedipine (Gilon, Yakel et al. 1997), indicating the presence of additional Ca^{2+} channel subtypes in the β-cell. The physiological roles of the non-L-type Ca^{2+} channels are unknown. A general $Ca_V2.3$-knockout ($Ca_V2.3^{-/-}$) mouse exhibits a slight glucose intolerance and reduced glucose induced insulin secretion (Pereverzev, Mikhna et al. 2002). $Ca_V2.3$ ablation is associated with a 23% decrease in β-cell Ca^{2+} current in $Ca_V2.3^{-/-}$ mice. This is in good agreement with the response to acute application of SNX482 in WT mice in which about one-quarter of the β-cell whole-cell Ca^{2+} current is sensitive to the R-type Ca^{2+} channel blocker SNX482. We demonstrate that pharmacological inhibition of R-type $Ca_V2.3$ Ca^{2+} channels using SNX482 does not affect first-phase insulin secretion, but reduces second-phase release a dramatic 80%. $Ca_V2.3^{-/-}$ mice exhibits a similar preferential suppression of late-phase insulin secretion. Previous evidence in neurons suggests that R-type channels are physically detached from the exocytotic machinery (Wu, Borst et al. 1998) and are not involved in rapid neurotransmission in mossy fibers (Dietrich, Kirschstein et al. 2003). It is possible that non-L-type Ca^{2+} channels fulfill functions in the β-cells other than initiation of exocytosis. For example, they may play a role in the refilling of the readily releasable pool (RRP) granules by mobilizing reserve pool (RP) granules. This would be consistent with the finding that whereas exocytosis elicited by the two first pulses during a train of ten 500 ms depolarizations is strongly inhibited in β-cells from $\beta Ca_V1.2^{-/-}$ mice and in control β-cells exposed to the L-type Ca^{2+} channel inhibitor isradipine, exocytosis during the latter part of the train is unaffected. Indeed, the R-type Ca^{2+} channel blocker SNX482 exerts its strongest effect on late exocytosis. The initial component

of exocytosis is not much affected in $Ca_V2.3^{-/-}$ β-cells. In fact, the overall reduction results exclusively from suppression of the late component of exocytosis. It appears that Ca^{2+} entry via L-type $Ca_V1.2$ and R-type $Ca_V2.3$ channels have distinct intracellular effects and may target different functional pools of insulin granules. Secretory granules in pancreatic β-cells exist in distinct functional pools and sequential release of these pools gives rise to kinetically separable components of exocytosis (Rorsman and Renstrom 2003). Granules belonging to RRP are release-competent and can undergo exocytosis without any further modification after stimulation. Release of such granules is believed to underlie a rapid component of release. The majority of granules belong to RP that must undergo a series of ATP-, Ca^{2+}-, time- and temperature-dependent reactions (collectively referred to as mobilization or priming) to gain release competence. Presumably, L-type Ca^{2+} channels trigger RRP granules exocytosis, but once the RRP is depleted, the supply of new granules from RP for release becomes rate limiting. It seems justifiable to conclude that Ca^{2+} entry via R-type $Ca_V2.3$ Ca^{2+} channels is functionally (and perhaps spatially) linked to granule mobilization and priming of insulin granules for release.

A transient peak in $Ca_V2.3$ channel expression in glial cells along specific CNS pathways has been demonstrated to coincide with postnatal myelinization of the white matter in the rat (Chen, Ren et al. 2000). It can be speculated that $Ca_V2.3$ channel expression exerts a similar action in defining the differentiated mature islet cell lineages. $Ca_V2.3$ ablation is associated with disturbances of glucagon secretion, possibly due to the appearance of atypical α/β-cells accounting for greater than 60% of the glucagon-expressing cells in these mice.

Supression of sulfonylurea- and glucose-induced insulin secretion in mice lacking the chloride transport protein ClC-3 (paper Ⅲ)

In paper Ⅰ and Ⅱ we demonstrated that Ca^{2+} influx through distinct Ca_V channels play different roles in biphasic insulin secretion. Previous functional experiments suggested that ClC-3 facilitates insulin secretion (Barg, Huang et al. 2001; Juhl, Hoy et al. 2003). In paper Ⅲ we investigated the role of ClC-3 chloride channel on insulin secretion using constitutive ClC-3 knock-out (KO) mice ($ClC3^{-/-}$ mice).

ClC-3 expression and localization in pancreatic islets

To investigate the expression of ClC-3 in islets, we performed immunohistochemistry on pancreatic islets using polyclonal antibodies against a mixture of two different peptides predicted from the ClC-3 sequence. It was shown that ClC-3 is strongly expressed in endocrine pancreas. Co-staining for insulin and glucagon showed that the protein is expressed in both α- and β-cells. The subcellular localisation of ClC-3 was investigated by immunocytochemistry. Subcellular fractionation analyses from primary β-cells and INS-1 cells revealed that ClC-3 was enriched in the fractions containing endosome and synaptic-like micro vesicles, but not in the fractions containing secretory granules. However, these data do not unequivocally demonstrate that ClC-3 is absent from the insulin granules. In fact granules isolated from INS-1 cells by GFP-labelling were enriched for insulin and did contain detectable levels of ClC-3 immunoreactivity.

ClC-3 ablation affects proton fluxes over the membrane

Effects of ClC-3 ablation on intragranular pH were investigated using the fluorescent probe LysoSensor Green DND-189. Addition of protonophore CCCP led to a prompt reduction of fluorescence in control cells as the intragranular pH increased and fluorescent probe moved out of the cell. The CCCP-induced fluorescence decrease at steady-state (90 s after addition of CCCP) was reduced from 41±9% in wildtype cells to 18±5% in $ClC3^{-/-}$ β-cells.

ClC-3 ablation does not affect intracellular Ca^{2+} homeostasis and insulin granule biogenesis

To investigate whether the lack of ClC-3 interferes with Ca^{2+} elevation, $[Ca^{2+}]_i$ was measured in islets isolated from WT and $ClC3^{-/-}$ mice using the fluorescent Ca^{2+}-indicator fura-2. Basal $[Ca^{2+}]_i$ levels were similar (88±6 nM and 106±15 nM in WT and $ClC3^{-/-}$ islets, respectively). Stimulation with 15 mM glucose, $[Ca^{2+}]_i$ rose to a peak value of 419±52 nM in WT and 452±29 nM in $ClC3^{-/-}$ islets. In both cases, this peak was followed by Ca^{2+} oscillations that are typical for β-cells. The addition of tolbutamide caused a comparable increase in $[Ca^{2+}]_i$ in both genotypes. These data indicate that the impaired secretory response of $ClC3^{-/-}$ islets cannot be attributed to abnormalities of intracellular Ca^{2+} handling, but is exclusively due to a later step in the intracellular signal cascade.

In addition, neither a change in the total number of secretory granules, nor in the number of docked vesicles was detected, in $ClC3^{-/-}$ β-cells. This fits well to the finding that there was no change in insulin content of ClC-3 deficient islets and supports the notion that there is no defect in granule biogenesis.

ClC-3 ablation affects insulin secretion at all levels

In vivo insulin secretion in response to elevation of glucose was impaired in constitutive $ClC3^{-/-}$ mice. Whereas control mice responded to the glucose load with an increase in their serum insulin secretion, no comparable rise in the insulin concentration was detected in $ClC3^{-/-}$ mice. Stimulation with glibenclamide also failed to enhance insulin secretion in ClC-3-deficient mice.

Since ClC-3 channels are expressed in many different tissues, it was of interest to see whether the reduced insulin secretion in $ClC3^{-/-}$ mice depends on systemic factors or reflects processes within the islets. To disrupt systemic effects, e.g. those exerted via neural inputs, insulin secretion from isolated islets was studied. Whereas increasing glucose from 1 to 20 mM stimulated insulin secretion of control islets on average by a factor of 10, secretion in islets from $ClC3^{-/-}$ mice was reduced by 67%. Insulin secretion in $ClC3^{-/-}$ islets stimulated by glibenclamide or high extracellular K^+ (50 mM) was largely abolished compared with control islets.

At the single cell level, the exocytotic response of the β-cell was studied using high-resolution capacitance measurements. Exocytosis was elicited by trains of ten 500-ms depolarizing pulses (from -70 mV to 0 mV) using the standard whole-cell configuration of the patch clamp technique. In control β-cells, exocytosis proceeded throughout the stimulus train. In $ClC3^{-/-}$ β-cells, the capacitance increases per pulse were drastically lower from the beginning (Figure 9),

and the total capacitance increase measured in ClC3$^{-/-}$ β-cells was significantly lower (-80%) than in control β-cells. The secretory response of ClC3$^{-/-}$ β-cells could be largely restored by infecting the cells with a recombinant Semliki Forest Virus (SFV) encoding ClC-3. Furthermore, exocytosis was also stimulated using an intracellular Ca^{2+} dialysis protocol. In this experiment, exocytotic rates reflect a sustained type of exocytosis in which mobilization of insulin granules to the plasma membrane (i.e. *priming*) becomes rate-limiting. Also in this experiment a clear reduction was observed in the ClC3$^{-/-}$ β-cells and exocytotic rates were suppressed by ~40%.

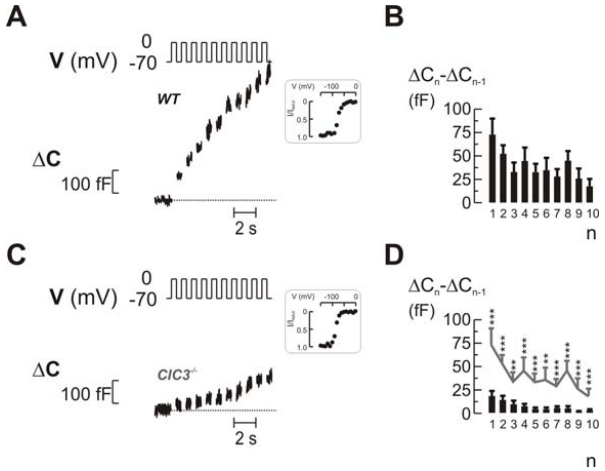

Figure 9: *(A) Increases in membrane capacitance (ΔC), evoked by a train of ten 500-ms voltage-clamp depolarisations from -70 mV to 0 mV (V) in a wildtype β-cell (identified by Na^+ current inactivation properties;inset). (B) Increases in membrane capacitance elicited by the individual pulses of the train stimulus (ΔC_n-ΔC_{n-1}). (C-D) Same as in (A-B) but using cells from ClC-3$^{-/-}$ mice.*

Interestingly, further support for a direct effect of ClC-3 on the β-cell was provided by RNA interference experiments in INS-1 cells. In these cells, down regulation of the ClC-3 protein reduced exocytosis by ~65%.

Discussion paper III

Secretory granules must undergo a priming reaction to gain release competence. In pancreatic β-cells, the pH of insulin granules is acidic. The low luminal pH of secretory granules is crucial for prohormone cleavage (Hutton 1989). In addition, the acidification of secretory vesicles may play a role in making them release-competent, an ATP-dependent process referred to as priming (Barg, Huang et al. 2001; Stiernet, Guiot et al. 2006). Acidification is carried out by a V-type H^+-ATPase that pumps H^+ into the vesicular lumen. Various members of the ClC family of Cl^- transport proteins facilitate the acidification of intracellular vesicles, most likely by limiting the generation of a transmembrane voltage by the H^+-ATPase. ClC-3 is present on endosomes and synaptic vesicles (Stobrawa, Breiderhoff et al. 2001; Salazar, Love et al. 2004), and acidification rates of both types of vesicles were reduced in ClC3$^{-/-}$ mice (Stobrawa, Breiderhoff et al. 2001; Yoshikawa, Uchida et al. 2002; Hara-Chikuma, Yang et al. 2005). In addition, ClC-3 has been reported to also reside on secretory granules of β-cells (Barg, Huang et al. 2001). Functional experiments based on the intracellular application of an antibody directed against ClC-3 suggested that ClC-3 facilitates insulin

secretion by enhancing the acidification of insulin-containing granules (Barg, Huang et al. 2001; Barg, Olofsson et al. 2002; Hoy, Olsen et al. 2003; Juhl, Hoy et al. 2003).

The strong expression of ClC-3 in pancreatic β-cells raised the interesting possibility that it might mediate the Cl^- conductance involved in the priming of the secretory granules. Indeed, the presence of ClC-3 in insulin granules was detected in a high-purification fraction of LDCVs obtained by phogrin-GFP labelling. Proton fluxes over the granule membrane were strongly reduced in $ClC3^{-/-}$ β-cells. Insulin secretion was severely affected in $ClC3^{-/-}$ mice. For instance, insulin secretion evoked by high extracellular K^+ was reduced by 56%. These findings are consistent with the concept that ClC-3-dependent processes have a strong impact on the size of the RRP. The present data support the scenario that granular Cl^--fluxes play an important role in the priming of secretory granules for release. The reduced capacity of $ClC3^{-/-}$ β-cells to replenish the releasable pool of granules is also evident from the Ca^{2+}-infusion experiments in which granule mobilization was suppressed by ~40%. Taken together, our data support the hypothesis that ClC-3 promotes granules mobilization by providing a shunt conductance that allows the granule interior to acidify; the latter leading to an increased release competence of granules by mechanisms that remain unestablished.

Interestingly, the $ClC3^{-/-}$ mice had normal basal plasma glucose (~10 mM) and insulin levels, though stimulated insulin secretion was strongly reduced both *in vitro* and *in vivo* in $ClC3^{-/-}$ mice. It argues that there must exist additional mechanisms for granule priming/acidification in the β-cell. These processes account for the normality of basal plasma insulin and glucose levels in the knockout animals.

Conclusions

In this thesis, we have investigated the effects of different ion channels on insulin secretion using a combination of gene knock-out mice, electrophysiology, Ca^{2+} microfluorimetry and hormone release measurements. The following conclusions were reached:

- (1)The L-type Ca^{2+} channel in mouse pancreatic β-cells is $Ca_V1.2$.
  (2)The disappearance of a rapid component of exocytosis in β$Ca_V1.2^{-/-}$ β-cells reflects the loss of a granule pool physically attached to the $Ca_V1.2$ channel.
  (3)The latter granule pool is required for first-phase insulin secretion and maintenance of systemic glucose tolerance.

- (1)R-type $Ca_V2.3$ channels do not associate with a pool of rapidly releasable insulin granules.
  (2) $Ca_V2.3$ Ca^{2+} channels mediate the Ca^{2+} entry needed for replenishment of the readily releasable pool of insulin granules.
  (3) $Ca_V2.3$ channel activity is primarily important during second-phase insulin secretion.

- (1)ClC-3 chloride channels are present intracellularly on the entire membrane system associated with regulated exocytosis, including the insulin granules.
  (2)ClC-3 channels affect proton (H^+) fluxes over the granule membrane.
  (3)ClC-3 channel activity is important for mobilization of insulin granules into the readily releasable pool of insulin granules.

Populärvetenskaplig sammanfattning

Insulin är kroppens enda blodsockersänkande hormon. Det frisätts till blodet från de pankreatiska betacellerna när man har ätit och halten av blodsocker (glukos) ökar. Glukosorsakad insulininsöndring i blodet sker i två faser: den första fasen är mycket intensiv, men varar bara 5-10 minuter innan insulininsöndringen till blodet sjunker. Under den andra fasen ökar insulinsekretionen sakta och kan sedan fortsätta i flera timmar, så länge blodsockervärdena förblir förhöjda.
Vi vet *att* insulinsekretionens bifasiska mönster är nödvändigt för att vi inte skall få typ 2-diabetes, men vi vet inte hur det uppkommer. I denna avhandling har jag undersökt hur olika s.k. *jonkanaler* påverkar bifasisk insulinsekretion. Jonkanaler är proteiner som normalt är stängda, men kan öppnas (aktiveras) när de utsätts för ett specifikt stimuli, t.ex. en ändrad elektrisk laddning.

Det finns flera olika typer av jonkanaler. Till exempel släpper vissa bara igenom kalciumjoner (Ca^{2+}). Kalciumjonkanalerna finns i cellens yta (plasmamembranet) och spelar en helt avgörande roll när en ökning av halten av glukos i blodet skall översättas till att starta insulinsekretion. De kalciumjoner (Ca^{2+}) som kommer in i betacellen leder till att insulin ansamlat i sekretkorn (insulingranula) tömmer sitt insulin i blodet.
Andra jonkanaler bara låter negativa kloridjoner (Cl^-) passera. Dessa typer av jonkanaler finns i membran inuti cellen.

I denna avhandling har jag undersökt båda dessa typer av jonkanaler och hur de påverar bifasisk insulinsekretion. Mina resultat visar att en typ av kalciumjonkanal, $Ca_V1.2$, utlöser första fasens insulinsekretion, medan en annan, $Ca_V2.3$, styr andra fasens insulinfrisättning. Detta resultat är mycket förvånande, eftersom båda kalciumjonkanalerna aktiveras när den pankreatiska betacellen blir mer positivt laddad. Förklaringen är att insulingranula i cellen binder till $Ca_V1.2$, men inte $Ca_V2.3$. Eftersom aktivering av kalciumjonkanaler är den händelse som utlöser glukosorsakad insulinsekretion, betyder det att $Ca_V1.2$ kommer att utlösa den snabba första fasens insulinfrisättning, medan $Ca_V2.3$ blir viktigare i ett senare skede och svarar för att utlösa den andra fasen.

I den sista delen av avhandlingen visar jag att kloridjonkanalen ClC3 finns på flera typer av membran inuti cellen, inklusive insulingranula. Den hjälper till att göra insulingranula kemiskt sura (lågt pH), vilket i sin tur leder till att de alls kan frisättas. ClC3 är alltså viktig för att vi överhuvudtaget skall kunna frisätta insulin.

Mina studier har givit ett viktigt bidrag till förståelsen av processer som diabetesforskare har tampats med under årtionden. Min förhoppning är att de skall kunna kopplas samman med den utveckling vi just nu observerar på diabetesgenetikens område och leda till nya behandlingsformer som förhindrar utvecklingen av typ 2-diabetes.

Acknowledgements

The work presented in this thesis would never have been possible without help and support from a lot of people. I am greatly indebted to you for your help.

I wish to thank:

Erik Renström, my supervisor, for inviting me to Lund and introducing me to the field of insulin secretion, for his scientific guidance, patience and encouragements, for his generosity and kindness, for fruitful discussion throughout my Ph D studies. Without his never-failing support, this study would never have been completed.

Lena Stenson Holst, my co-supervisor, for encouragement and positive attitude, for sharing her ideas and wisdom with me in Yeast-two Hybrid project.

Patrik Rorsman, for welcoming me to this laboratory.

The **colleagues** in the Endocrinology Division at the Department of Clinical Sciences, Malmö, Lena Eliasson, for general advice, for inviting me to her beautiful house to taste Swedish food; Albert Salehi, for insulin release measurements; Kristina Borglid, for invaluable technical assistance and for helping me with buying a bicycle when I was a newcomer; Britt-Marie Nilsson, for expert technical help with cell culture; Rosita Ivarsson, for nice and fruitful collaborations; Daiqing Li, for teaching me Western Blot and for many interesting discussions about almost everything; Anders Rosengren, for enthusiasm and for fun during conferences; all other former and present colleagues, for creating a nice and friendly atmosphere.

The **co-authors** in my articles, for scientific collaboration.

Chinese friends, no one mentioned, no one forgotten, for our friendship and happy time spent over the years.

My family, **Shujing Wang** and **Lihang Jing,** because you are the best! You are the most important in my life!

References

Aizawa, T., M. Komatsu, et al. (1998). "Glucose action 'beyond ionic events' in the pancreatic beta cell." Trends Pharmacol Sci **19**(12): 496-9.

Ammala, C., F. M. Ashcroft, et al. (1993). "Calcium-independent potentiation of insulin release by cyclic AMP in single beta-cells." Nature **363**(6427): 356-8.

Ammon, H. P. and J. Steinke (1972). "6-Amnionicotinamide (6-AN) as a diabetogenic agent. In vitro and in vivo studies in the rat." Diabetes **21**(3): 143-8.

Andrews, R. C. and B. R. Walker (1999). "Glucocorticoids and insulin resistance: old hormones, new targets." Clin Sci (Lond) **96**(5): 513-23.

Arai, H., S. Pink, et al. (1989). "Interaction of anions and ATP with the coated vesicle proton pump." Biochemistry **28**(7): 3075-82.

Ashcroft, F. M. and F. M. Gribble (1998). "Correlating structure and function in ATP-sensitive K+ channels." Trends Neurosci **21**(7): 288-94.

Ashcroft, F. M. and P. Rorsman (1989). "Electrophysiology of the pancreatic beta-cell." Prog Biophys Mol Biol **54**(2): 87-143.

Ashcroft, S. J. and M. R. Christie (1979). "Effects of glucose on the cytosolic ration of reduced/oxidized nicotinamide-adenine dinucleotide phosphate in rat islets of Langerhans." Biochem J **184**(3): 697-700.

Atkinson, M. A. and N. K. Maclaren (1993). "Islet cell autoantigens in insulin-dependent diabetes." J Clin Invest **92**(4): 1608-16.

Atkinson, M. A. and N. K. Maclaren (1994). "The pathogenesis of insulin-dependent diabetes mellitus." N Engl J Med **331**(21): 1428-36.

Baekkeskov, S., H. J. Aanstoot, et al. (1990). "Identification of the 64K autoantigen in insulin-dependent diabetes as the GABA-synthesizing enzyme glutamic acid decarboxylase." Nature **347**(6289): 151-6.

Barasch, J., M. D. Gershon, et al. (1988). "Thyrotropin induces the acidification of the secretory granules of parafollicular cells by increasing the chloride conductance of the granular membrane." J Cell Biol **107**(6 Pt 1): 2137-47.

Barg, S., L. Eliasson, et al. (2002). "A subset of 50 secretory granules in close contact with L-type Ca2+ channels accounts for first-phase insulin secretion in mouse beta-cells." Diabetes **51 Suppl 1**: S74-82.

Barg, S., P. Huang, et al. (2001). "Priming of insulin granules for exocytosis by granular Cl(-) uptake and acidification." J Cell Sci **114**(Pt 11): 2145-54.

Barg, S., C. S. Olofsson, et al. (2002). "Delay between fusion pore opening and peptide release from large dense-core vesicles in neuroendocrine cells." Neuron **33**(2): 287-99.

Barthel, A., D. Schmoll, et al. (2001). "Differential regulation of endogenous glucose-6-phosphatase and phosphoenolpyruvate carboxykinase gene expression by the forkhead transcription factor FKHR in H4IIE-hepatoma cells." Biochem Biophys Res Commun **285**(4): 897-902.

Bean, B. P. (1989). "Classes of calcium channels in vertebrate cells." Annu Rev Physiol **51**: 367-84.

Betz, H. (1990). "Ligand-gated ion channels in the brain: the amino acid receptor superfamily." Neuron **5**(4): 383-92.

Bhattacharjee, A., R. M. Whitehurst, Jr., et al. (1997). "T-type calcium channels facilitate insulin secretion by enhancing general excitability in the insulin-secreting beta-cell line, INS-1." Endocrinology **138**(9): 3735-40.

Bittner, M. A. and R. W. Holz (1992). "A temperature-sensitive step in exocytosis." J Biol Chem **267**(23): 16226-9.

Blackmore, C. G., A. Varro, et al. (2001). "Measurement of secretory vesicle pH reveals intravesicular alkalinization by vesicular monoamine transporter type 2 resulting in inhibition of prohormone cleavage." J Physiol **531**(Pt 3): 605-17.

Bokvist, K., L. Eliasson, et al. (1995). "Co-localization of L-type Ca2+ channels and insulin-containing secretory granules and its significance for the initiation of exocytosis in mouse pancreatic B-cells." Embo J **14**(1): 50-7.

Bonifacio, E., V. Lampasona, et al. (1995). "Identification of protein tyrosine phosphatase-like IA2 (islet cell antigen 512) as the insulin-dependent diabetes-related 37/40K autoantigen and a target of islet-cell antibodies." J Immunol **155**(11): 5419-26.

Bratanova-Tochkova, T. K., H. Cheng, et al. (2002). "Triggering and augmentation mechanisms, granule pools, and biphasic insulin secretion." Diabetes **51 Suppl 1**: S83-90.

Brisseau, G. F., S. Grinstein, et al. (1996). "Interleukin-1 increases vacuolar-type H+-ATPase activity in murine peritoneal macrophages." J Biol Chem **271**(4): 2005-11.

Brown, D. and S. Breton (2000). "H(+)V-ATPase-dependent luminal acidification in the kidney collecting duct and the epididymis/vas deferens: vesicle recycling and transcytotic pathways." J Exp Biol **203**(Pt 1): 137-45.

Brun, T., E. Roche, et al. (1996). "Evidence for an anaplerotic/malonyl-CoA pathway in pancreatic beta-cell nutrient signaling." Diabetes **45**(2): 190-8.

Bruns, D. and R. Jahn (2002). "Molecular determinants of exocytosis." Pflugers Arch **443**(3): 333-8.

Cain, C. C., D. M. Sipe, et al. (1989). "Regulation of endocytic pH by the Na+,K+-ATPase in living cells." Proc Natl Acad Sci U S A **86**(2): 544-8.

Catterall, W. A. (1999). "Interactions of presynaptic Ca2+ channels and snare proteins in neurotransmitter release." Ann N Y Acad Sci **868**: 144-59.

Catterall, W. A. (2000). "Structure and regulation of voltage-gated Ca2+ channels." Annu Rev Cell Dev Biol **16**: 521-55.

Catterall, W. A., J. Striessnig, et al. (2003). "International Union of Pharmacology. XL. Compendium of voltage-gated ion channels: calcium channels." Pharmacol Rev **55**(4): 579-81.

Cavaghan, M. K., D. A. Ehrmann, et al. (2000). "Interactions between insulin resistance and insulin secretion in the development of glucose intolerance." J Clin Invest **106**(3): 329-33.

Chen, S., A. Ogawa, et al. (1994). "More direct evidence for a malonyl-CoA-carnitine palmitoyltransferase I interaction as a key event in pancreatic beta-cell signaling." Diabetes **43**(7): 878-83.

Chen, S., Y. Q. Ren, et al. (2000). "Alpha 1E subunit of the R-type calcium channel is associated with myelinogenesis." J Neurocytol **29**(10): 719-28.

Corkey, B. E., M. C. Glennon, et al. (1989). "A role for malonyl-CoA in glucose-stimulated insulin secretion from clonal pancreatic beta-cells." J Biol Chem **264**(36): 21608-12.

Curry, D. L., L. L. Bennett, et al. (1968). "Dynamics of insulin secretion by the perfused rat pancreas." Endocrinology **83**(3): 572-84.

Daniel, S., M. Noda, et al. (1999). "Identification of the docked granule pool responsible for the first phase of glucose-stimulated insulin secretion." Diabetes **48**(9): 1686-90.

Davalli, A. M., E. Biancardi, et al. (1996). "Dihydropyridine-sensitive and -insensitive voltage-operated calcium channels participate in the control of glucose-induced insulin release from human pancreatic beta cells." J Endocrinol **150**(2): 195-203.

Dean, P. M. (1973). "Ultrastructural morphometry of the pancreatic -cell." Diabetologia **9**(2): 115-9.

Dean, P. M. and E. K. Matthews (1968). "Electrical activity in pancreatic islet cells." Nature **219**(5152): 389-90.
Del Prato, S. (2003). "Loss of early insulin secretion leads to postprandial hyperglycaemia." Diabetologia **46 Suppl 1**: M2-8.
Detimary, P., S. Dejonghe, et al. (1998). "The changes in adenine nucleotides measured in glucose-stimulated rodent islets occur in beta cells but not in alpha cells and are also observed in human islets." J Biol Chem **273**(51): 33905-8.
Detimary, P., G. Van den Berghe, et al. (1996). "Concentration dependence and time course of the effects of glucose on adenine and guanine nucleotides in mouse pancreatic islets." J Biol Chem **271**(34): 20559-65.
Devuyst, O. (2004). "Chloride channels and endocytosis: new insights from Dent's disease and CLC-5 knockout mice." Bull Mem Acad R Med Belg **159**(Pt 2): 212-7.
Dietrich, D., T. Kirschstein, et al. (2003). "Functional specialization of presynaptic Cav2.3 Ca2+ channels." Neuron **39**(3): 483-96.
Dirksen, R. T., J. Nakai, et al. (1997). "The S5-S6 linker of repeat I is a critical determinant of L-type Ca2+ channel conductance." Biophys J **73**(3): 1402-9.
Dutzler, R., E. B. Campbell, et al. (2002). "X-ray structure of a ClC chloride channel at 3.0 A reveals the molecular basis of anion selectivity." Nature **415**(6869): 287-94.
Eberhart, M., O. C., et al. (2004). "Prevalence of Overweight and Obesity Among Adults with Diagnosed Diabetes --- United States, 1988--1994 and 1999--2002." Morbidity and Mortality Weekly Report 53 (45): 1066-1068. : 1066-1068. .
Eliasson, L., E. Renstrom, et al. (1997). "Rapid ATP-dependent priming of secretory granules precedes Ca(2+)-induced exocytosis in mouse pancreatic B-cells." J Physiol **503 (Pt 2)**: 399-412.
Ellinor, P. T., J. F. Zhang, et al. (1993). "Functional expression of a rapidly inactivating neuronal calcium channel." Nature **363**(6428): 455-8.
Ertel, E. A., K. P. Campbell, et al. (2000). "Nomenclature of voltage-gated calcium channels." Neuron **25**(3): 533-5.
Fasshauer, M. and R. Paschke (2003). "Regulation of adipocytokines and insulin resistance." Diabetologia **46**(12): 1594-603.
Flink, M. T. and W. D. Atchison (2003). "Ca2+ channels as targets of neurological disease: Lambert-Eaton Syndrome and other Ca2+ channelopathies." J Bioenerg Biomembr **35**(6): 697-718.
Fuchs, R., S. Schmid, et al. (1989). "A possible role for Na+,K+-ATPase in regulating ATP-dependent endosome acidification." Proc Natl Acad Sci U S A **86**(2): 539-43.
Futai, M., T. Oka, et al. (1998). "Diverse roles of single membrane organelles: factors establishing the acid lumenal pH." J Biochem (Tokyo) **124**(2): 259-67.
Gembal, M., P. Detimary, et al. (1993). "Mechanisms by which glucose can control insulin release independently from its action on adenosine triphosphate-sensitive K+ channels in mouse B cells." J Clin Invest **91**(3): 871-80.
Gembal, M., P. Gilon, et al. (1992). "Evidence that glucose can control insulin release independently from its action on ATP-sensitive K+ channels in mouse B cells." J Clin Invest **89**(4): 1288-95.
Gentet, L. J., G. J. Stuart, et al. (2000). "Direct measurement of specific membrane capacitance in neurons." Biophys J **79**(1): 314-20.
Gilon, P., J. Yakel, et al. (1997). "G protein-dependent inhibition of L-type Ca2+ currents by acetylcholine in mouse pancreatic B-cells." J Physiol **499 (Pt 1)**: 65-76.
Glickman, J., K. Croen, et al. (1983). "Golgi membranes contain an electrogenic H+ pump in parallel to a chloride conductance." J Cell Biol **97**(4): 1303-8.

Grabe, M. and G. Oster (2001). "Regulation of organelle acidity." J Gen Physiol **117**(4): 329-44.
Graham, J. and D. Rickwood (1997). Subcellular fractionation—a practical approach., Oxford University Press, Oxford.
Grynkiewicz, G., M. Poenie, et al. (1985). "A new generation of Ca2+ indicators with greatly improved fluorescence properties." J Biol Chem **260**(6): 3440-50.
Hamill, O. P., A. Marty, et al. (1981). "Improved patch-clamp techniques for high-resolution current recording from cells and cell-free membrane patches." Pflugers Arch **391**(2): 85-100.
Hamilton, D. L. and K. Abremski (1984). "Site-specific recombination by the bacteriophage P1 lox-Cre system. Cre-mediated synapsis of two lox sites." J Mol Biol **178**(2): 481-6.
Hara-Chikuma, M., B. Yang, et al. (2005). "ClC-3 chloride channels facilitate endosomal acidification and chloride accumulation." J Biol Chem **280**(2): 1241-7.
Henquin, J. C. (2000). "Triggering and amplifying pathways of regulation of insulin secretion by glucose." Diabetes **49**(11): 1751-60.
Hockerman, G. H., B. Z. Peterson, et al. (1997). "Molecular determinants of drug binding and action on L-type calcium channels." Annu Rev Pharmacol Toxicol **37**: 361-96.
Hofmann, F., M. Biel, et al. (1994). "Molecular basis for Ca2+ channel diversity." Annu Rev Neurosci **17**: 399-418.
Horn, R. and A. Marty (1988). "Muscarinic activation of ionic currents measured by a new whole-cell recording method." J Gen Physiol **92**(2): 145-59.
Hoy, M., H. L. Olsen, et al. (2003). "The imidazoline NNC77-0020 affects glucose-dependent insulin, glucagon and somatostatin secretion in mouse pancreatic islets." Naunyn Schmiedebergs Arch Pharmacol **368**(4): 284-93.
Hutton, J. C. (1989). "The insulin secretory granule." Diabetologia **32**(5): 271-81.
Inagaki, N., T. Gonoi, et al. (1995). "Reconstitution of IKATP: an inward rectifier subunit plus the sulfonylurea receptor." Science **270**(5239): 1166-70.
Ivarsson, R., X. Jing, et al. (2005). "Myosin 5a controls insulin granule recruitment during late-phase secretion." Traffic **6**(11): 1027-35.
Ivarsson, R., R. Quintens, et al. (2005). "Redox control of exocytosis: regulatory role of NADPH, thioredoxin, and glutaredoxin." Diabetes **54**(7): 2132-42.
Jentsch, T. J., V. Stein, et al. (2002). "Molecular structure and physiological function of chloride channels." Physiol Rev **82**(2): 503-68.
Jones, P. M., J. Stutchfield, et al. (1985). "Effects of Ca2+ and a phorbol ester on insulin secretion from islets of Langerhans permeabilised by high-voltage discharge." FEBS Lett **191**(1): 102-6.
Juhl, K., M. Hoy, et al. (2003). "cPLA2alpha-evoked formation of arachidonic acid and lysophospholipids is required for exocytosis in mouse pancreatic beta-cells." Am J Physiol Endocrinol Metab **285**(1): E73-81.
Kim, J. H., L. Johannes, et al. (1998). "Noninvasive measurement of the pH of the endoplasmic reticulum at rest and during calcium release." Proc Natl Acad Sci U S A **95**(6): 2997-3002.
Kruger., D. F., C. L. Martin, et al. (2006). "New insights into glucose regulation." The Diabetes Educator **32**: 221-228.
Lang, J. (1999). "Molecular mechanisms and regulation of insulin exocytosis as a paradigm of endocrine secretion." Eur J Biochem **259**(1-2): 3-17.
Langin, D. (2001). "Diabetes, insulin secretion, and the pancreatic beta-cell mitochondrion." N Engl J Med **345**(24): 1772-4.
Li, X., T. Wang, et al. (2002). "The ClC-3 chloride channel promotes acidification of lysosomes in CHO-K1 and Huh-7 cells." Am J Physiol Cell Physiol **282**(6): C1483-91.

Li, Y. P., W. Chen, et al. (1999). "Atp6i-deficient mice exhibit severe osteopetrosis due to loss of osteoclast-mediated extracellular acidification." Nat Genet **23**(4): 447-51.
Ligon, B., A. E. Boyd, 3rd, et al. (1998). "Class A calcium channel variants in pancreatic islets and their role in insulin secretion." J Biol Chem **273**(22): 13905-11.
Lin, R. C. and R. H. Scheller (2000). "Mechanisms of synaptic vesicle exocytosis." Annu Rev Cell Dev Biol **16**: 19-49.
Liu, G., N. Hilliard, et al. (2004). "Cav1.3 is preferentially coupled to glucose-induced [Ca2+]i oscillations in the pancreatic beta cell line INS-1." Mol Pharmacol **65**(5): 1269-77.
Lizcano, J. M. and D. R. Alessi (2002). "The insulin signalling pathway." Curr Biol **12**(7): R236-8.
Llinas, R., M. Sugimori, et al. (1992). "Distribution and functional significance of the P-type, voltage-dependent Ca2+ channels in the mammalian central nervous system." Trends Neurosci **15**(9): 351-5.
Maechler, P. and C. B. Wollheim (1999). "Mitochondrial glutamate acts as a messenger in glucose-induced insulin exocytosis." Nature **402**(6762): 685-9.
Maechler, P. and C. B. Wollheim (2000). "Mitochondrial signals in glucose-stimulated insulin secretion in the beta cell." J Physiol **529 Pt 1**: 49-56.
McGarry, J. D., G. P. Mannaerts, et al. (1977). "A possible role for malonyl-CoA in the regulation of hepatic fatty acid oxidation and ketogenesis." J Clin Invest **60**(1): 265-70.
Meglasson, M. D. and F. M. Matschinsky (1986). "Pancreatic islet glucose metabolism and regulation of insulin secretion." Diabetes Metab Rev **2**(3-4): 163-214.
Mellman, I., R. Fuchs, et al. (1986). "Acidification of the endocytic and exocytic pathways." Annu Rev Biochem **55**: 663-700.
Miesenbock, G., D. A. De Angelis, et al. (1998). "Visualizing secretion and synaptic transmission with pH-sensitive green fluorescent proteins." Nature **394**(6689): 192-5.
Miljanich, G. P. and J. Ramachandran (1995). "Antagonists of neuronal calcium channels: structure, function, and therapeutic implications." Annu Rev Pharmacol Toxicol **35**: 707-34.
Neher, E. (1998). "Vesicle pools and Ca2+ microdomains: new tools for understanding their roles in neurotransmitter release." Neuron **20**(3): 389-99.
Neher, E., B. Sakmann, et al. (1978). "The extracellular patch clamp: a method for resolving currents through individual open channels in biological membranes." Pflugers Arch **375**(2): 219-28.
Newcomb, R., B. Szoke, et al. (1998). "Selective peptide antagonist of the class E calcium channel from the venom of the tarantula Hysterocrates gigas." Biochemistry **37**(44): 15353-62.
Nishi, T. and M. Forgac (2002). "The vacuolar (H+)-ATPases--nature's most versatile proton pumps." Nat Rev Mol Cell Biol **3**(2): 94-103.
Nowycky, M. C., A. P. Fox, et al. (1985). "Three types of neuronal calcium channel with different calcium agonist sensitivity." Nature **316**(6027): 440-3.
Ohkuma, S. and B. Poole (1978). "Fluorescence probe measurement of the intralysosomal pH in living cells and the perturbation of pH by various agents." Proc Natl Acad Sci U S A **75**(7): 3327-31.
Olofsson, C. S., S. O. Gopel, et al. (2002). "Fast insulin secretion reflects exocytosis of docked granules in mouse pancreatic B-cells." Pflugers Arch **444**(1-2): 43-51.
Palmer, J. P., C. M. Asplin, et al. (1983). "Insulin antibodies in insulin-dependent diabetics before insulin treatment." Science **222**(4630): 1337-9.
Parsons, T. D., J. R. Coorssen, et al. (1995). "Docked granules, the exocytic burst, and the need for ATP hydrolysis in endocrine cells." Neuron **15**(5): 1085-96.

Pereverzev, A., M. Mikhna, et al. (2002). "Disturbances in glucose-tolerance, insulin-release, and stress-induced hyperglycemia upon disruption of the Ca(v)2.3 (alpha 1E) subunit of voltage-gated Ca(2+) channels." Mol Endocrinol **16**(4): 884-95.

Pereverzev, A., R. Vajna, et al. (2002). "Reduction of insulin secretion in the insulinoma cell line INS-1 by overexpression of a Ca(v)2.3 (alpha1E) calcium channel antisense cassette." Eur J Endocrinol **146**(6): 881-9.

Prentki, M. and F. M. Matschinsky (1987). "Ca2+, cAMP, and phospholipid-derived messengers in coupling mechanisms of insulin secretion." Physiol Rev **67**(4): 1185-248.

Prentki, M., S. Vischer, et al. (1992). "Malonyl-CoA and long chain acyl-CoA esters as metabolic coupling factors in nutrient-induced insulin secretion." J Biol Chem **267**(9): 5802-10.

Proks, P., L. Eliasson, et al. (1996). "Ca(2+)- and GTP-dependent exocytosis in mouse pancreatic beta-cells involves both common and distinct steps." J Physiol **496 (Pt 1)**: 255-64.

Quinton, P. M. (1990). "Cystic fibrosis: a disease in electrolyte transport." Faseb J **4**(10): 2709-17.

Randall, A. and R. W. Tsien (1995). "Pharmacological dissection of multiple types of Ca2+ channel currents in rat cerebellar granule neurons." J Neurosci **15**(4): 2995-3012.

Renstrom, E., L. Eliasson, et al. (1996). "Cooling inhibits exocytosis in single mouse pancreatic B-cells by suppression of granule mobilization." J Physiol **494 (Pt 1)**: 41-52.

Renstrom, E., L. Eliasson, et al. (1997). "Protein kinase A-dependent and -independent stimulation of exocytosis by cAMP in mouse pancreatic B-cells." J Physiol **502 (Pt 1)**: 105-18.

Reuter, H. (1967). "The dependence of slow inward current in Purkinje fibres on the extracellular calcium-concentration." J Physiol **192**(2): 479-92.

Reuter, H. (1983). "Calcium channel modulation by neurotransmitters, enzymes and drugs." Nature **301**(5901): 569-74.

Riordan, J. R., J. M. Rommens, et al. (1989). "Identification of the cystic fibrosis gene: cloning and characterization of complementary DNA." Science **245**(4922): 1066-73.

Rizzuto, R. and T. Pozzan (2003). "When calcium goes wrong: genetic alterations of a ubiquitous signaling route." Nat Genet **34**(2): 135-41.

Rorsman, P., L. Eliasson, et al. (2000). "The Cell Physiology of Biphasic Insulin Secretion." News Physiol Sci **15**: 72-77.

Rorsman, P. and E. Renstrom (2003). "Insulin granule dynamics in pancreatic beta cells." Diabetologia **46**(8): 1029-45.

Rother, K. I. (2007). "Diabetes treatment--bridging the divide." N Engl J Med **356**(15): 1499-501.

Rubi, B., H. Ishihara, et al. (2001). "GAD65-mediated glutamate decarboxylation reduces glucose-stimulated insulin secretion in pancreatic beta cells." J Biol Chem **276**(39): 36391-6.

Salazar, G., R. Love, et al. (2004). "AP-3-dependent mechanisms control the targeting of a chloride channel (ClC-3) in neuronal and non-neuronal cells." J Biol Chem **279**(24): 25430-9.

Saltiel, A. R. and C. R. Kahn (2001). "Insulin signalling and the regulation of glucose and lipid metabolism." Nature **414**(6865): 799-806.

Satin, L. S. and D. L. Cook (1985). "Voltage-gated Ca2+ current in pancreatic B-cells." Pflugers Arch **404**(4): 385-7.

Sato, Y., T. Aizawa, et al. (1992). "Dual functional role of membrane depolarization/Ca2+ influx in rat pancreatic B-cell." Diabetes **41**(4): 438-43.
Sato, Y. and J. C. Henquin (1998). "The K+-ATP channel-independent pathway of regulation of insulin secretion by glucose: in search of the underlying mechanism." Diabetes **47**(11): 1713-21.
Schapiro, F. B. and S. Grinstein (2000). "Determinants of the pH of the Golgi complex." J Biol Chem **275**(28): 21025-32.
Schmoll, D., K. S. Walker, et al. (2000). "Regulation of glucose-6-phosphatase gene expression by protein kinase Balpha and the forkhead transcription factor FKHR. Evidence for insulin response unit-dependent and -independent effects of insulin on promoter activity." J Biol Chem **275**(46): 36324-33.
Schuit, F. C., P. Huypens, et al. (2001). "Glucose sensing in pancreatic beta-cells: a model for the study of other glucose-regulated cells in gut, pancreas, and hypothalamus." Diabetes **50**(1): 1-11.
Seino, S., T. Iwanaga, et al. (2000). "Diverse roles of K(ATP) channels learned from Kir6.2 genetically engineered mice." Diabetes **49**(3): 311-8.
Seksek, O., J. Biwersi, et al. (1995). "Direct measurement of trans-Golgi pH in living cells and regulation by second messengers." J Biol Chem **270**(10): 4967-70.
Sher, E., F. Giovannini, et al. (2003). "Voltage-operated calcium channel heterogeneity in pancreatic beta cells: physiopathological implications." J Bioenerg Biomembr **35**(6): 687-96.
Sipe, D. M. and R. F. Murphy (1987). "High-resolution kinetics of transferrin acidification in BALB/c 3T3 cells: exposure to pH 6 followed by temperature-sensitive alkalinization during recycling." Proc Natl Acad Sci U S A **84**(20): 7119-23.
Stevens, T. H. and M. Forgac (1997). "Structure, function and regulation of the vacuolar (H+)-ATPase." Annu Rev Cell Dev Biol **13**: 779-808.
Stiernet, P., Y. Guiot, et al. (2006). "Glucose acutely decreases pH of secretory granules in mouse pancreatic islets. Mechanisms and influence on insulin secretion." J Biol Chem **281**(31): 22142-51.
Stobrawa, S. M., T. Breiderhoff, et al. (2001). "Disruption of ClC-3, a chloride channel expressed on synaptic vesicles, leads to a loss of the hippocampus." Neuron **29**(1): 185-96.
Straub, S. G. and G. W. Sharp (2002). "Glucose-stimulated signaling pathways in biphasic insulin secretion." Diabetes Metab Res Rev **18**(6): 451-63.
Sutton, R. B., D. Fasshauer, et al. (1998). "Crystal structure of a SNARE complex involved in synaptic exocytosis at 2.4 A resolution." Nature **395**(6700): 347-53.
Sweet, I. R. and M. Gilbert (2006). "Contribution of calcium influx in mediating glucose-stimulated oxygen consumption in pancreatic islets." Diabetes **55**(12): 3509-19.
Tabcharani, J. A., W. Low, et al. (1990). "Low-conductance chloride channel activated by cAMP in the epithelial cell line T84." FEBS Lett **270**(1-2): 157-64.
Taguchi, N., T. Aizawa, et al. (1995). "Mechanism of glucose-induced biphasic insulin release: physiological role of adenosine triphosphate-sensitive K+ channel-independent glucose action." Endocrinology **136**(9): 3942-8.
Takahashi, M., M. J. Seagar, et al. (1987). "Subunit structure of dihydropyridine-sensitive calcium channels from skeletal muscle." Proc Natl Acad Sci U S A **84**(15): 5478-82.
Trout, K. K., C. Homko, et al. (2007). "Methods of measuring insulin sensitivity." Biol Res Nurs **8**(4): 305-18.
Tsien, R. W., D. Lipscombe, et al. (1988). "Multiple types of neuronal calcium channels and their selective modulation." Trends Neurosci **11**(10): 431-8.

Tycko, B., C. H. Keith, et al. (1983). "Rapid acidification of endocytic vesicles containing asialoglycoprotein in cells of a human hepatoma line." J Cell Biol **97**(6): 1762-76.
Tycko, B. and F. R. Maxfield (1982). "Rapid acidification of endocytic vesicles containing alpha 2-macroglobulin." Cell **28**(3): 643-51.
Urbe, S., A. S. Dittie, et al. (1997). "pH-dependent processing of secretogranin II by the endopeptidase PC2 in isolated immature secretory granules." Biochem J **321 (Pt 1)**: 65-74.
Vajna, R., U. Klockner, et al. (2001). "Functional coupling between 'R-type' Ca2+ channels and insulin secretion in the insulinoma cell line INS-1." Eur J Biochem **268**(4): 1066-75.
van Renswoude, J., K. R. Bridges, et al. (1982). "Receptor-mediated endocytosis of transferrin and the uptake of fe in K562 cells: identification of a nonlysosomal acidic compartment." Proc Natl Acad Sci U S A **79**(20): 6186-90.
Watkins, D. T. and M. Moore (1977). "Uptake of NADPH by islet secretion granule membranes." Endocrinology **100**(5): 1461-7.
Waxman, S. G. (2001). "Transcriptional channelopathies: an emerging class of disorders." Nat Rev Neurosci **2**(9): 652-9.
WHO (2006). "Definition and diagnosis of diabetes mellitus and intermediate hyperglycemia." World Health Organization: Geneva.
Wiser, O., M. Trus, et al. (1999). "The voltage sensitive Lc-type Ca2+ channel is functionally coupled to the exocytotic machinery." Proc Natl Acad Sci U S A **96**(1): 248-53.
Voets, T., E. Neher, et al. (1999). "Mechanisms underlying phasic and sustained secretion in chromaffin cells from mouse adrenal slices." Neuron **23**(3): 607-15.
Wollheim, C. B. and G. W. Sharp (1981). "Regulation of insulin release by calcium." Physiol Rev **61**(4): 914-73.
Wu, L. G., J. G. Borst, et al. (1998). "R-type Ca2+ currents evoke transmitter release at a rat central synapse." Proc Natl Acad Sci U S A **95**(8): 4720-5.
Wu, M. M., M. Grabe, et al. (2001). "Mechanisms of pH regulation in the regulated secretory pathway." J Biol Chem **276**(35): 33027-35.
Xie, X. S., D. K. Stone, et al. (1983). "Determinants of clathrin-coated vesicle acidification." J Biol Chem **258**(24): 14834-8.
Yamashiro, D. J. and F. R. Maxfield (1987). "Acidification of morphologically distinct endosomes in mutant and wild-type Chinese hamster ovary cells." J Cell Biol **105**(6 Pt 1): 2723-33.
Yang, S. N. and P. O. Berggren (2006). "The role of voltage-gated calcium channels in pancreatic beta-cell physiology and pathophysiology." Endocr Rev **27**(6): 621-76.
Yang, S. N., O. Larsson, et al. (1999). "Syntaxin 1 interacts with the L(D) subtype of voltage-gated Ca(2+) channels in pancreatic beta cells." Proc Natl Acad Sci U S A **96**(18): 10164-9.
Yoshikawa, M., S. Uchida, et al. (2002). "CLC-3 deficiency leads to phenotypes similar to human neuronal ceroid lipofuscinosis." Genes Cells **7**(6): 597-605.
Zhang, J. F., A. D. Randall, et al. (1993). "Distinctive pharmacology and kinetics of cloned neuronal Ca2+ channels and their possible counterparts in mammalian CNS neurons." Neuropharmacology **32**(11): 1075-88.
Zhao, Y. F. and C. Chen (2007). "Regulation of pancreatic beta-cell function by adipocytes." Sheng Li Xue Bao **59**(3): 247-52.

I

The EMBO Journal Vol. 22 No. 15 pp. 3844–3854, 2003

Impaired insulin secretion and glucose tolerance in β cell-selective $Ca_V1.2$ Ca^{2+} channel null mice

Verena Schulla[1], Erik Renström[2,3], Robert Feil[1], Susanne Feil[1], Isobel Franklin[4], Asllan Gjinovci[4], Xing-Jun Jing[2], Dirk Laux[1], Ingmar Lundquist[2], Mark A.Magnuson[5], Stefanie Obermüller[2], Charlotta S.Olofsson[2], Albert Salehi[2], Anna Wendt[2], Norbert Klugbauer[1], Claes B.Wollheim[4], Patrik Rorsman[2] and Franz Hofmann[1]

[1]Institut für Pharmakologie und Toxikologie, TU München, Biedersteiner Strasse 29, D-80802 München, Germany, [2]Department of Physiological Sciences, Lund University, BMC F11, SE-221 84 Lund, Sweden, [4]Division of Clinical Biochemistry, University Medical Center, 1 rue Michel-Servet, CH-1211 Geneva 4, Switzerland and [5]Department of Molecular Physiology and Biophysics, Vanderbilt University School of Medicine, Nashville, TN 37232, USA

[3]Corresponding author
e-mail: erik.renstrom@mphy.lu.se

Insulin is secreted from pancreatic β cells in response to an elevation of cytoplasmic Ca^{2+} resulting from enhanced Ca^{2+} influx through voltage-gated Ca^{2+} channels. Mouse β cells express several types of Ca^{2+} channel (L-, R- and possibly P/Q-type). β cell-selective ablation of the gene encoding the L-type Ca^{2+} channel subtype $Ca_v1.2$ ($\beta Ca_v1.2^{-/-}$ mouse) decreased the whole-cell Ca^{2+} current by only ~45%, but almost abolished first-phase insulin secretion and resulted in systemic glucose intolerance. These effects did not correlate with any major effects on intracellular Ca^{2+} handling and glucose-induced electrical activity. However, high-resolution capacitance measurements of exocytosis in single β cells revealed that the loss of first-phase insulin secretion in the $\beta Ca_v1.2^{-/-}$ mouse was associated with the disappearance of a rapid component of exocytosis reflecting fusion of secretory granules physically attached to the $Ca_v1.2$ channel. Thus, the conduit of Ca^{2+} entry determines the ability of the cation to elicit secretion.

Keywords: Ca^{2+} channels/diabetes/exocytosis/insulin secretion/pancreatic β cells

Introduction

Insulin secretion occurs upon elevation of the blood glucose concentration, when the pancreatic β cell depolarizes and regenerative electrical activity consisting of Ca^{2+}-dependent action potentials is initiated (Henquin and Meissner, 1984; Ashcroft and Rorsman, 1989). The resultant elevation of the cytoplasmic Ca^{2+} concentration culminates in exocytosis of insulin-containing secretory granules (Barg *et al*., 2001; (Maecheler and Wollheim, 2001). Mouse pancreatic β cells contain dihydropyridine-sensitive L-type Ca^{2+} channels and glucose-induced insulin secretion is almost abolished by pharmacological inhibitors of L-type Ca^{2+} channels such as nifedipine. The molecular identity of the pancreatic β cell L-type Ca^{2+} channel has not been established and it has variably been reported to be $Ca_v1.2$ ($\alpha 1_C$) (Barg *et al*., 2001) or $Ca_v1.3$ ($\alpha 1_D$) (Yang *et al*., 1999). A significant fraction (~50%) of the whole-cell Ca^{2+} current is resistant to nifedipine (Gilon *et al*., 1997), indicating the presence of additional Ca^{2+} channel subtypes in the β cell. The physiological roles of the non-L-type Ca^{2+} channels are unknown.

Glucose-induced insulin secretion follows a biphasic time-course. A transient first phase lasting 5–10 min is followed by a sustained second phase (Curry *et al*., 1968). The cellular background to the two phases of release remains unknown but it has been suggested to reflect the sequential release of distinct pools of granules, which vary with regard to release competence (Barg *et al*., 2002; Bratanova-Tochkova *et al*., 2002). In support of this idea, high-resolution capacitance measurements have documented two components of exocytosis (Renström *et al*., 1996; Eliasson *et al*., 1997). The rapid component is believed to reflect the release of a limited pool of readily releasable granules in close proximity to the L-type Ca^{2+} channels (Barg *et al*., 2001), whereas replenishment of this pool by mobilization of granules originally residing in a large reserve pool gives rise to the slower component. Interestingly, the initial component can selectively be prevented by intracellular addition of a recombinant peptide corresponding to the loop connecting domains II and III of $Ca_v1.2$ (Wiser *et al*., 1999; Barg *et al*., 2001), suggesting that the assembly of a tight Ca^{2+} channel/insulin granule complex is required for rapid exocytosis in the β cell.

Here we have investigated the role of the L-type $Ca_v1.2$ Ca^{2+} channel for insulin secretion by combining a targeted gene knockout approach with time-resolved insulin release assays and high-resolution single-cell capacitance measurements of exocytosis. Our results suggest that $Ca_v1.2$ Ca^{2+} channels are required for first-phase insulin release and maintenance of systemic glucose tolerance. Collectively, these data raise the interesting possibility that polymorphisms of genes encoding proteins involved in the formation of the exocytotic core/Ca^{2+} channel complex may lead to an impairment of rapid insulin secretion, a hallmark of human type-2 diabetes.

Results

Generation of $\beta Ca_v1.2^{-/-}$ mice

Mice lacking the $Ca_v1.2$ L-type Ca^{2+} channel die *in utero* before day 15 post-coitum (Seisenberger *et al*., 2000). To circumvent embryonic lethality, the Cre/loxP recombination system was used to selectively inactivate the $Ca_v1.2$ gene in pancreatic β cells (Figure 1A; see Materials and

 Published by Oxford University Press

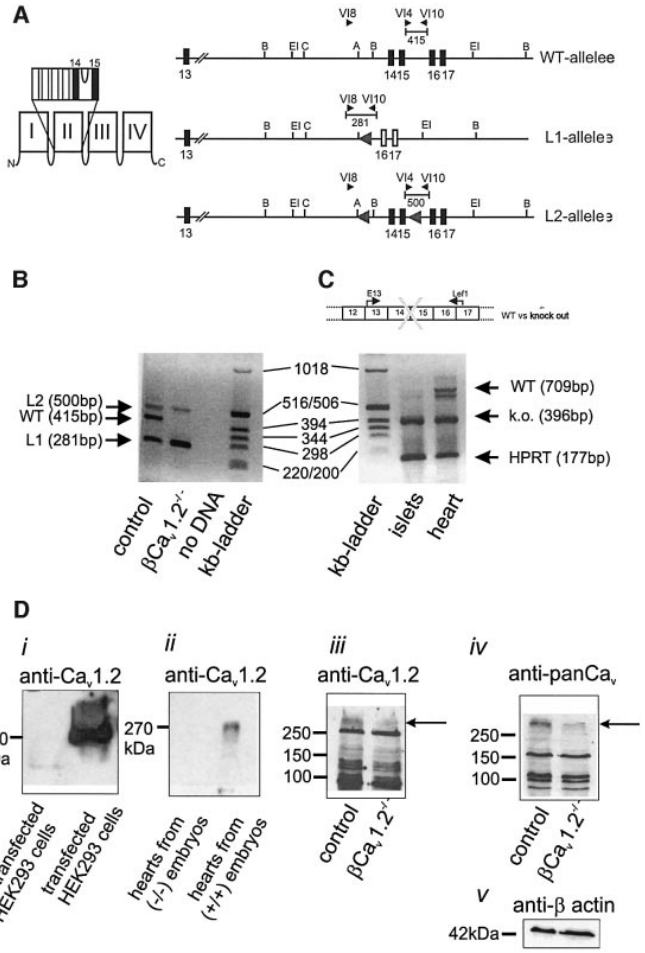

Fig. 1. β cell-specific inactivation of the $Ca_v1.2$ gene. (**A**) To the left, a schematic drawing of the location of the transmembrane segments and the pore loop encoded by exons 14 and 15. To the right, the genomic structures of the wild-type and of the mutated $Ca_v1.2$ genes, respectively, are shown. The black arrows indicate the position of the primers used for genotyping and the fragment length of the PCR products. The numbers indicate the exon number. Schematic representation of the wild-type allele, the knockout allele (L1) and the conditional $Ca_v1.2$ (L2) allele, which contains two loxP sites flanking exons 14 and 15. (**B**) PCR analysis of genomic DNA from control, β$Ca_v1.2^{-/-}$ islets and control reaction (no DNA) and kb marker lane as indicated below the lanes. (**C**) RT–PCR analysis of islets and heart from a β$Ca_v1.2^{-/-}$ mouse ($Ca_V1.2^{L1/L2}$/RIP-Cre$^{+/tg}$) and kb marker as indicated. The scheme (top) represents the locations of the primer pair E13 and Lef1 used in RT–PCR (lower). The double band in heart was sequenced. The upper band represents wild-type mRNA, whereas the lower band consists of wild-type mRNA missing 80 bp. Because the control mice are heterozygous, the heart also expresses the L2 gene transcript (396 bp). As an internal standard, the hypoxanthine phosphoribosyl transferase (HPRT) cDNA was amplified together with the $Ca_v1.2$ cDNA. (**D**) Western blots of protein extracts from control islets and β$Ca_v1.2^{-/-}$ islets (as indicated) using a $Ca_v1.2$-specific antibody (iii, top), a panCa_v-specific antibody (iv) and a β-actin antibody (v, bottom). The specificity of the $Ca_v1.2$ antibody was confirmed using HEK293 cells stably transfected with $Ca_v1.2$ cells (i) and by heart preparations from (+/+) or (–/–) embryos (ii) (Seisenberger *et al.*, 2000). Please note: $Ca_v1.2$ shows an apparently higher mol. wt of 270 kDa in this SDS–PAGE system (11%, low cross-linking).

methods for details). β cell-specific Cre/loxP recombination was achieved by expressing the Cre-recombinase under the control of the rat insulin 2 promoter and was ascertained by PCR analysis using DNA isolated from islets of control and β$Ca_v1.2^{-/-}$ mice (Figure 1B). The islets of β$Ca_v1.2^{-/-}$ mice still contained detectable amounts of the 'floxed' $Ca_v1.2$ gene (L2 allele). This we attribute to contribution of DNA from islet cells not expressing the insulin 2 promoter, i.e. α, δ and PP cells. No Cre-mediated recombination was detectable in heart and lung (data not shown). Islet expression of $Ca_v1.2$ mRNA in β$Ca_v1.2^{-/-}$ mice consisted predominantly of the 'knockout' variety of

$Ca_v1.2$ mRNA and only very low amounts of the wild-type transcript could be detected (Figure 1C). By contrast, the wild-type mRNA was still present in heart (Figure 1C), indicating that Cre-mediated recombination did not occur in this tissue. The successful tissue-selective ablation of $Ca_v1.2$ in β cells was supported by western blot analysis (Figure 1D) using both a $Ca_v1.2$-specific (Diii) and a pan α_1 antibody recognizing high voltage-gated Ca^{2+} channels (Div). Equal loading of the gels shown in (Diii) and (Div) was ascertained by staining for β-actin. The specificity of the $Ca_v1.2$ antibody was confirmed using HEK293 cells stably transfected with $Ca_v1.2$ (Di) and by heart preparations from (+/+) or (–/–) embryos (Dii) (mouse line A in Seisenberger *et al*., 2000). Although both antibodies recognize several proteins, it is clear that a band with the mass expected for $Ca_v1.2$ selectively disappears following knockout of $Ca_v1.2$.

Complete and selective loss of L-type Ca^{2+} currents in $\beta Ca_v1.2^{-/-}$ β cells

We studied the functional consequences of β cell-selective ablation of the $Ca_v1.2$ gene using perforated-patch whole-cell Ca^{2+}-current measurements. Figure 2A shows whole-cell Ca^{2+} currents recorded from a control β cell during a 100 ms depolarization from –70 to –10 mV (close to the peak of the β cell action potential; Henquin and Meissner, 1984) under control conditions and after addition of 1 μM specific L-type Ca^{2+} channel agonist BayK8644. The peak Ca^{2+} current elicited by a depolarization to 0 mV in the control β cells (–58 ± 5 pA) was similar to that observed in β cells from NMRI mice (–49 ± 5 pA) under the same experimental conditions (Larsson-Nyrén *et al*., 2001). The effects of BayK8644 on the integrated Ca^{2+} currents (Q) evoked by depolarizations to voltages (V) between –50 and +20 mV are summarized in Figure 2B. The agonist stimulated the Ca^{2+} current to about the same extent at all voltages, and at –10 mV Ca^{2+} influx increased 2.6 ± 0.6-fold ($P < 0.05$, $n = 5$).

Ca^{2+} currents were reduced in β cells from $\beta Ca_v1.2^{-/-}$ mice. The integrated Ca^{2+} current observed at –10 mV only amounted to 2.4 ± 0.3 pC ($n = 10$), ~55% of the 4.4 ± 0.4 pC ($n = 11$) seen in control β cells. However, it is noteworthy that, up to –30 mV, the amplitude of the Ca^{2+} current was identical in the control and $\beta Ca_v1.2^{-/-}$ β cells. Even at the peak of the β cell action potential (approximately –18 mV; dotted line in Figure 2D), the effects of $Ca_v1.2$ disruption were limited to ~30%. Importantly, BayK8644, as well as the potent L-type Ca^{2+} channel antagonist isradipine (2 μM), were ineffective in these β cells (Figure 2C). The Q–V relationships in $\beta Ca_v1.2^{-/-}$ β cells recorded in the absence and presence of BayK8644 or isradipine are shown in Figure 2D, and are compared with the relationship recorded under control conditions in

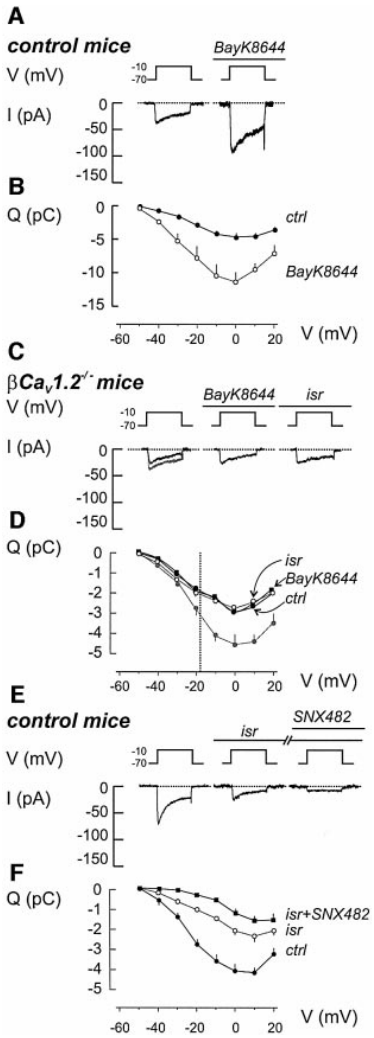

Fig. 2. Ca^{2+} currents in β cells from control and $\beta Ca_v1.2^{-/-}$ mice. (**A**) Whole-cell Ca^{2+} currents (*I*) during 100 ms depolarizations from –70 to –10 mV (*V*) in the absence (left) and presence (right) of 1 μM BayK8644. The dotted line represents the zero current level. (**B**) Charge (*Q*)–voltage (*V*) relationships recorded in the absence (filled circles) and presence of BayK8644 (open circles). Depolarizations were 100 ms long and went to voltages between –50 and +20 mV. Mean values ± SEM of five experiments. $P < 0.05$ for voltages above –40 mV. (**C** and **D**) As in (A and B) but recordings were conducted on β cells from $\beta Ca_v1.2^{-/-}$ mice. The effects of the L-type channel activator BayK8644 (1 μM) as well as the L-type channel inhibitor isradipine (2 μM) were evaluated. The *Q–V* relationship recorded from control β cells under control conditions has been superimposed (gray). Data represent mean values ± SEM of 10, 10 and 5 experiments carried out under control conditions, in the presence of BayK8644 or after addition of isradipine, respectively. $P < 0.01$ for voltages beyond –20 mV when comparing control currents recorded in $\beta Ca_v1.2^{-/-}$ and control mice. The dotted vertical line indicates the average peak voltage attained during the action potential (approximately –18 mV). (**E** and **F**) as (A and B) but isradipine (2 μM) and SNX482 (0.1 μM) were included sequentially as indicated above the voltage trace. Mean values ± SEM of nine experiments. When comparing currents recorded before and after addition of isradipine, $P < 0.01$ at voltages beyond –30 mV. For currents detected before and after addition of SNX482 and in the continued presence of isradipine, $P < 0.05$ at voltages –30 to 0 mV.

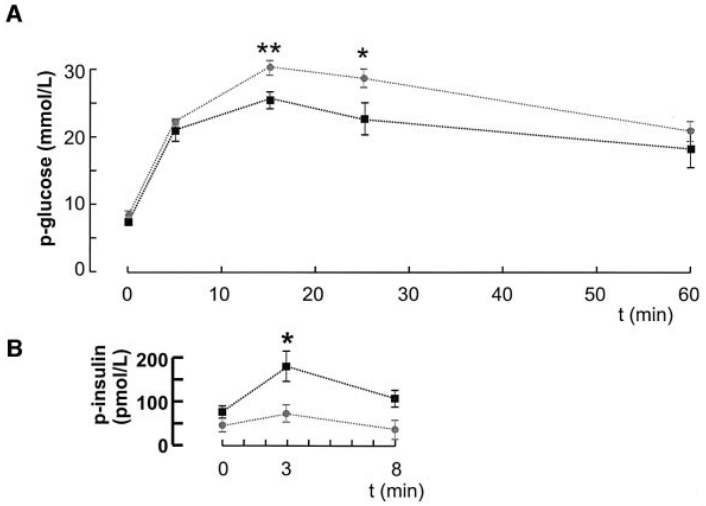

Fig. 3. Impaired glucose tolerance and *in vivo* insulin secretion in $\beta Ca_v1.2^{-/-}$ mice. (**A**) Changes in plasma glucose (p-glucose) in response to an intraperitoneal glucose challenge (2 g/kg body weight) applied at time zero in control (black squares) and $\beta Ca_v1.2^{-/-}$mice (gray squares). Data are mean values ± SEM of nine animals for both data sets. (**B**) Plasma insulin levels (p-insulin) measured in control (black squares) and $\beta Ca_v1.2^{-/-}$ mice (gray squares) at 0, 3 and 8 min after glucose injection.

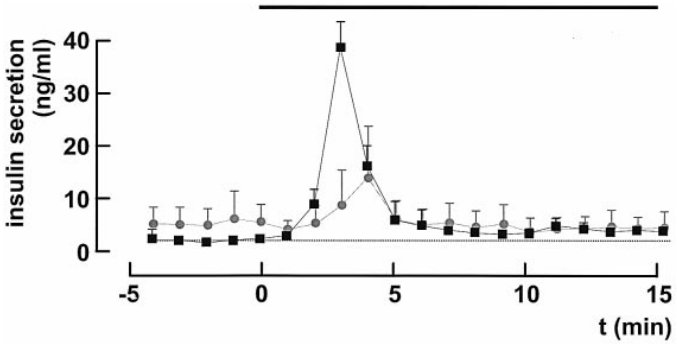

Fig. 4. Blunted first-phase insulin secretion in $\beta Ca_v1.2^{-/-}$ pancreata. Insulin release from *in situ* perfused pancreatic glands from control (black squares) and $\beta Ca_v1.2^{-/-}$ mice (gray circles) before and after elevating glucose from 1 to 10 mM (black horizontal bar). The dotted horizontal line corresponds to the pre-stimulatory rate of insulin release in control mice. Data represent mean values ± SEM of four animals in both groups.

control β cells (gray line). Cell capacitance was nearly identical in $\beta Ca_v1.2^{-/-}$ and control β cells (5.9 ± 0.2 and 5.8 ± 0.3 pF, respectively), demonstrating that the smaller Ca^{2+} current in $\beta Ca_v1.2^{-/-}$ β cells indeed reflects a reduced Ca^{2+} channel density.

To confirm the β cell-selective ablation of $Ca_v1.2$, we measured whole-cell Ca^{2+} currents in glucagon-producing α cells. As expected, the amplitude of the Ca^{2+} current in α cells (identified by the presence of a Na^+ current activated at physiological membrane potentials; Barg *et al.*, 2000) was unaffected in $\beta Ca_v1.2^{-/-}$ mice. The mean charge entry during a 100 ms depolarization to –10 mV amounted to –4.4 ± 0.4 pC (n = 18) and –4.5 ± 0.5 pC (n = 8) in α cells from $\beta Ca_v1.2^{-/-}$ and control mice, respectively (data not shown). The effects of BayK8644 (1 μM) on the α cell Ca^{2+} current in $\beta Ca_v1.2^{-/-}$ mice were tested in four cells and increased the Ca^{2+} current by 58 ± 8% ($P < 0.01$, n = 4; data not shown).

The consequences of ablating $Ca_v1.2$ on the β cell Ca^{2+} current are similar to those obtained using isradipine (Figure 2E). Isradipine blocked the Ca^{2+} current to the same extent at all voltages and the integrated current observed at –10 mV was reduced by 53 ± 6% (n = 9). Nifedipine (20 μM) likewise reduced the β cell Ca^{2+}

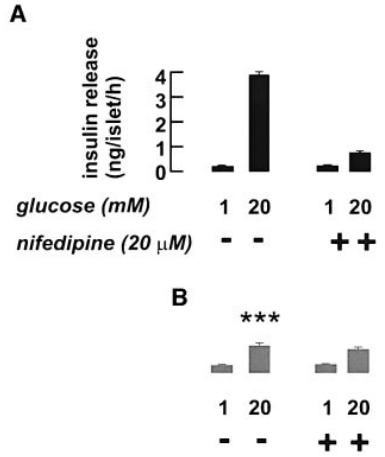

Fig. 5. Loss of a nifedipine-sensitive component of insulin release in isolated $Ca_v1.2^{-/-}$ islets. Insulin secretion measured in isolated islets from control (**A**, black bars) and $Ca_v1.2^{-/-}$ mice (**B**, gray bars) in the presence of 1 or 20 mM glucose with or without 20 μM nifedipine as indicated. Data are mean values ± SEM of six experiments. ***$P < 0.001$ versus the same condition in control mice.

current by 51 ± 4% ($n = 5$; data not shown). We also tested the R-type Ca^{2+} channel antagonist SNX482 (Vajna *et al.*, 2001) on the isradipine-resistant component. The action of SNX482 was voltage-dependent and it blocked ⩾60% of the isradipine-resistant component at voltages up to –10 mV. A cocktail of isradipine, SNX482 and the P-/Q-type Ca^{2+} channel inhibitors ω-conotoxin MVIIC (0.5 μM) or ω-agatoxin IVA (0.1 μM) reduced Ca^{2+} current elicited by depolarizations to –10 mV by 97 ± 4% ($n = 4$; data not shown).

βCa$_v$1.2$^{-/-}$ mice exhibit impaired glucose tolerance and insulin secretion in vivo

We next determined the consequences of β cell-selective disruption of the $Ca_v1.2$ gene on systemic glucose homeostasis and insulin release. The $\beta Ca_v1.2^{-/-}$ mice exhibited a slight hyperglycemia under basal and fasted (6 h) conditions. Fasting glucose levels averaged 6.8 ± 0.4 mM ($n = 8$) and 7.7 ± 0.4 mM ($P < 0.001$, $n = 7$) in control and $\beta Ca_v1.2^{-/-}$ mice, respectively (data not shown). An intraperitoneal glucose challenge (2 g/kg body weight) in fed mice (Figure 3A) revealed an impaired glucose tolerance in $\beta Ca_v1.2^{-/-}$ mice, glucose concentrations as high as ~30 mM being attained. This correlated with a slight reduction of basal plasma insulin levels and marked reduction of glucose-induced first-phase insulin secretion (measured 3 min after the glucose challenge) in the $\beta Ca_v1.2^{-/-}$mice (Figure 3B).

Loss of first-phase insulin secretion in βCa$_v$1.2$^{-/-}$ mice in vitro

To allow comparison between the kinetics of glucose-induced insulin secretion in control and $\beta Ca_v1.2^{-/-}$ mice, *in situ* pancreatic perfusions were carried out (Figure 4). In control animals, elevating the glucose concentration (from 1 to 10 mM) produced a ~20-fold enhancement of secretion that peaked 3 min after onset of stimulation (compare parts in Figure 3B). In $\beta Ca_v1.2^{-/-}$ mice, first-phase (<5 min) secretion was inhibited by 78 ± 12% ($P < 0.01$) and the remaining secretory response peaked ~1 min later than in control animals. No difference in insulin secretion between control and $\beta Ca_v1.2^{-/-}$ mice was observed ⩾5 min after onset of stimulation.

We correlated these observations to insulin secretion *in vitro* using isolated islets. In control mice (Figure 5A), an increase in extracellular glucose from 1 to 20 mM stimulated insulin secretion 16-fold. The L-type Ca^{2+} channel blocker nifedipine (20 μM) had no effect on basal secretion but inhibited glucose-induced release by close to 80%. The R-type channel inhibitor SNX482 (100 nM) likewise failed to affect basal insulin release, but inhibited glucose-elicited insulin secretion by a mere 10% ($n = 6$; data not shown). In agreement with these results, glucose remained capable of stimulating insulin secretion 3.1-fold even in the presence of nifedipine. The latter effect we attribute to Ca^{2+} entry through non-L-type Ca^{2+} channels. In islets from $\beta Ca_v1.2^{-/-}$ mice (Figure 5B), basal insulin secretion was unaffected, but glucose-induced insulin secretion was much lower than in the control mice and comparable to that seen after blockage of the Ca^{2+} channels with nifedipine (2.7-fold enhancement). As expected, given that $Ca_v1.2$ channels appear to constitute the only L-type Ca^{2+} channels in the β cell (Figure 2C and D), nifedipine had no effect on glucose-induced insulin secretion in the knockout mice. The suppressed insulin secretory capacity in islets from $\beta Ca_v1.2^{-/-}$ mice could not be attributed to reduced total insulin content, which amounted to 25 ± 1 ng/islet ($n = 13$) and 23 ± 2 ng/islet ($n = 8$) in islets from control and $\beta Ca_v1.2^{-/-}$ mice, respectively.

Intracellular Ca^{2+} handling and electrical activity are unperturbed in β cells from βCa$_v$1.2$^{-/-}$ mice

The impaired insulin secretory capacity of $\beta Ca_v1.2^{-/-}$ islets is not attributable to abnormalities of intracellular Ca^{2+} handling (Figure 6A and B) or glucose-induced electrical activity (Figure 6C and D). Basal $[Ca^{2+}]_i$ averaged 103 ± 8 nM ($n = 8$) and 112 ± 12 nM ($n = 8$) in control and $\beta Ca_v1.2^{-/-}$ islets, respectively. Following stimulation with 10 mM glucose, $[Ca^{2+}]_i$ rose to a peak value of 279 ± 25 nM in control islets and 325 ± 55 nM in islets from the knockout mice. The time-averaged $[Ca^{2+}]_i$ measured both at 10 and 20 mM glucose were likewise not different in the two strains of mice (data not shown). The latency between glucose addition and the initial increase in $[Ca^{2+}]_i$ averaged 257 ± 24 s in control islets and 327 ± 18 s ($P < 0.05$) in $\beta Ca_v1.2^{-/-}$ islets.

We ascertained that steady-state electrical activity was not significantly affected by ablation of $Ca_v1.2$. In control mice, the membrane potential changed from a resting potential of –62 ± 3 mV ($n = 4$) in the absence of glucose to –17 ± 5 mV (measured at the peak of the action potential) in the presence of 10 mM glucose. The corresponding values in the β cells from $\beta Ca_v1.2^{-/-}$ mice averaged –64 ± 5 and –19 ± 4 mV ($n = 4$). It is evident that the pattern of action potential firing in β cells from

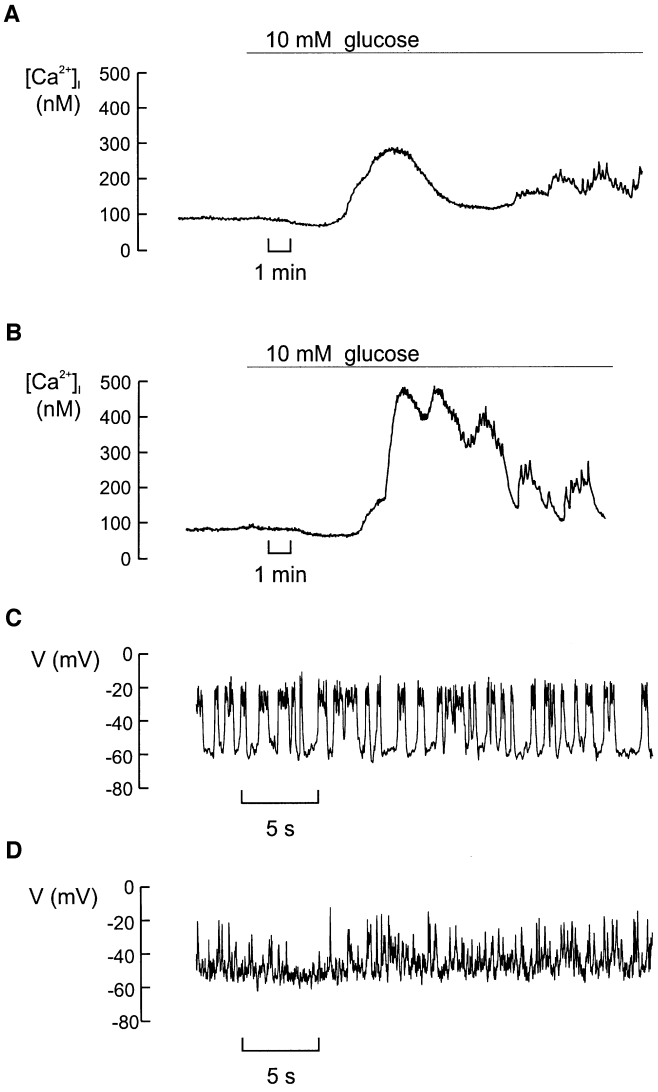

Fig. 6. Intracellular Ca^{2+} handling and glucose-induced electrical activity are only moderately affected by disruption of the $Ca_v1.2$ gene. (**A**) Cytoplasmic Ca^{2+} ($[Ca^{2+}]_i$) measured before and after addition of 10 mM glucose in an islet isolated from a control mouse. (**B**) As in (A) but using an islet isolated from a $\beta Ca_v1.2^{-/-}$ mouse. Data are representative of eight recordings in each group. (**C**) Recording of the membrane potential from a β cell in a small cell cluster isolated from control islets exposed to 10 mM glucose at steady state. (**D**) The same as in (C) but in a β cell from a $\beta Ca_v1.2^{-/-}$ mouse. Data are representative of four recordings in both groups that lasted long enough to permit multiple changes of the external solutions (>20 min).

$\beta Ca_v1.2^{-/-}$ mice was somewhat different from that observed in the control mice in not being grouped to short bursts. It might seem surprising that $Ca_v1.2$ ablation had no effect on the peak voltage of the action potential given that the peak Ca^{2+} current was reduced by ~30% at –20 mV (Figure 2D). However, several processes in addition to the Ca^{2+}-current amplitude influence the shape of the action potential. These include, for example, the magnitude of the resting and voltage-gated K^+ conductances.

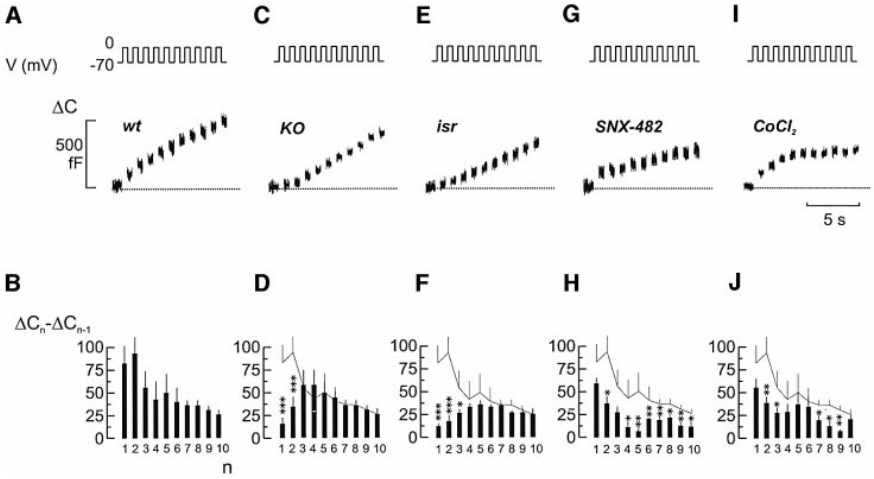

Fig. 7. Loss of rapid exocytosis in $\beta Ca_v1.2^{-/-}$ β cells. (**A**) Increase in cell capacitance (ΔC, lower) elicited by a train of ten 500 ms depolarizations from –70 to 0 mV (V, upper). The dotted line indicates the pre-stimulatory level. (**B**) Increment in cell capacitance by each depolarization ($\Delta C_n - \Delta C_{n-1}$) displayed against pulse number (*n*). Data are mean values ± SEM of nine experiments. (**C** and **D**) The same as in (A and B) but using a β cell obtained from a $\beta Ca_v1.2^{-/-}$ mouse. Data are mean values ± SEM of 15 experiments. (**E** and **F**) As in (A and B) but in the presence of 2 μM isradipine. Data are mean values ± SEM of eight experiments. (**G** and **H**) As in (A and B) but in the presence of 0.1 μM SNX482. Data are mean values ± SEM of seven experiments. (**I** and **J**) As in (A and B) but in the presence of 0.5 mM Co^{2+}. Data are mean values ± SEM of 11 experiments. In (D, F, H and J), the superimposed gray line denotes the data in control β cells from (A). ***$P < 0.001$, **$P < 0.01$ and *$P < 0.05$ versus responses in the control β cells (gray line).

Loss of rapid Ca^{2+}-dependent exocytosis in β cells from $\beta Ca_v1.2^{-/-}$ mice

The mild consequences of ablating $Ca_v1.2$ in β cells on intracellular Ca^{2+} suggest that impaired glucose tolerance and insulin secretion may result from direct interference with the exocytotic apparatus. Indeed, it has been shown previously that $Ca_v1.2$ Ca^{2+} channels co-assemble with fusion proteins including synaptotagmin, syntaxin and SNAP-25 (Wiser *et al*., 1999; Ji *et al*., 2002). We used cell capacitance measurements to study the kinetics of depolarization-evoked exocytosis in single β cells from control and $\beta Ca_v1.2^{-/-}$ mice. Figure 7A shows changes in cell capacitance in response to a train of ten 500 ms depolarizations. The data of a total of nine experiments are summarized in Figure 7B. Typically, the capacitance increase per pulse decreased during the train, from 80 to 100 fF in response to the initial depolarizations to a steady-state rate of 25 fF/pulse. This behavior is expected if the cell contains a limited pool of releasable granules, which are gradually depleted during repetitive stimulation (Neher, 1998; Barg *et al*., 2000, 2001, 2002). When the same experiments were conducted in β cells from $\beta Ca_v1.2^{-/-}$ mice (Figure 7C and D), exocytosis in response to the initial depolarizations was markedly reduced whereas that elicited later during the train was not affected. The Ca^{2+} current elicited by the depolarizations was reduced to an equal extent (~45%) throughout the train (data not shown). The acute effects of applying the L-type Ca^{2+} channel antagonist isradipine were identical to those resulting from $Ca_v1.2$ disruption (Figure 7E and F). By contrast, inhibition of R-type Ca^{2+} channels with SNX482, which reduced the Ca^{2+} current by ~25%, affected late exocytosis but had no significant effect on the response to the first depolarization (Figure 7G and H). The differential effects of selective L- and R-type channel inhibition on rapid and sustained exocytosis, respectively, are at variance with the effect of the non-selective Ca^{2+} channel blocker Co^{2+} (0.5 mM), which inhibited Ca^{2+} entry by ~50% (i.e. the same as that produced by ablation of $Ca_v1.2$), and reduced exocytosis to an equal extent (45 ± 6%; Figure 7I and J) throughout the train.

Discussion

General considerations

Here we have studied the effects of ablating the L-type Ca^{2+} channel gene $Ca_v1.2$ *in vivo*, at the whole-organ level, in isolated islets and individual islet cells. The combination of techniques makes it possible to correlate the consequences of a single-cell defect on the complex systems physiology of insulin release and plasma glucose homeostasis. The genetic model we have chosen strictly depends on the comparison of litter-matched animals of a control group ($Ca_v1.2^{+/L2}$/RIP-$Cre^{+/tg}$ resulting in the genotype $Ca_v1.2^{+/L1}$/RIP-$Cre^{+/tg}$ only in the β cells) and of a knockout group ($Ca_v1.2^{L1/L2}$/RIP-$Cre^{+/tg}$ resulting in the genotype $Ca_v1.2^{L1/L1}$/RIP-$Cre^{+/tg}$ only in the β cells). These animals are identical with the exception of one functional $Ca_v1.2$ allele in the control group. Therefore, we compare animals with two knockout alleles with those with one wild-type allele, allowing us to establish the specific function of $Ca_v1.2$. Careful analysis of the L-type

Ca^{2+}-current densities in embryonic cardiomyocytes for all three genotypes and two differently constructed mouse lines (stop codon in exon 3 versus deletion of exons 14/15 and stop in 16) failed to detect significant differences between (+/+) and (+/–) cells (Seisenberger *et al*., 2000). We have also analyzed mice in which the $Ca_v1.2$ channel was specifically deleted in smooth muscle cells. $Ca_v1.2$ current densities were identical in litter-matched animals for the genotypes (+/–) or (+/+) (N.Klugbauer and F.Hofmann, unpublished data). These considerations indicate that a gene dose effect does not account for the present results.

In the following, we will consider the molecular identity of the L-type Ca^{2+} channel in the pancreatic β cell, the importance of the L-type $Ca_v1.2$ channel for systemic glucose control and first-phase insulin secretion, as well as the functional roles fulfilled by other Ca^{2+} channel subtypes expressed in β cells. Finally, we discuss the possibility that defects of the release machinery and/or Ca^{2+} entry contribute to the impaired insulin secretion seen in human type-2 diabetes.

Mouse L-type Ca^{2+} channel variety expressed in β cells is $Ca_v1.2$

The present data unequivocally establish the central role of $Ca_v1.2$ L-type Ca^{2+} channels in insulin secretion. Previous studies have indicated that $Ca_v1.3$ ($\alpha1_D$) might be of importance in insulin release (Yang *et al*., 1999; Namkung *et al*., 2001). However, the finding that the entire DHP-sensitive Ca^{2+} current is lost following inactivation of the $Ca_v1.2$ gene reinforces our previous immunochemical and electrophysiological data that $Ca_v1.2$ is the only L-type Ca^{2+} channel variety expressed in mouse β cells (Barg *et al*., 2001). In addition to the L-type Ca^{2+} channels, mouse β cells also express R- and P/Q-type Ca^{2+} channels. Although the L-type current component accounts for only ~50% of the total Ca^{2+} current, its inhibition reduces glucose-induced insulin secretion *in vitro* by 80% and nearly abolishes insulin release *in vivo*. Thus, it appears that the conduit of Ca^{2+} entry determines the biological efficacy of the ion and that influx through L-type Ca^{2+} channels is more tightly coupled to insulin secretion than that occurring via P/Q- and R-type Ca^{2+} channels.

$Ca_V1.2$ Ca^{2+} channels are required for first-phase insulin secretion and rapid exocytosis in pancreatic β cells

We have previously demonstrated that $Ca_v1.2$ Ca^{2+} channels functionally associate with insulin granules in the β cells, and that the loop connecting the second and third homologous domains physically tethers the channel to components of the exocytotic core complex (Wiser *et al*., 1999). It is therefore pertinent that the effects of isradipine and genetic ablation of $Ca_v1.2$ are indistinguishable from those of intracellular application of the synprint peptide (Barg *et al*., 2001). We propose that in $\beta Ca_v1.2^{-/-}$ mice, the $Ca_v1.2$/granule complex is disrupted, leading to selective suppression of fast exocytosis. We emphasize that the effects of inhibition of L-type Ca^{2+} channels or ablation of the $Ca_v1.2$ gene are not simply attributable to the fact that the whole-cell Ca^{2+} current is reduced by 50%. This possibility can be discarded by the finding that addition of the non-selective Ca^{2+} channel blocker Co^{2+} (0.5 mM), which reduces the total whole-cell Ca^{2+} current (i.e. that flowing through both L- and non-L-type Ca^{2+} channels) by 50%, does not affect the release kinetics but simply reduces the amplitude of the responses observed during the train by ~50%.

The role of the non-L-type Ca^{2+} channels in β cell exocytosis remains enigmatic, but it is worth pointing out that a DHP-resistant component of insulin secretion can be detected both in the insulin-release experiments (Figure 5) as well as the capacitance measurements (Figure 7). It is possible that non-L-type Ca^{2+} channels fulfill functions in the β cells other than initiation of exocytosis. For example, they may play a role in the refilling of the readily releasable pool of granules by mobilizing reserve granules. This would be consistent with the finding that whereas exocytosis elicited by the two first pulses during a train of ten 500 ms depolarizations is strongly inhibited in β cells from $\beta Ca_v1.2^{-/-}$ mice and in control β cells exposed to the L-type Ca^{2+} channel inhibitor isradipine (Figure 7A–F), exocytosis during the latter part of the train is unaffected. Indeed, the R-type Ca^{2+} channel blocker SNX482 exerts its strongest effect on late exocytosis (Figure 7H). In addition, influx of Ca^{2+} through non-L-type Ca^{2+} channels may regulate exocytosis of GABA-containing synaptic-like microvesicles (SLMV; the presence of which has been documented in β cells; Reetz *et al*., 1991) rather than the large insulin-containing secretory granules (compare with Takahashi *et al*., 1997). We have ascertained that exocytosis of SLMVs only contributes ~1% of the total capacitance (M.Braun, A.Wendt and P.Rorsman, manuscript in preparation) increase. It is therefore safe to conclude that the data presented in this study reflect exocytosis of insulin-containing large dense core vesicles. Finally, non-L-type Ca^{2+} channels may not be important for exocytosis, but rather in the generation of glucose-induced electrical activity (Pereverzev *et al*., 2002) or gene expression (Wang *et al*., 2002).

Ca^{2+} signaling is unperturbed in $\beta Ca_v1.2^{-/-}$ mice

Surprisingly, given the strong effects on insulin secretion, ablation of $Ca_v1.2$ had no detectable effects on intracellular Ca^{2+} signaling except that the glucose-induced increase in cytoplasmic Ca^{2+} was delayed by ~1 min relative to that observed in control β cells. The latter effect nicely echoes the slower time-course of insulin release observed *in situ* (~1 min; Figure 4). Possibly, the latter observations are the consequence of L-type Ca^{2+} channels contributing to the initiation of electrical activity in the β cell (Ribalet and Beigelman, 1981).

Why are measured Ca^{2+} concentrations unchanged in $\beta Ca_v1.2^{-/-}$ β cells? The preservation of normal Ca^{2+} signaling is unexpected in view of previous data showing that glucose-induced increases in cytoplasmic Ca^{2+} concentration are suppressed following the addition of L-type Ca^{2+} channel blockers such as nifedipine (Rosario *et al*., 1993). This may result from a compensatory up-regulation of non-L-type Ca^{2+} channels, as suggested by the finding that the peak Ca^{2+} current measured at –20 mV in $Ca_v1.2^{-/-}$ β cells is 50% larger than that observed in control β cells exposed to isradipine (compare Figure 2D, black circles with F, white circles). In fact, the reduction of the whole-cell Ca^{2+} current in the knockout mice was limited to ~30% at voltages up to –20 mV, i.e. the range of voltages

covered by the action potential. This makes the strong inhibition of insulin secretion (~80%; Figures 3–5) even more remarkable and provides additional arguments that exocytosis in the β cell is tightly coupled to Ca^{2+} entry through $Ca_v1.2$.

We emphasize that microfluorimetry reports the global intracellular Ca^{2+} concentration ($[Ca^{2+}]_i$) within the β cell. We have previously documented the existence of steep Ca^{2+} gradients in mouse pancreatic β cells and these are not resolved in the present recordings of $[Ca^{2+}]_i$ in intact pancreatic islets. Our failure to detect any gross abnormalities in cellular Ca^{2+} signaling therefore does not exclude the possibility that $[Ca^{2+}]_i$ at the release sites is affected. The significance of microdomains of high $[Ca^{2+}]_i$ close to the release sites is illustrated by the finding that whereas glucose-induced insulin secretion is nearly abolished in the presence of nifedipine (Figure 5), exocytosis during the latter part of the train of voltage–clamp depolarizations is hardly affected (Figure 7E and F). This apparent discrepancy we attribute to the fact that the stimulus used for the capacitance measurements (trains of 500 ms depolarizations to 0 mV) is much stronger than that normally triggering insulin secretion (50 ms action potentials to ~15 mV; Atwater *et al*., 1979). During the train of depolarizations, $[Ca^{2+}]_i$ equilibrates in the β cell (Bokvist *et al*., 1995) and rises sufficiently throughout the cell to initiate exocytosis of granules that are not in the immediate vicinity of the Ca^{2+} channels. This does not occur during the brief action potentials when exocytotic levels of $[Ca^{2+}]_i$ ($\geqslant$10 μM) are only attained close to the Ca^{2+} channels (Barg *et al*., 2001, 2002).

Does human type-2 diabetes result from defective assembly of Ca^{2+} channels and secretory granules?

It is tempting to consider the significance of these findings to human type-2 diabetes. Like the $\beta Ca_v1.2^{-/-}$ mice, early cases of type-2 diabetes exhibit mild basal hyperglycemia, impaired glucose tolerance and lack of first-phase insulin secretion (UKPDS16, 1995). We are not implying that loss-of-function mutations of the $Ca_v1.2$ gene cause diabetes. However, polymorphisms that result in subtle changes in gating of the Ca^{2+} channel or its ability to interact with the exocytotic machinery (Nagamatsu *et al*., 1999; Wiser *et al*., 1999; Zhang *et al*., 2002) can be envisaged to result in impaired insulin secretion. The significance of such interactions is illustrated by the fact that whereas the SNARE proteins SNAP-25 and syntaxin1A inhibit the L-type Ca^{2+} channel when expressed individually, channel activity is actually stimulated when these proteins are co-expressed (Wiser *et al*., 1999; Ji *et al*., 2002). Interestingly, SNARE protein expression is reduced in the GK rat model of human type-2 diabetes (Nagamatsu *et al*., 1999; Zhang *et al*., 2002) and several proteins known to be important for the anchoring of the insulin granules to the Ca^{2+} channels localize to chromosomal regions linked to human type-2 diabetes. These include the insulin granule proteins synaptotagmins 5 and 7 (Haeger *et al*., 1998; Norman *et al*., 1998; Pratley *et al*., 1998), putative Ca^{2+} sensors in β cell exocytosis (Ji *et al*., 2002), the granular fusion protein VAMP-2/synaptobrevin-2 (Regazzi *et al*., 1995; Parker *et al*., 2001; Lindgren *et al*., 2002) and the plasma membrane-associated fusion protein SNAP-25 (Imperatore *et al*., 1998; Ji *et al*., 2002). Indeed, a single nucleotide polymorphism in the gene encoding syntaxin1A has recently been found to associate with human type-2 diabetes (Tsunoda *et al*., 2001). Ca^{2+} channels and proteins involved in exocytosis therefore deserve to be regarded as interesting candidate genes in genetic studies of type-2 diabetes. We point out that the functional consequences of the polymorphisms must be small as we are not born with type-2 diabetes. This suggests that the changes in protein function resulting from the polymorphisms only become significant when combined with other β cell abnormalities such as age-dependent reduction in glucose metabolism (due to accumulating mitochondrial mutations; Maechler and Wollheim, 2001) with resultant impairment of electrical activity and Ca^{2+} entry. This concept is indeed entirely compatible with the current view that diabetes results from a combination of genetic factors, age and environmental factors (McCarthy and Froguel, 2002). Genes encoding proteins involved in exocytosis (SNARE proteins as well as Ca^{2+} channels) should accordingly be considered as candidate genes in future studies of the genetics of type-2 diabetes.

Materials and methods

Conditional inactivation of the $Ca_v1.2$ gene in pancreatic β cells

As described previously (Seisenberger *et al*., 2000), two different $Ca_v1.2$ alleles were generated by Cre-mediated recombination in ES cells (L1 and L2; Figure 1A). In L1, exons 14 and 15 that encode the IIS5 and IIS6 transmembrane segments and the pore loop in domain II were deleted. In addition, this deletion causes incorrect splicing from exon 13 to an intron upstream of exon 16, and thereby generates a premature stop codon in exon 16 and a loss-of-function allele. L2 contains the 'floxed' exons 14 and 15, and encodes a functional $Ca_v1.2$ gene. To generate β cell-specific $Ca_v1.2$-deficient mice, the $Ca_v1.2^{+/L1}$ mouse (i.e. a mouse carrying one L1 allele and one wild-type allele) was crossed with a mouse expressing the Cre-recombinase under the control of the rat insulin 2 promoter ($RipCre^{+/tg}$) (Postic *et al*., 1999). The resulting $Ca_v1.2^{+/L1}$,$RipCre^{+/tg}$ mice were then mated with $Ca_v1.2^{L2/L2}$ mice (i.e. mice homozygous for the L2 allele) to obtain the β cell-specific knockout $Ca_v1.2^{L1/L2}$,$RipCre^{+/tg}$ (i.e. $\beta Ca_v1.2^{-/-}$ mice) and control animals ($Ca_v1.2^{+/L2}$,$RipCre^{+/tg}$). Both lines were viable and showed no gross abnormalities. Genotyping was performed using primers VI4 (5′-TGGCCCCTAAGCAATGA-3′), VI8 (5′-AGGGGTGTTCAGAGCAA-3′) and VI10 (5′-CCCCAGCCAA-TAGAATGCCAAT-3′). The background mouse strain was C57BL/6.

Isolation of pancreatic islets

Mice (3–4 months old) were killed by cervical dislocation, the pancreas quickly excised and pancreatic islets isolated by standard collagenase digestion (Salehi *et al*., 1999). The surgical procedures used in the *in vitro* and *in vivo* studies were approved by the ethical committee at Lund University, the Regierung von Oberbayern or by the Veterinary Office of the canton of Geneva.

DNA isolation from islets and PCR analysis

Islets were digested for 5 min at 55°C in 19 μl of buffer containing 50 mM Tris pH 8.0, 20 mM NaCl, 1 mM EDTA, 1% SDS and 1 mg/ml proteinase K. Proteinase K was subsequently inactivated by increasing the temperature of the digest to 95°C for 5 min. The digest (0.1 μl) was taken for PCR analysis using the $Ca_v1.2$-specific primers VI4, VI8 and VI10.

RT–PCR on mRNA of islets

Freshly prepared islets were cultured overnight in RPMI 1640 medium (Gibco™) at 37°C. PolyA mRNA was isolated using Dynabeads Oligo $(dT)_{25}$ (Dynal Biotech, Oslo, Norway). The following buffers were used: GTC buffer [4 M guanidine thiocyanate, 20 mM Na acetate pH 5.4, 0.1 mM DTT, 0.5% lauroyl sarcosinat (w/v), 6.5 μl/ml mercaptoethanol],

binding buffer (100 mM Tris–HCl pH 8.0, 20 mM EDTA, 400 mM LiCl) and washing buffer (10 mM Tris–HCl pH 8.0, 0.15 M LiCl, 1 mM EDTA). The mRNA was eluted with DEPC-treated water. Random hexamer primers and Superscript Reverse Transkriptase II (Life Technologies) were used for cDNA synthesis. The following primers were used: for amplifying $Ca_v1.2$ (E13 5′-ACAGCCAATAAAG-CCCTCCT-3′ and Lef 1 5′-GGCTTCTCCATCACCTCCTGTT-3′), for HPRT (QG 197 5′-GTAATGATCAGTCAACGGGGGAC-3′ and QG 198 5′-CCAGCAAGCTTGCAACCTTAACCA-3′).

Western blot analysis

Approximately 900 islets of control and $\beta Ca_v1.2^{-/-}$ mice were cultured in RPMI 1640 for 48 h at 37°C. Thereafter, the islets were homogenized after one freeze–thaw cycle in a hypotonic buffer (20 mM K_2HPO_4/KH_2PO_4 pH 7.2, 1 mM EDTA) containing protease inhibitors [1 mM benzamidine, 0.1 mM PMSF and Protease Inhibitor Cocktail (1:500; Sigma)]. The homogenates (40 μg protein) were separated on an 11% SDS–PAGE (lower crosslinking with 0.2% bis-acrylamide). Peptides were blotted on a PVDF membrane (Millipore) and probed with a $Ca_v1.2$-(Chemicon) and a panCa_v-specific antibody (Calbiochem). Equal loading of the slots was ascertained using a monoclonal β-actin antibody (Abcam). Antibodies were visualized by the ECL system (NEN).

Glucose and insulin measurements

In the *in vivo* studies, glucose [11.1 mmol (equal to 2 g)/kg body weight] was dissolved in 0.9% NaCl and delivered by intraperitoneal injection. Blood sampling, detection of plasma insulin by RIA and enzymatic determination of plasma glucose concentrations were performed as described previously (Salehi *et al*., 1999). *In situ* pancreatic perfusions were performed as detailed in Maechler *et al*. (2002), except that the basal and stimulatory glucose concentrations in the perfusate were 1 and 10 mM, respectively. Insulin release *in vitro* was measured in batch incubations. Briefly, freshly isolated islets were pre-incubated for 30 min at 37°C in a Krebs–Ringer bicarbonate buffer pH 7.4 supplemented with 7 mM glucose, 10 mM HEPES and 0.1% bovine serum albumin, and gassed with 95% O_2 and 5% CO_2. Groups of 10 islets were then incubated in 1 ml for 60 min at 37°C in KRB supplemented with glucose and nifedipine as specified. Total insulin islet content was determined by extraction with acidic ethanol and insulin was assayed by RIA.

Electrophysiology

Isolated islets (see above) were dissociated into single cells by shaking in Ca^{2+}-free medium. Insulin-secreting β cells and glucagon-producing α cells were identified electrophysiologically by the absence and presence, respectively, of Na^+ currents at physiological membrane potentials (Barg *et al*., 2000). The measurements were conducted using an EPC-7 patch–clamp amplifier in conjunction with the software Pulse (version 8.53; HEKA Elektronik, Lambrecht/Pfalz, Germany). Whole-cell Ca^{2+} currents and glucose-induced electrical activity were recorded from metabolically intact cells using the perforated-patch whole-cell approach (Renström *et al*., 1996). Exocytosis was monitored using standard whole-cell measurements that allow control of the cytosol, by recordings of cell capacitance using the sine+DC mode of the lock-in amplifier included in the Pulse software suite. The extracellular bath solution contained (in mM) 138 NaCl, 5.6 KCl, 2.6 $CaCl_2$, 1.2 $MgCl_2$, 5 glucose (unless otherwise indicated) and 5 HEPES (pH 7.4 with NaOH). For the recordings of the whole-cell Ca^{2+} currents, 20 mM NaCl was equimolarly replaced by the K^+ channel blocker TEA-Cl. The pipette solution in the perforated-patch recordings of membrane potential contained (in mM) 76 K_2SO_4, 10 NaCl, 10 KCl, 1 $MgCl_2$, 5 HEPES (pH 7.35 with KOH) and 0.24 mg/ml amphotericin B (Renström *et al*., 1996). For the whole-cell Ca^{2+} current recordings, the K^+ salts in the pipette solution were replaced by the corresponding Cs^+ salts. The intracellular medium used in the capacitance measurements consisted of (in mM): 125 Cs glutamate, 10 CsCl, 10 NaCl, 1 $MgCl_2$, 5 HEPES, 3 Mg ATP, 0.1 cAMP and 0.05 EGTA (pH 7.2 with CsOH). The dihydropyridines nifedipine, isradipine (Pfizer) and BayK8644 were prepared as stock solutions in DMSO (final concentration ≤0.1%). The R-type blocker SNX482 (Peptide Institute Inc., Osaka, Japan) was dissolved directly in the extracellular medium. All other reagents were from Sigma. Effects of agonists and antagonists were determined in the steady state. The bath (~1.5 ml) was continuously perfused (6 ml/min) and the temperature maintained at ~32°C.

Microfluorimetry

$[Ca^{2+}]_i$ in intact pancreatic islets was measured by dual-wavelength microfluorimetry using fura-2 and a D104 PTI microfluorimetry system (Monmouth Junction, NJ). The temperature of the experimental chamber was +32°C. Procedures for loading and calibration of the fluorescence signal were as detailed in Olofsson *et al*. (2002).

Data analysis

Data are given as mean values ± SEM. Statistical significances were evaluated by either ANOVA followed by Dunnet's ad hoc tests for unpaired comparisons, or by paired Student's *t*-test when comparing data obtained in the same cell.

Acknowledgements

We thank Mrs K.Borglid, Mrs B-M.Nilsson and Mrs S.Paparisto for expert technical assistance. and Dr Cecilia Lindgren for help with diabetes genetics. Supported by the JDRF, the Swedish Research Council (grant nos 08647, 13509, 12234), the Swedish Diabetes Association, the NovoNordisk Foundation, the European Commission (HPRN-CT-2000-00082), the Deutsche Forschungsgemeinschaft, Fond der Chemischen Industrie, Swiss National Science Foundation (grant no 32-66907.01) and the Swiss Federal Office for Education and Science (grant no 01.0260).

References

Ashcroft,F.M. and Rorsman,P. (1989) Electrophysiology of the pancreatic β-cell. *Prog. Biophys. Mol. Biol.*, **54**, 87–143.

Atwater,I., Dawson,C.M., Ribalet,B. and Rojas,E. (1979) Potassium permeability activated by intracellular calcium ion concentration in the pancreatic β cell. *J. Physiol.*, **288**, 575–588.

Barg,S., Galvanovskis,J., Göpel,S., Rorsman,P. and Eliasson,L. (2000) Tight coupling between electrical activity and exocytosis in mouse glucagon-secreting α-cells. *Diabetes*, **49**, 1500–1510.

Barg,S. *et al*. (2001) Fast exocytosis with few Ca^{2+} channels in insulin-secreting mouse pancreatic B cells. *Biophys. J.*, **81**, 3308–3323.

Barg,S., Eliasson,L., Renström,E. and Rorsman,P. (2002) A subset of 50 secretory granules in close contact with l-type ca^{2+} channels accounts for first-phase insulin secretion in mouse β-Cells. *Diabetes*, **51**, S74–S82.

Bokvist,K., Eliasson,L., Ämmälä,C., Renström,E. and Rorsman,P. (1995) Co-localization of L-type Ca^{2+} channels and insulin-containing secretory granules and its significance for the initiation of exocytosis in mouse pancreatic B-cells. *EMBO J.*, **14**, 50–57.

Bratanova-Tochkova,T.K. *et al*. (2002) Triggering and augmentation mechanisms, granule pools, and biphasic insulin secretion. *Diabetes,* **51**, S83–S90.

Curry,D.L., Bennett,L.L. and Grodsky,G.M. (1968) Dynamics of insulin secretion by the perfused rat pancreas. *Endocrinology*, **83**, 572–584.

Eliasson,L., Renstrom,E., Ding,W.G., Proks,P. and Rorsman,P. (1997) Rapid ATP-dependent priming of secretory granules precedes Ca^{2+}-induced exocytosis in mouse pancreatic B-cells. *J. Physiol.*, **503**, 399–412.

Gilon,P., Yakel,J., Gromada,J., Zhu,Y., Henquin,J.C. and Rorsman P. (1997) G protein-dependent inhibition of L-type Ca^{2+} currents by acetylcholine in mouse pancreatic B-cells. *J. Physiol.*, **499**, 65–76.

Hager,J. *et al*. (1998) A genome-wide scan for human obesity genes reveals a major susceptibility locus on chromosome 10. *Nat. Genet.*, **20**, 304–308.

Henquin,J.C. and Meissner,H.P. (1984) Significance of ionic fluxes and changes in membrane potential for stimulus–secretion coupling in pancreatic β-cells. *Experientia*, **40**, 1043–1052.

Imperatore,G., Hanson,R.L., Pettitt,D.J., Kobes,S., Bennett,P.H. and Knowler,W.C. (1998) Sib-pair linkage analysis for susceptibility genes for microvascular complications among Pima Indians with type 2 diabetes. Pima Diabetes Genes Group. *Diabetes*, **47**, 821–830.

Ji,J,. Yang,S.N., Huang,X., Li,X., Sheu,L., Diamant,N., Berggren,P-O. and Gaisano,H.Y. (2002) Modulation of L-type Ca^{2+} channels by distinct domains within SNAP-25. *Diabetes*, **51**, 1425–1436.

Larsson-Nyrén,G., Sehlin,J., Rorsman,P. and Renstrom,E. (2001) Perchlorate stimulates insulin secretion by shifting the gating of L-type Ca^{2+} currents in mouse pancreatic B-cells towards negative potentials. *Pflugers Arch.*, **441**, 587–595.

Lindgren,C.M. *et al*. (2002) Contribution of known and unknown susceptibility genes to early-onset diabetes in Scandinavia: evidence for heterogeneity. *Diabetes*, **51**, 1609–1617.

Maechler,P. and Wollheim,C.B. (2001) Mitochondrial funtion in normal and diabetic β-cells *Nature*, **414**, 807–812.

Maechler,P., Gjinovci,A. and Wollheim,C.B. (2002) Implication of glutamate in the kinetics of insulin secretion in rat and mouse perfused pancreas. *Diabetes*, **51**, (Suppl. 1), S99–S102.

McCarthy,M.I. and Froguel,P. (2002) Genetic approaches to the molecular understanding of type 2 diabetes. *Am. J. Physiol. Endocrinol. Metab.*, **283**, E217–E225.

Nagamatsu,S., Nakamichi,Y., Yamamura,C., Matsushima,S., Watanabe,T., Ozawa,S., Furukawa,H. and Ishida,H. (1999) Decreased expression of t-SNARE, syntaxin 1, and SNAP-25 in pancreatic β-cells is involved in impaired insulin secretion from diabetic GK rat islets: restoration of decreased t-SNARE proteins improves impaired insulin secretion. *Diabetes*, **48**, 2367–2373.

Namkung,Y. *et al*. (2001) Requirement for the L-type Ca^{2+} channel $\alpha 1_D$ subunit in postnatal pancreatic β cell generation. *J. Clin. Invest.*, **108**, 1015–1022.

Neher,E. (1998) Vesicle pools and Ca^{2+} microdomains: new tools for understanding their roles in neurotransmitter release. *Neuron*, **20**, 389–399.

Norman,R.A. *et al*. (1998) Autosomal genomic scan for loci linked to obesity and energy metabolism in Pima Indians *Am. J. Hum. Genet.*, **62**, 659–668.

Olofsson,C.S., Göpel,S.O., Barg,S., Galvanovskis,J., Ma,X., Salehi,A., Rorsman,P. and Eliasson,L. (2002) Fast insulin secretion reflects exocytosis of docked granules in mouse pancreatic B-cells. *Pflugers Arch.*, **444**, 43–51.

Parker,A. *et al*. (2001) A gene conferring susceptibility to type 2 diabetes in conjunction with obesity is located on chromosome 18p11. *Diabetes*, **50**, 675–680.

Pereverzev,A., Vajna,R., Pfitzer,G., Hescheler,J., Klockner,U. and Schneider,T. (2002) Reduction of insulin secretion in the insulinoma cell line INS-1 by overexpression of a $Ca_v2.3$ ($\alpha 1_E$) calcium channel antisense cassette. *Eur. J. Endocrinol.* **146**, 881–889.

Postic,C. *et al*. (1999) Dual roles for glucokinase in glucose homeostasis as determined by liver and pancreatic β cell-specific gene knockouts using Cre recombinase. *J. Biol. Chem.*, **274**, 305–315.

Pratley,R.E. *et al*. (1998) An autosomal genomic scan for loci linked to prediabetic phenotypes in Pima Indians. *J. Clin. Invest.*, **101**, 1757–1764.

Reetz,A., Solimena,M., Matteoli,M., Folli,F., Takei,K. and De Camilli,P. (1991) GABA and pancreatic β cells: colocalization of glutamic acid decarboxylase (GAD) and GABA with synaptic-like microvesicles suggests their role in GABA storage and secretion. *EMBO J.*, **10**, 1275–1284.

Regazzi,R. *et al*. (1995) VAMP-2 and cellubrevin are expressed in pancreatic β-cells and are essential for Ca^{2+}- but not for GTPγS-induced insulin secretion. *EMBO J.*, **14**, 2723–2730.

Renström,E., Eliasson,L., Bokvist,K. and Rorsman,P. (1996) Cooling inhibits exocytosis in single mouse pancreatic B-cells by suppression of granule mobilization. *J. Physiol.*, **494**, 41–52.

Ribalet,B. and Beigelman,P.M. (1981) Effects of divalent cations on β-cell electrical activity. *Am. J. Physiol.*, **241**, 59–67.

Rosario,L.M., Barbosa,R.M., Antunes,C.M., Silva,A.M., Abrunhosa,C.M. and Santos,R.M. (1993) Bursting electrical activity in pancreatic β-cells: evidence that the channel underlying the burst is sensitive to Ca^{2+} influx through L-type Ca^{2+} channels. *Pflugers Arch.*, **424**, 439–447.

Salehi,A., Chen,D., Håkansson,R., Nordin,G. and Lundquist,I. (1999) Gastrectomy induces impaired insulin and glucagon secretion: evidence for a gastro-insular axis in mice. *J. Physiol.*, **514**, 579–593.

Seisenberger,C. *et al*. (2000) Functional embryonic cardiomyocytes after disruption of the L-type α_{1C} ($Ca_v1.2$) calcium channel gene in the mouse. *J. Biol. Chem.*, **275**, 39193–3999.

Takahashi,N., Kadowaki,T., Yazaki,Y., Miyashita,Y. and Kasai,H. (1997) Multiple exocytotic pathways in pancreatic β cells. *J. Cell Biol.*, **138**, 55–64.

Tsunoda,K., Sanke,T., Nakagawa,T., Furuta,H. and Nanjo,K. (2001) Single nucleotide polymorphism (D68D, T to C) in the syntaxin 1A gene correlates to age at onset and insulin requirement in Type II diabetic patients. *Diabetologia*, **44**, 2092–2097.

UKPDS16 (United Kingdom Prospective Diabetes Study Group) (1995) Overview of 6 years therapy of type II diabetes: a progressive disease (UKPDS16). *Diabetes*, **44**, 1249–1258.

Vajna,R. *et al*. (2001) Functional coupling between 'R-type' Ca^{2+} channels and insulin secretion in the insulinoma cell line INS-1. *Eur. J. Biochem.*, **268**, 1066–1075.

Wang,W., Xu,J. and Kirsch,T. (2002) Annexin-mediated Ca^{2+} influx regulates growth plate chondrocyte maturation and apoptosis. *J. Biol. Chem.*, in press.

Wiser,O., Trus,M., Hernandez,A., Renström,E., Barg,S., Rorsman,P. and Atlas,D. (1999) The voltage sensitive Lc-type Ca^{2+} channel is functionally coupled to the exocytotic machinery. *Proc. Natl Acad. Sci. USA.*, **96**, 248–253.

Yang,S.N. *et al*. (1999) Syntaxin 1 interacts with the L(D) subtype of voltage-gated Ca^{2+} channels in pancreatic β cells. *Proc. Natl Acad. Sci. USA*, **96**, 10164–10169.

Zhang,W., Khan,A., Östenson,C-G., Berggren,P-O., Efendic,S. and Meister,B. (2002) Down-regulated expression of exocytotic proteins in pancreatic islets of diabetic GK rats. *Biochem. Biophys. Res. Commun.*, **291**, 1038–1044.

Received February 2, 2003; revised May 15, 2003; accepted June 16, 2003

II

Research article Related Commentary, page 16

$Ca_V2.3$ calcium channels control second-phase insulin release

Xingjun Jing,[1] Dai-Qing Li,[1] Charlotta S. Olofsson,[1] Albert Salehi,[1] Vikas V. Surve,[1] José Caballero,[1] Rosita Ivarsson,[1] Ingmar Lundquist,[1] Alexey Pereverzev,[2] Toni Schneider,[2] Patrik Rorsman,[3] and Erik Renström[1]

[1]Diabetes Programme at Lund University, Lund, Sweden. [2]Institute of Neurophysiology and Center of Molecular Medicine Cologne, University of Cologne, Cologne, Germany. [3]Diabetes Research Laboratories, Oxford Centre for Diabetes, Endocrinology and Metabolism, the Churchill Hospital, Oxford, United Kingdom.

Concerted activation of different voltage-gated Ca^{2+} channel isoforms may determine the kinetics of insulin release from pancreatic islets. Here we have elucidated the role of R-type $Ca_V2.3$ channels in that process. A 20% reduction in glucose-evoked insulin secretion was observed in $Ca_V2.3$-knockout ($Ca_V2.3^{-/-}$) islets, close to the 17% inhibition by the R-type blocker SNX482 but much less than the 77% inhibition produced by the L-type Ca^{2+} channel antagonist isradipine. Dynamic insulin-release measurements revealed that genetic or pharmacological $Ca_V2.3$ ablation strongly suppressed second-phase secretion, whereas first-phase secretion was unaffected, a result also observed in vivo. Suppression of the second phase coincided with an 18% reduction in oscillatory Ca^{2+} signaling and a 25% reduction in granule recruitment after completion of the initial exocytotic burst in single $Ca_V2.3^{-/-}$ β cells. $Ca_V2.3$ ablation also impaired glucose-mediated suppression of glucagon secretion in isolated islets (27% versus 58% in WT), an effect associated with coexpression of insulin and glucagon in a fraction of the islet cells in the $Ca_V2.3^{-/-}$ mouse. We propose a specific role for $Ca_V2.3$ Ca^{2+} channels in second-phase insulin release, that of mediating the Ca^{2+} entry needed for replenishment of the releasable pool of granules as well as islet cell differentiation.

Introduction

Systemic glucose tolerance is orchestrated by the regulated release of insulin and glucagon from the β and α cells of the pancreatic islets of Langerhans. The α and β cells are electrically excitable and use electrical signals to couple changes in blood glucose concentration to stimulation or inhibition of hormone release. In both cell types, influx of extracellular Ca^{2+} through voltage-gated Ca^{2+} channels with resultant elevation of intracellular Ca^{2+} concentration ($[Ca^{2+}]_i$) triggers exocytosis of the hormone-containing secretory granules. Like other electrically excitable cells, both α and β cells contain several types of voltage-gated Ca^{2+} channel (1, 2). Assigning physiological functions to the respective Ca^{2+} channels is central to the understanding of electrical and secretory activities in these cells.

Voltage-gated Ca^{2+} channels are divided into 3 subfamilies: (a) L-type high voltage–activated (HVA) Ca^{2+} channel family that comprises the $Ca_V1.1$, 1.2, 1.3, and 1.4 channels and is inhibited by dihydropyridines (DHPs) (1, 3, 4); (b) non–L-type HVA channels $Ca_V2.1$ (P/Q-type), 2.2 (N-type), and 2.3 (R-type) that are sensitive to ω-agatoxin IVA and ω-conotoxin GVIA and SNX482, respectively (1, 4, 5); and (c) the low voltage–activated (LVA) T-type Ca^{2+} channel family ($Ca_V3.1$, 3.2, and 3.3). The latter subtype differs electrophysiologically from the HVA Ca^{2+} channels in opening transiently already upon modest depolarization (6, 7) and fulfilling important roles in pacemaker cells (8).

The chain of events that couples an elevation in blood glucose to initiation of β cell electrical activity is well established and involves facilitated transport of the sugar into the β cell and its subsequent metabolic degradation by glycolysis and mitochondrial oxidation, resulting in closure of the ATP-sensitive K^+ channels (K_{ATP} channels) and β cell depolarization, with resultant activation of voltage-gated Ca^{2+} channels and regulated insulin exocytosis (9). Glucose-stimulated insulin secretion consists of a rapid first-phase of insulin secretion that lasts for approximately 10 minutes before declining to near-basal levels, followed by less prominent but sustained second-phase insulin secretion that can last for several hours (10, 11). The cellular mechanisms underlying biphasic insulin release remain unclear, but consensus exists that an elevation in $[Ca^{2+}]_i$ is required for both first- and second-phase insulin secretion (12). Type 2 diabetes is associated with a shift from biphasic to monophasic insulin release (10), and it is therefore important to establish the cell biology of insulin release kinetics.

In mouse pancreatic β cells, 50% of the whole cell Ca^{2+} current exhibits properties typical for L-type channels, is inhibited by DHP channel blockers such as isradipine or nifedipine, and is activated by BayK8644. The molecular identity of the β cell L-type Ca^{2+} channel involved in insulin secretion has been debated, but recent studies have established that $Ca_V1.2$ or $\alpha 1_C$ channels play a decisive role (13, 14).

In mouse β cells, there is evidence suggesting that the secretory granules and the L-type Ca^{2+} channels assemble into a tight functional complex (13, 15–17). Thanks to this organization, the β cells are capable of exocytosis at rates comparable to those encountered in chromaffin cells, although the Ca^{2+} channel density is only 5–10% of that in the latter cell type. This arrangement bears strong resemblance to the tight coupling of P/Q-type $Ca_V2.1$ as well as N-type $Ca_V2.2$ channels to rapid synaptic transmission (18, 19). No such interaction has been demonstrated for the R-type Cav2.3 channels.

Nonstandard abbreviations used: $[Ca^{2+}]_i$, intracellular Ca^{2+} concentration; $Ca_V2.3^{-/-}$, $Ca_V2.3$-knockout; DHP, dihydropyridine; fF, femtofarad(s); HVA, high voltage–activated; K_{ATP}, ATP-sensitive K^+; LVA, low voltage–activated; RRP, readily releasable pool.

Conflict of interest: The authors have declared that no conflict of interest exists.

Citation for this article: *J. Clin. Invest.* **115**:146–154 (2005). doi:10.1172/JCI200522518.

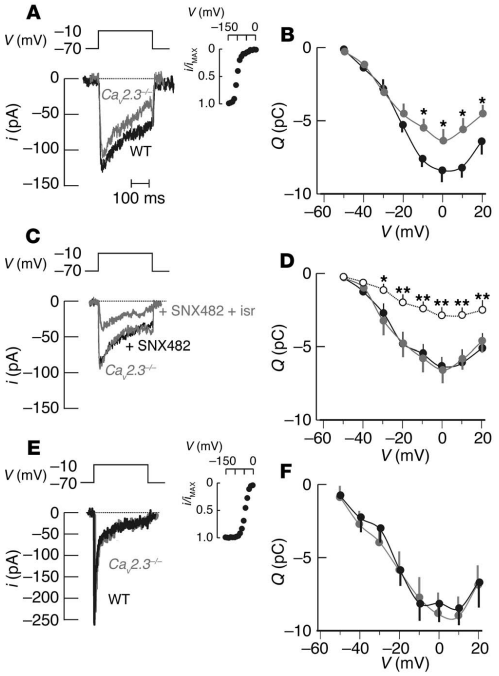

Figure 1
Whole-cell Ca^{2+} currents in islet cells from WT and $Ca_V2.3^{-/-}$ mice. (**A**) Whole-cell Ca^{2+} currents (*i*) evoked by a 300-ms voltage-clamp depolarization (*V*) in WT $Ca_V2.3^{+/+}$ (black) and $Ca_V2.3^{-/-}$ (gray) β cells. β cells were identified by exhibiting half-maximal Na^+ channel inactivation at membrane potentials (*V*) lower than –100 mV (half-maximal inactivation at –102 mV; inset). (**B**) Average integrated current-voltage (*Q-V*) relationships. Data are mean values ± SEM in 10 WT (filled circles) and 10 $Ca_V2.3^{-/-}$ (shaded circles) β cells. $^*P < 0.05$. (**C**) Whole-cell Ca^{2+} currents were recorded as in **A**, but using $Ca_V2.3^{-/-}$ β cells. The recordings were made under control conditions (lower gray line) in the presence of R-type Ca^{2+} channel blocker SNX482 (100 nM; black line) and after addition of L-type Ca^{2+} channel inhibitor isradipine (isr) (2 μM; upper gray line). (**D**) Average *Q-V* relationships representing mean values ± SEM in 4 $Ca_V2.3^{-/-}$ β cells under control conditions (shaded circles), in the presence of SNX482 (filled circles), and after addition of isradipine (open circles). $^*P < 0.05$, $^{**}P < 0.01$, control versus SNX482 plus isradipine. (**E**) Whole-cell Ca^{2+} currents were recorded as in **A**, but in α cells identified by Na^+ channel inactivation at membrane potentials greater than –100 mV (half-maximal inactivation at –49 mV; inset). (**F**) *Q-V* relationships in α cells. Data represent average values ± SEM in 8 WT (filled circles) and 4 $Ca_V2.3^{-/-}$ (shaded circles) α cells. pC, picocoulombs.

By contrast, recent evidence in neurons suggests that R-type channels are physically detached from the exocytotic machinery (20) and are not involved in rapid neurotransmission in mossy fibers (21).

About one-quarter of the β cell whole-cell Ca^{2+} current is sensitive to the R-type Ca^{2+} channel blocker SNX482, but the role of R-type Ca^{2+} channels in insulin secretion remains elusive. A general $Ca_V2.3$-knockout ($Ca_V2.3^{-/-}$) mouse has been established. It exhibits a relatively modest neurological phenotype, including altered pain responses (22), impaired spatial memory (23), and enhanced fear reaction (24). Pancreatic islets express the endocrine splice variant of $Ca_V2.3$ (25), and previous investigations of glucose homeostasis in $Ca_V2.3^{-/-}$ mice have demonstrated a slight glucose intolerance and reduced glucose-induced insulin secretion (26). Here we have extended these initial observations by performing in vivo glucose tolerance tests, dynamic measurements of phasic insulin secretion in situ, static pancreatic hormone–release experiments in isolated islets, as well as single cell recordings of whole-cell Ca^{2+} currents and exocytosis and ratiometric measurements of the cytoplasmic Ca^{2+} concentration in WT and $Ca_V2.3^{-/-}$ islets. We demonstrate that whereas R-type Ca^{2+} channels play a minor role in rapid insulin release, their significance becomes more apparent during second-phase secretion. These data point to an emerging picture where Ca^{2+} influx through different β cell Ca^{2+} channels play distinct functional roles.

Results

Whole cell Ca^{2+} currents in α and β cells from $Ca_V2.3^{+/+}$ and $Ca_V2.3^{-/-}$ mice. Integrated Ca^{2+} current versus voltage (*Q-V*) relations were measured in dissociated single pancreatic islet cells using the perforated-patch whole cell configuration. Insulin-releasing β cells were identified by the absence of voltage-gated Na^+ currents at membrane potentials relevant for β cell electrical activity, that is, between the β cell resting membrane potential (–70 mV) and the peak of the β cell action potential (–10 mV; Figure 1A, inset). In β cells from $Ca_V2.3^{-/-}$ mice, the integrated Ca^{2+} currents observed at membrane potentials less than or equal to –10 mV were reduced compared with WT cells. At –10 mV, the reduction averaged approximately 23% ($P < 0.05$; Figure 1B). The $Ca_V2.3^{-/-}$ mice exhibited a selective loss of a high-voltage Ca^{2+} current component, and current amplitudes at voltages below –10 mV were not affected. The R-type Ca^{2+} channel blocker SNX482 (100 nM) had no effect on voltage-gated Ca^{2+} currents in $Ca_V2.3^{-/-}$ mice, whereas the L-type inhibitor isradipine (2 μM) significantly reduced Ca^{2+} influx approximately 60% at potentials greater than or equal to –30 mV ($P < 0.05$; Figure 1, C and D).

Cells exhibiting Na^+ currents when holding at –70 mV (Figure 1E, inset) were classified as non–β cells and likely represent glucagon-releasing α cells (27). The frequency of α cells was much lower in dispersed islet cells from $Ca_V2.3^{-/-}$ mice than cells made from WT islets. Counting all cells that could be functionally defined as belonging to either group, only approximately 7% of the $Ca_V2.3^{-/-}$ cells could be classified as α cells versus approximately 27% of the WT cells. In 4 cells from $Ca_V2.3^{-/-}$ mice with the electrophysiological properties expected for α cells, the Ca^{2+} current amplitude was not different from that observed in WT cells (Figure 1, E and F).

Single cell exocytosis in $Ca_V2.3^{-/-}$ and $Ca_V2.3^{+/+}$ mice. Ca^{2+}-elicited exocytosis in β cells was monitored as increases in whole-cell membrane capacitance and was elicited by trains of 10 500-ms voltage

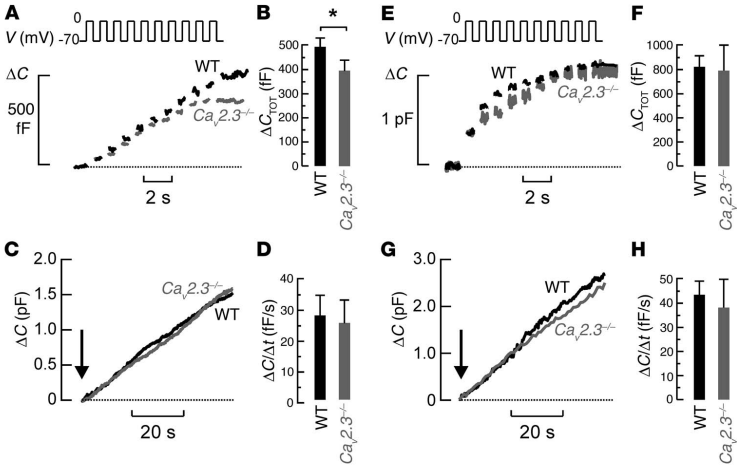

Figure 2
Effects of $Ca_V2.3$ ablation on single-cell exocytosis in islet cells. (**A**) Exocytosis evoked by trains of 10 depolarizations (*V*) and monitored as increases in cell capacitance (Δ*C*) in WT $Ca_V2.3^{+/+}$ (black) and $Ca_V2.3^{-/-}$ (gray) β cells. (**B**) Average total increase in capacitance evoked by the trains (ΔC_{TOT}). Data are mean values ± SEM in 6 WT (black bars) and 7 $Ca_V2.3^{-/-}$ (gray bars) β cells. *$P < 0.05$. (**C**) Δ*C* evoked by intracellular dialysis of a Ca^{2+}-containing patch electrode solution (free $[Ca^{2+}]_i$, approximately 1.5 μM) in WT (black) and $Ca_V2.3^{-/-}$ (gray) β cells. (**D**) Average rates of exocytosis ($\Delta C/\Delta t$) ± SEM evoked by Ca^{2+} dialysis in 10 WT (black bars) and 10 $Ca_V2.3^{-/-}$ (gray bars) β cells. (**E** and **F**) Exocytosis and average Δ*C* were recorded as in **A** and **B**, but results are from α cells, and averages represent 5 WT (black) and 3 $Ca_V2.3^{-/-}$ (gray) α cells. (**G** and **H**) Δ*C* and average rates of exocytosis were recorded as in **C** and **D**, but the data are from α cells, and mean responses are from 6 WT (black) and 3 $Ca_V2.3^{-/-}$ (gray) α cells. pF, picofarads.

clamp depolarizations from the holding potential –70 mV to 0 applied at 1 Hz (Figure 2, A and B). In β cells from $Ca_V2.3^{-/-}$ mice, the increase in cell capacitance during the train averaged 392 ± 47 femtofarads (fF) ($n = 7$). The latter value is 21% less than the exocytotic response evoked by the same stimulus in WT mice ($P < 0.05$; 496 ± 42 fF; $n = 6$). Interestingly, the early component of exocytosis (in response to the first depolarization) was not affected and averaged 55 ± 19 fF and 57 ± 22 fF in WT and $Ca_V2.3^{-/-}$ β cells, respectively. Instead, selective suppression of the late component of exocytosis was observed. The 23% reduction of the whole cell Ca^{2+} current observed in the $Ca_V2.3^{-/-}$ β cells corresponded nicely with the overall reduction in exocytosis, suggesting that exocytotic capacity as such was not affected. This idea was reinforced by the observation that exocytotic rates, measured during intracellular dialysis of a Ca^{2+}-containing pipette solution using the standard whole-cell configuration, were identical in β cells from both mouse strains (Figure 2, C and D). In the few α cells that could be identified in $Ca_V2.3^{-/-}$ mice, exocytosis was not different from that observed in WT, either when elicited by train depolarizations ($n = 3$) or Ca^{2+} buffer dialysis ($n = 3$; Figure 2, E–H).

Effects of $Ca_V2.3$ ablation on intracellular Ca^{2+} homeostasis. Insulin secretion is initiated by changes in the submembrane cytoplasmic free $[Ca^{2+}]_i$ (28, 29), which are determined by β cell electrical activity. We therefore monitored $[Ca^{2+}]_i$ under basal conditions as well as after the addition of glucose, the K_{ATP} channel blocker tolbutamide, or following depolarization with high extracellular K^+ (Figure 3). Resting $[Ca^{2+}]_i$ measured at 5 mM glucose was identical in islets from $Ca_V2.3^{-/-}$ and WT mice and averaged approximately 90 nM. In WT islets, elevation of extracellular glucose from 5 to 15 mM evoked an initial robust elevation in $[Ca^{2+}]_i$ after 204 ± 33 seconds ($n = 7$). This initial peak decayed slowly (over 4–10 minutes) toward baseline and was eventually followed by a pattern of repetitive $[Ca^{2+}]_i$ oscillations. Subsequent depolarization by the nonmetabolizable stimuli tolbutamide and high K^+ in the continued presence of glucose elicited a rapid elevation of $[Ca^{2+}]_i$ but did not result in oscillatory activity. In $Ca_V2.3^{-/-}$ islets, the glucose-evoked initial peak in $[Ca^{2+}]_i$ occurred 227 ± 15 seconds ($n = 9$) after elevating the glucose concentration. This initial amplitude was almost unaffected (7% decrease), but the time-averaged $[Ca^{2+}]_i$ during the subsequent oscillatory phase was 17% lower than in WT islets ($P < 0.01$). In addition, the oscillatory activity was 29% slower

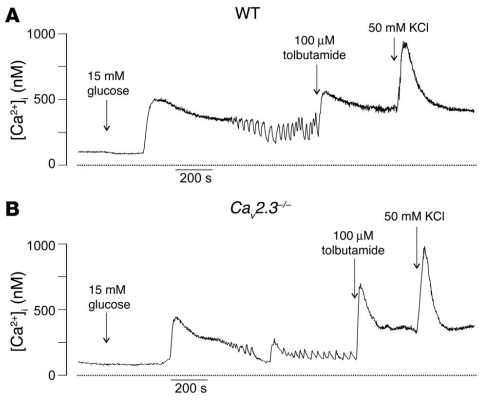

Figure 3
Ca^{2+} homeostasis in WT and $Ca_V2.3^{-/-}$ islets. (**A**) $[Ca^{2+}]_i$ in an intact WT $Ca_V2.3^{+/+}$ islet assayed by ratiometric fura-2 measurements. The islets were stimulated at the time points indicated by the arrows in the continued presence of previously added stimuli. (**B**) $[Ca^{2+}]_i$ was determined as in **A**, but the experiment was performed in an intact $Ca_V2.3^{-/-}$ islet. Recordings selected for display are representative of 7 and 9 separate experiments in WT and $Ca_V2.3^{-/-}$ islets, respectively. Statistical significances are provided in the text.

Table 1
Insulin secretion in response to in vivo glucose challenge in WT $Ca_V2.3^{+/+}$ and $Ca_V2.3^{-/-}$ mice

	Time after i.p. glucose challenge (min)	WT	$Ca_V2.3^{-/-}$
Plasma glucose (mmol/l)	0	9.8 ± 0.6	11.5 ± 0.8[A]
	3	16.4 ± 2.1	18.9 ± 1.7
	8	23.0 ± 2.1	26.5 ± 2.1[A]
Plasma insulin (pmol/l)	0	163.0 ± 15.5	170.1 ± 14.8
	3	229.4 ± 29.6	207.5 ± 11.1
	8	244.4 ± 17.8	185.2 ± 18.5[A]
Plasma glucagon (ng/l)	0	194.0 ± 15.1	175.7 ± 6.1
	3	169.6 ± 13.2	197.0 ± 7.7[A]
	8	148.5 ± 13.5	130.3 ± 4.9

Average values for plasma glucose, insulin, and glucagon concentrations ± SEM immediately before and 3 and 8 minutes after an i.p. glucose challenge (2 g/kg body weight) in 8 WT and 9 $Ca_V2.3^{-/-}$ mice. Levels of statistical significance are shown only for comparisons between WT and $Ca_V2.3^{-/-}$ data. [A]$P < 0.05$.

in the $Ca_V2.3^{-/-}$ islets (1.8 ± 0.1 versus 2.5 ± 0.2 bursts/minute in $Ca_V2.3^{-/-}$ and WT islets, respectively; $P < 0.01$). By contrast, the peaks in $[Ca^{2+}]_i$ induced by depolarization with tolbutamide or high K^+ were, if anything, slightly augmented in the $Ca_V2.3^{-/-}$ islets (NS versus control). The finding that no $[Ca^{2+}]_i$ oscillations were observed at 5 mM glucose and that elevating the glucose concentration to 15 mM increased Ca^{2+} signaling suggests that the signal principally reflects the behavior of the pancreatic β cells (see ref. 30).

In vivo glucose tolerance and pancreatic hormone release in $Ca_V2.3^{-/-}$ mice. In vivo glucose homeostasis was investigated by intraperitoneal glucose challenges (2 g/kg body weight; Table 1). Basal (nonfasted) plasma glucose levels averaged 9.8 ± 0.6 mmol/l ($n = 8$) in WT $Ca_V2.3^{+/+}$ mice and increased 67% and 135% 3 and 8 minutes after the glucose load, respectively. In $Ca_V2.3^{-/-}$ mice, basal glucose levels were elevated by 17% compared with WT ($P < 0.05$ versus WT; $n = 9$), and the plasma glucose concentrations measured 3 and 8 minutes after challenge were also elevated approximately 15% ($P < 0.05$ for values at 8 minutes versus WT). Basal plasma insulin levels did not differ between the $Ca_V2.3^{-/-}$ and $Ca_V2.3^{+/+}$ strains, although the plasma glucose concentration was somewhat higher in the former mice. In WT mice, glucose increased plasma insulin concentrations 43% and 52% 3 and 8 minutes after the challenge, respectively. In $Ca_V2.3^{-/-}$ mice, the glucose-induced increase in circulating insulin was similar to that in WT mice 3 minutes after challenge, but after 8 minutes it was limited to less than 10% ($P < 0.05$ versus WT). These findings reinforce previous observations indicating an impaired glucose tolerance of the $Ca_V2.3^{-/-}$ mice (26).

We also monitored plasma glucagon concentrations during the glucose challenge. Basal glucagon levels in $Ca_V2.3^{-/-}$ mice were modestly decreased (approximately 10%) compared with $Ca_V2.3^{+/+}$ littermates. In WT mice, the glucose load reduced circulating glucagon 15% already at 3 minutes after challenge, and an additional 8% decrease was observed at 8 minutes. In $Ca_V2.3^{-/-}$ mice, the inhibition of glucagon release was sluggish. At 3 minutes after challenge, plasma glucagon concentrations actually *increased* 18% ($P < 0.05$ versus basal; $n = 9$).

Insulin and glucagon release in vitro in pancreatic islets. Pancreatic islets in situ receive extensive neuronal input from parasympathetic nerve endings (31). Since $Ca_V2.3$ Ca^{2+} channels are also expressed in neuronal tissue, their ablation might affect pancreatic hormone release in vivo by indirect mechanisms and not by directly affecting α and β cell function. Insulin and glucagon secretion was therefore also investigated in isolated islets. The first set of experiments investigated the effects of L-type and R-type channel blockers isradipine and SNX482, respectively, in WT $Ca_V2.3^{+/+}$ islets (Table 2). Basal insulin release (1 mM glucose) was low and was unaffected by either channel blocker. Elevation of extracellular glucose to 20 mM stimulated insulin release more than 15-fold. Isradipine (2 μM) suppressed glucose-stimulated insulin release 77%, whereas SNX482 (100 nM) reduced insulin secretion 17% (Table 2). The latter value agrees favorably with the inhibition observed in capacitance measurements (see Figure 2, A and B). Glucagon release was measured under the same conditions. At 1 mM glucose glucagon release was high and remained unchanged by either isradipine or SNX482. Elevating the glucose concentration (20 mM) reduced glucagon secretion 70% ($P < 0.001$; low versus high glucose). At high glucose, blockade of R-type channels by SNX482 failed to affect glucagon release, whereas isradipine *stimulated* glucagon secretion under the same condition.

We next compared the effects of the Ca^{2+} channel blockers with the consequences of $Ca_V2.3$ gene ablation on pancreatic hormone release (Table 3). In WT $Ca_V2.3^{+/+}$ islets, elevating glucose from 1 to 20 mM again stimulated insulin release more than 15-fold. In $Ca_V2.3^{-/-}$ islets, glucose-stimulated insulin release was reduced approximately 25% compared with WT. The effects of isradipine on glucose-stimulated insulin release were comparable in WT (66% reduction) and in $Ca_V2.3^{-/-}$ islets (68% suppression). Insulin secretion elicited by stimulation with high extracellular K^+ (50 mM) resulted in a 75% enhancement of release relative to that observed in the presence of glucose alone in WT islets. A similar relative stimulation was observed in $Ca_V2.3^{-/-}$ islets (96%), but in absolute terms, the response in the latter type of islets was reduced 13% compared with WT islets. Surprisingly, whereas elevating glucose from 1 to 20 mM suppressed glucagon release 58% in WT $Ca_V2.3^{+/+}$ islets ($P < 0.001$; low versus high glucose), the inhibitory action of the sugar was severely impaired in the $Ca_V2.3^{-/-}$ islets and amounted to a mere 27% ($P < 0.01$ versus WT). Isradipine exerted divergent actions in WT and $Ca_V2.3^{-/-}$ islets. As discussed above, in WT islets the

Table 2
Effects of Ca^{2+} channel inhibitors on in vitro insulin and glucagon release in WT $Ca_V2.3^{+/+}$ islets

Condition	Insulin secretion (ng/islet/h)	Glucagon secretion (pg/islet/h)
1 mM glucose	0.2 ± 0.03	38.4 ± 3.0
1 mM glucose + 2 μM isradipine	0.2 ± 0.05	36.7 ± 6.1
1 mM glucose + 100 nM SNX482	0.3 ± 0.03	38.5 ± 4.5
20 mM glucose	2.6 ± 0.2[A]	12.8 ± 4.7[A]
20 mM glucose + 2 μM isradipine	0.7 ± 0.08[A,B]	22.8 ± 2.1[A,C]
20 mM glucose + 100 nM SNX482	2.3 ± 0.2[A]	16.2 ± 4.1[D]

Average values for insulin and glucagon release ± SEM measured in 60-minute batch incubations of 10 islets from WT $Ca_V2.3^{+/+}$ mice under conditions as indicated. Data are from 10 independent experiments. [A]$P < 0.001$, [D]$P < 0.05$ versus the same condition in 1 mM glucose; [B]$P < 0.001$, [C]$P < 0.05$ versus 20 mM glucose alone.

Table 3
Effects of $Ca_V2.3$ ablation on in vitro insulin and glucagon release

	Insulin release (ng/islet/h)		Glucagon release (pg/islet/h)	
	WT	$Ca_V2.3^{-/-}$	WT	$Ca_V2.3^{-/-}$
1 mM glucose	0.2 ± 0.02	0.4 ± 0.05	39.8 ± 1.3	40.9 ± 1.8
20 mM glucose	3.1 ± 0.3	2.4 ± 0.1[A]	16.9 ± 1.5	29.8 ± 3.5[A]
20 mM glucose + 2 μM isradipine	0.8 ± 0.09[B]	1.1 ± 0.1[B]	25.7 ± 1.9[C]	20.3 ± 2.3[D]
20 mM glucose + 50 mM K^+	5.4 ± 0.2[B]	4.7 ± 0.3[B,D]	71.7 ± 6.5[E]	94.8 ± 10.6[A,B]

Average values for insulin and glucagon release measured in 60-minute batch incubations of 10 WT $Ca_V2.3^{+/+}$ and $Ca_V2.3^{-/-}$ islets under conditions as indicated. Data represent means ± SEM of 18 experiments in each group. [A]$P < 0.01$, [E]$P < 0.05$ for comparisons between WT and $Ca_V2.3^{-/-}$; [B]$P < 0.001$, [C]$P < 0.01$, [D]$P < 0.05$ versus results obtained in 20 mM glucose alone.

L-type Ca^{2+} channel antagonist stimulated glucagon release 52% when applied in the presence of 20 mM glucose. By contrast, isradipine reduced glucagon secretion in $Ca_V2.3^{-/-}$ islets 32% under high-glucose conditions. Increasing extracellular K^+ enhanced glucagon secretion massively, approximately 320% in WT and 220% in $Ca_V2.3^{-/-}$ islets.

Phasic insulin release measured by in situ pancreatic perfusion. To assess the role of $Ca_V2.3$ in dynamic insulin release, we performed in situ pancreatic perfusions with fractionated sampling. When WT $Ca_V2.3^{+/+}$ pancreata were perfused (Figure 4A) with a low-glucose solution (3.3 mM), insulin release was barely detectable. After increasing the glucose concentration to 16.7 mM (at t = 11 minutes), first-phase insulin release was initiated with a 2-minute delay. The peak in first-phase insulin secretion was attained 2 minutes after onset of release (t = 15 minutes) and measured 8.8 ± 1.7 ng/ml (n = 4). Insulin release then exhibited a transient nadir phase (t = 18–21 minutes) during which release rates averaged 4–5 ng/ml, before accelerating again during second-phase insulin secretion to approximately 18 ng/ml at t = 36 minutes and later. When the same experiment was repeated in $Ca_V2.3^{-/-}$ pancreata (Figure 4B), the peak in first-phase insulin secretion was only slightly reduced (19%) and measured 7.1 ± 2.1 ng/ml (NS; n = 4). More importantly, second-phase insulin release was markedly suppressed and averaged 9.4 ± 2.7 ng/ml at t = 40 minutes, representing a 46% reduction compared with WT ($P < 0.05$).

Genetic ablation of Cav2.3 may result in compensatory mechanisms resulting in rearrangements of the Ca^{2+} channels in the β cell itself or neighboring α and δ cells. In addition, we wanted to verify that the observed effects of $Ca_V2.3$ on insulin secretion are not limited to the background C57B mouse strain. Similar experiments were therefore made in pancreata from standard inbred NMRI mice, but instead $Ca_V2.3$ channel function was inhibited by SNX482. In the absence of the channel inhibitor, first-phase insulin secretion was initiated with a 2-minute delay and peaked 1 minute, 30 seconds later when it measured 15.3 ± 2.5 ng/ml (n = 6).

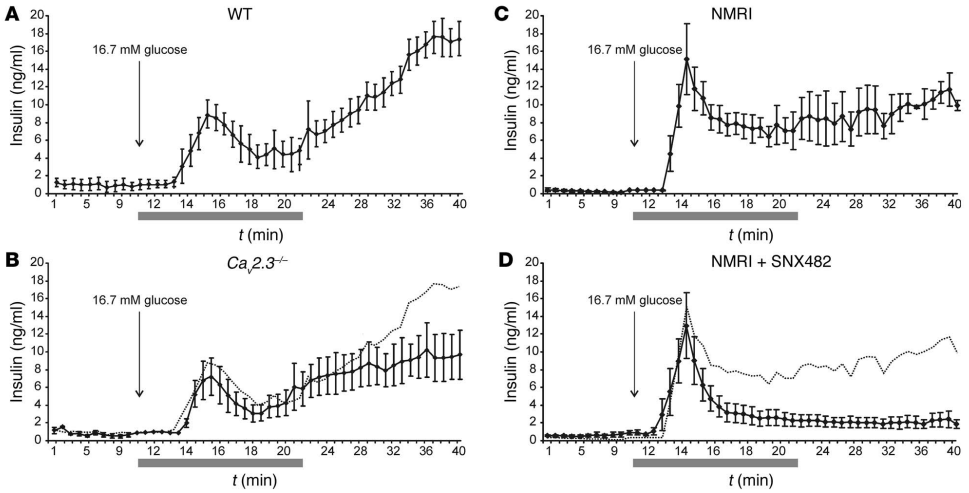

Figure 4
Dynamics of insulin release. (**A**) Insulin release measured in WT $Ca_V2.3^{+/+}$ pancreata before and after increasing the glucose concentration in the perfusate from 3.3 mM to 16.7 mM at t = 11 minutes. Samples were taken at 60-second intervals, except during the first 10 minutes after increasing the glucose concentration (t = 11 to 21 minutes, as indicated by the gray bar) when the sample interval was 30 seconds. (**B**) Insulin release was measured as in **A**, but the experiments were performed in $Ca_V2.3^{-/-}$ mice. To facilitate comparison with WT, mean values measured under that condition are indicated by the dotted line. Data in **A** and **B** represent means ± SEM from 4 and 5 experiments in WT and $Ca_V2.3^{-/-}$ mice, respectively. (**C**) Insulin release was measured as in **A**, but the experiments were performed in NMRI mice. (**D**) Insulin release was measured as in **C**, but SNX482 (100 nM) was included in the high-glucose solution. To facilitate comparison with mean values measured in the absence of SNX482, these values are denoted by the dotted line. Data in **C** and **D** represent means ± SEM from 6 experiments performed with and without SNX482, respectively. Statistical significance is provided in Results.

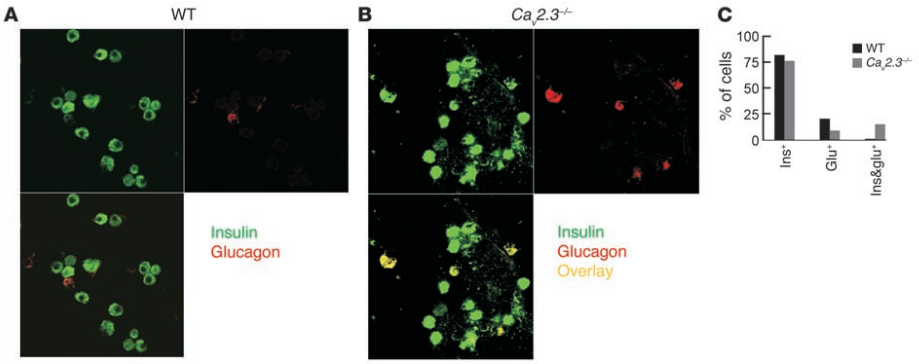

Figure 5
Confocal immunocytochemistry of insulin and glucagon immunoreactivity in single islet cells. (**A**) Insulin and glucagon immunoreactivity in dispersed WT islet cells visualized by confocal microscopy. (**B**) Insulin and glucagon immunoreactivity was visualized as in **A**, but cells are from $Ca_V2.3^{-/-}$ islets. (**C**) Relative distribution of insulin, glucagon, and double immunoreactivity (Ins^+, Glu^+, and $Ins\&glu^+$, respectively) in WT $Ca_V2.3^{+/+}$ (black bars) and $Ca_V2.3^{-/-}$ (gray bars) islet cells. Data represent more than 200 cells in each group and are from 3 different experiments.

Insulin release then decayed toward a lower plateau level of approximately 8 ng/ml and increased slightly to approximately 10 ng/ml during the second phase (Figure 4C). When SNX482 (100 nM) was included in the perfusate (Figure 4D), first-phase insulin release was largely unaffected, and peak values averaged 13.0 ± 3.7 ng/ml (n = 6). By contrast, second-phase insulin secretion was reduced more than 80% (e.g., 1.8 ± 0.6 ng/ml versus 10.0 ± 0.6 ng/ml at t = 40 minutes in the presence or absence of SNX482, respectively; $P < 0.01$). It was verified that the glucose concentration in the effluent medium was identical in all experiments.

Insulin and glucagon immunoreactivity in WT and $Ca_V2.3^{-/-}$ islet cells. Islet cells were finally dispersed and investigated by confocal immunocytochemistry (Figure 5). In WT islet cells, 80% of the dispersed cells revealed immunoreactivity for insulin and approximately 20% stained positive for glucagons in double-labeling experiments. The relative frequency of α and β cells suggested by this analysis compares favorably with the electrophysiological data. Only 1 out of 230 cells investigated revealed immunoreactivity for both insulin and glucagons. A rather different picture emerged in the $Ca_V2.3^{-/-}$ islet cell preparation. Whereas 75% and 9% of the cells could readily be characterized as β and α cells, respectively, 16% of the 210 cells coexpressed insulin and glucagons.

Discussion

Insulin-producing β cells contain multiple types of Ca^{2+} channel. Whereas the role of L-type Ca^{2+} channels in insulin secretion is amply documented, that of the non–L-type Ca^{2+} channels is less well understood. The advent of subtype-specific Ca^{2+} channel blockers in combination with the generation of transgenic knockout mice provides a unique opportunity for an in-depth analysis of the function(s) fulfilled by the different Ca^{2+} channel subtypes. Here we have used SNX482 and $Ca_V2.3$-null mice to study the significance of R-type $Ca_V2.3$ Ca^{2+} channels in islet insulin and glucagon secretion in vivo and in vitro.

The role of $Ca_V2.3$ channels for β cell $[Ca^{2+}]_i$ homeostasis and insulin secretion. Here we demonstrate that pharmacological inhibition of R-type $Ca_V2.3$ Ca^{2+} channels using SNX482 does not affect first-phase insulin secretion, but reduces second-phase release a dramatic 80%. A similar preferential effect on late-phase insulin secretion is observed in $Ca_V2.3^{-/-}$ mice (Figure 4). At the single β cell level, close inspection of the capacitance recordings (Figure 2, A and B) reveals that the initial component of exocytosis is not much affected in $Ca_V2.3^{-/-}$ β cells. In fact, the overall reduction results exclusively from suppression of the late component of exocytosis (elicited by the third and subsequent depolarizations). We have previously demonstrated that opening of L-type $Ca_V1.2$ Ca^{2+} channels is tightly associated with rapid exocytosis and first-phase secretion. Thus, it appears that Ca^{2+} entry via L-type $Ca_V1.2$ and R-type $Ca_V2.3$ channels have distinct intracellular effects.

$Ca_V2.3$ ablation is associated with a 23% decrease in β cell Ca^{2+} current in $Ca_V2.3^{-/-}$ mice (Figure 1). This is in good agreement with the response to acute application of SNX482 in WT mice (13), suggesting that there is little compensatory upregulation of other Ca^{2+} channels in the knockout mice. We acknowledge that $Ca_V2.3$ channel activity may represent only part of the R-type current component (24, 32). In addition, other reports suggest that all R-type current components are not blocked by SNX482 with the same efficacy (33). The observation that SNX482 fails to affect whole cell Ca^{2+} currents in $Ca_V2.3^{-/-}$ β cells (Figure 1, C and D), however, indicates at least that SNX482, at the concentration used here (100 nM), does not affect any Ca^{2+} channels other than $Ca_V2.3$, but we cannot exclude the contribution of an SNX482-insensitive R-type Ca^{2+} current component. Indeed, approximately 40% of the whole cell Ca^{2+} current is unaffected by either SNX482 or the L-type blocker isradipine in $Ca_V2.3^{-/-}$ β cells. Although most of this current probably represents P/Q-type Ca^{2+} currents as previously shown for WT β cells (13), it is possible that part of it reflects a SNX482-resistant portion of the R-type Ca^{2+} current.

How do $Ca_V2.3$ Ca^{2+} channels regulate second-phase insulin secretion? Secretory granules in pancreatic β cells can be classified according to their release competence (34). A limited (1–5%) pool is immediately available for rapid exocytosis upon stimulation (readily releasable pool, RRP). Once this pool of granules has been

released, exocytosis proceeds at a slower rate determined by the supply of granules newly mobilized from a much larger reserve pool (35). The observation that only a late component of exocytosis is affected in $Ca_V2.3^{-/-}$ β cells (Figure 2, A and B) argues that $Ca_V2.3$ channels are not tightly coupled to exocytosis but are more important for the recruitment of new granules for release. We also demonstrate that genetic ablation of the $Ca_V2.3$ Ca^{2+} channels results in approximately 20% reduction of the glucose-induced steady-state time-averaged $[Ca^{2+}]_i$ (more than 5 minutes after initial response; Figure 3). Can these 2 pieces of information be reconciled? We have reported previously that a moderate (40%) but protracted elevation of $[Ca^{2+}]_i$ results in strong enhancement of the exocytotic capacity (36). It is of interest that this effect is mediated by a global rather than a localized increase in $[Ca^{2+}]_i$ and is operational already at concentrations as low as 200–300 nM, that is, 10-fold lower than those required to elicit fast exocytosis. Thus, even moderate reduction of Ca^{2+} entry and $[Ca^{2+}]_i$ following inhibition of $Ca_V2.3$ Ca^{2+} channels can have strong effects on insulin secretion in the longer term by inhibition of granule recruitment. Presumably, L-type Ca^{2+} channels still trigger granule exocytosis, but once the RRP is depleted, the supply of new granules for release becomes rate limiting. This would explain how ablation of the approximately 20% $Ca_V2.3$ Ca^{2+} channel component can result in approximately 50% (knockout) to 80% (SNX482) reduction of second-phase insulin secretion. Thus, it seems justifiable to conclude that Ca^{2+} entry via R-type $Ca_V2.3$ Ca^{2+} channels is functionally (and perhaps spatially) linked to granule mobilization and priming of insulin granules for release.

$Ca_V2.3$ ablation and glucagon secretion. $Ca_V2.3$ ablation is associated with disturbances of glucagon secretion. In isolated islets, the ability of glucose to suppress glucagon secretion is severely impaired (Table 3). These abnormalities are also detectable at the systemic level. In the in vivo glucose challenge test, 3-minute values for plasma glucagon were *stimulated* approximately 15% in $Ca_V2.3^{-/-}$ mice, whereas in WT they were *reduced* approximately 20% (Table 1). The observations that whole cell Ca^{2+} currents (Figure 1, E and F) and single cell exocytosis (Figure 2, E–H) are unaffected in $Ca_V2.3^{-/-}$ α cells, taken together with the finding that the R-type blocker SNX482 fails to affect glucagon release in WT islets (Table 2), make it unlikely that these effects are the direct consequence of the loss of $Ca_V2.3$ in the α cell. Rather, the explanation for the perturbation of glucose-inhibited glucagon release in $Ca_V2.3$-ablated mice appears to be due to the appearance of atypical α/β cells accounting for greater than 60% of the glucagon-expressing cells in these mice (Figure 5, B and C). Taken together with the scarcity of cells with α cell electrophysiological properties in preparations from $Ca_V2.3^{-/-}$ mice (7% compared with 27% in WT mice), this suggests that the α/β cells electrical behavior is more like that of the β cells. This idea is supported by the results in Table 3, showing that whereas isradipine suppresses glucagon release in $Ca_V2.3^{-/-}$ islets, it has the opposite effect in WT islets. This observation also provides a clue to the relative failure of glucose to suppress glucagon release in $Ca_V2.3^{-/-}$ islets both in vitro and (acutely) in vivo. The fact that glucagon eventually decreases after a glucose challenge in vivo may be related to neuronal input or paracrine effects that are known to be of great importance for the control of the hyperglycemic hormone (37). Surprisingly, basal glucagon release (at low glucose) is unaffected in $Ca_V2.3^{-/-}$ islets. One possibility is that the reduced population of normal α cells have a very large capacity for exocytosis, but the capacitance measurements (Figure 2, E–H) provide no support for this notion. Another explanation is that the α/β cells exhibit poorly regulated exocytosis and constitutively release both glucagon and insulin. This idea is reinforced by the observation that basal insulin release in $Ca_V2.3^{-/-}$ islets is higher than in WT islets (0.4 ± 0.05 versus 0.2 ± 0.02 ng/islet/hour in $Ca_V2.3^{-/-}$ and WT, respectively; Table 3). Yet another possibility is that glucagon coreleased with insulin from the α/β cells potentiates further secretion by a cAMP-dependent mechanism. We have reported elsewhere that glucagon increases β cell exocytosis 5-fold (38). The significance of paracrine mechanisms within the islet is apparent from the strong stimulatory action of isradipine on glucagon secretion in WT islets (Tables 2 and 3). The latter effect may reflect the relief from paracrine inhibition of glucagon secretion exerted by Zn^{2+} and GABA cosecreted with insulin from the β cells (39, 40). Preliminary data from our laboratory indicate that R-type $Ca_V2.3$ Ca^{2+} channels play a decisive role in somatostatin secretion from the δ cells (Q. Zhang, A. Salehi, E. Renström, and P. Rorsman, unpublished observations). We can exclude that the loss of physiological glucose inhibition of glucagon secretion is secondary to relief from paracrine inhibition by somatostatin, however, since the dysregulation of glucagon secretion in $Ca_V2.3^{-/-}$ islets is not mimicked by SNX482.

Role of $Ca_V2.3$ in islet cell differentiation. A surprising finding in the present study is that the majority of the glucagon immunoreactive cells in $Ca_V2.3^{-/-}$ islets coexpress insulin, indicating that $Ca_V2.3$ channels play a role in the development of mature α cells. A transient peak in $Ca_V2.3$ channel expression in glial cells along specific CNS pathways has been demonstrated to coincide with postnatal myelinization of the white matter in the rat (41). It can be speculated that $Ca_V2.3$ channel expression exerts a similar action in defining the differentiated mature islet cell lineages, but the exact underlying mechanism remains to be established.

Pathophysiological implications. Although R-type $Ca_V2.3$ channels appear to be of little importance for first-phase insulin secretion and their contribution becomes apparent only during late exocytosis/second-phase insulin secretion, this does not mean that they are unimportant for systemic glucose homeostasis. Indeed, the $Ca_V2.3^{-/-}$ mice exhibited basal hyperglycemia (Table 1). In humans, $Ca_V2.3$ is encoded by the *CACNA1E* gene, which is located on chromosome 1q25–31. Interestingly, a chromosomal region around 1q25 reveals linkage to type 2 diabetes in several independent studies in different populations. These include early onset type 2 diabetes in Pima Indians (42), Utah Caucasians (43), and English sib pairs (44). In addition, the 1q25–32 region demonstrates linkage with elevated blood glucose levels in the Framingham Heart Study (45). It is also pertinent that the above region confers defective insulin secretion in type 2 diabetes in Pima Indians (46). Type 2 diabetes is a multifactorial polygenic disorder. Clearly, polymorphisms in the *CACNA1E* gene alone are not sufficient to trigger disease. Given the present functional data, however, it is tempting to speculate that dysfunctional $Ca_V2.3$ Ca^{2+} channels may frequently be involved in creating the disturbed β cell phenotype in type 2 diabetes.

Methods

Experimental animals. As previously reported (26), the *CACNA1E* gene encoding $Ca_v2.3$ was disrupted in vivo by deleting a region containing exon 2 on mating $Ca_v2.3^{fl/+}$ and deleter mice on a C57Bl/6 background

that expresses *Cre* recombinase constitutively under the control of the CMV promoter. $Ca_V2.3^{+/-}$ mice containing 1 cre transgene were inbred, and pups with the $Ca_V2.3^{-/-}$ genotype were selected and transferred by embryo transfer into a SPF facility. The transfer included breeding with C57Bl/6 mice and resulted in heterozygous $Ca_V2.3^{+/-}$ mice. Only cre-negative pups were selected and inbred, yielding either $Ca_V2.3^{+/+}$ or $Ca_V2.3^{-/-}$ mice. Thus, the $Ca_V2.3^{+/+}$ and $Ca_V2.3^{-/-}$ mice used in this study have an identical genetic background. In Figure 4, inbred NMRI mice purchased from Charles River Wiga GmbH were used.

The mice were housed at a constant temperature (22–23°C) and 12-hour light cycles (6:00 a.m.–6:00 p.m.), with access to standard pellet food and water ad libitum. All experiments were evaluated and approved by the local ethical committee Malmö/Lund djurförsöksetiska nämnd, Lund District Court, Sweden.

Islet isolation and islet cell preparation. The mice were sacrificed by cervical dislocation, and collagenase was administered into the pancreas by retrograde injection via the pancreatic duct. After 15–20 minutes' incubation at 37°C, the islet suspension was washed 4 times with HBSS (4°C) before being manually collected. The islets were cultured in RPMI-1640 medium (Invitrogen Corp.) supplemented with 10% FCS, penicillin, and streptomycin. For the preparation of single cells, islets obtained by collagenase digestion were dissociated by incubation and gentle triculation in Ca^{2+}-free medium. The resulting cell suspension was centrifuged, the supernatant discarded, and the pellet (containing the cells) was resuspended in RPMI-1640 medium, plated on plastic Nunc 35-mm Petri dishes, and maintained in tissue culture for up to 2 days.

Electrophysiology. The measurements were conducted using an EPC-10 patch-clamp amplifier in conjunction with the PULSE software suite (version 8.53; HEKA Elektronik). Whole-cell Ca^{2+} currents were measured in intact cells using the perforated-patch whole-cell approach (Figure 1) using a pipette solution consisting of 76 mM Cs_2SO_4, 10 mM NaCl, 10 mM CsCl, 1 mM $MgCl_2$, 5 mM HEPES (pH 7.35 with KOH), and 0.24 mg/ml amphotericin B (47). Exocytosis was monitored as increases in cell capacitance using the sine + DC mode of the lock-in amplifier included in the PULSE software and the standard whole cell configuration. When eliciting exocytosis by trains of ten 500-ms voltage clamp depolarizations (Figure 2, A and E), the pipette solution consisted of 125 mM Cs-glutamate, 10 mM CsCl, 10 mM NaCl, 1 mM $MgCl_2$, 5 mM HEPES, 3 mM Mg-ATP, 0.1 mM cAMP, and 0.05 mM EGTA (pH 7.2 with CsOH). In Figure 2, C and G, this pipette solution was slightly modified to include 10 mM EGTA and 9 mM $CaCl_2$, and all Cs^+ salts were replaced by corresponding K^+ salts. The resulting free intracellular Ca^{2+} concentration of this Ca^{2+}/EGTA buffer was estimated to 1.5 μM using the binding constants of Martell and Smith (48, 49). The extracellular bath solution contained 138 mM NaCl, 5.6 mM KCl, 2.6 mM $CaCl_2$, 1.2 mM $MgCl_2$, 5 mM glucose, and 5 mM HEPES (pH 7.4 with NaOH). In the recordings of whole-cell Ca^{2+} currents (Figure 1) and depolarization-evoked exocytosis (Figure 2, A and E), 20 mM of NaCl was equimolarly replaced by the K^+ channel blocker TEA-Cl to facilitate the separation of the small voltage-gated Ca^{2+} currents from the large outward K^+ current. The DHP isradipine (Pfizer Inc.) was prepared as stock solution in DMSO (final concentration less than or equal to 0.1%). The R-type blocker SNX482 (Peptide Institute Inc.) was dissolved directly in the extracellular medium. All other reagents were from Sigma-Aldrich. Effects were determined in the steady state. The bath (approximately 1.5 ml) was continuously perfused (6 ml/min) and the temperature maintained at approximately 32°C.

In vivo glucose challenges. For the in vivo studies, glucose (11.1 mmol [equivalent to 2 g]/kg body weight) was dissolved in 0.9% NaCl and delivered by intraperitoneal injection. Blood sampling, detection of plasma insulin by RIA, and enzymatic determination of plasma glucose concentrations were performed as described previously (50).

In situ/ex vivo pancreatic perfusion. Experiments were performed in the morning at 10:00 a.m. in nonfasted mice. Anesthesia was given by intraperitoneal injection of midazolam (Hofmann-La Roche AG; 0.4 mg/25 g body weight) and fentanyl (Janssen Pharmaceuticals Inc.; 0.02 mg/25 g body weight). The experimental procedures were essentially identical to those described by Bonnevie-Nielsen et al. (51). Briefly, the mice were kept on a heating pad during the entire experiment. After opening the abdominal cavity and ligating the renal, hepatic, and splenic arteries, the aorta was tied off above the level of the pancreatic artery. The pancreas was perfused with modified Krebs-Ringer HEPES buffer preheated to 37°C (1 ml/min) via a silicone catheter placed in the aorta. The perfusate was collected via a silicone catheter from the portal vein at 30- or 60-second intervals, as indicated, in 2.5-ml Eppendorf tubes containing 25 μl Trasylol. Insulin and glucose concentrations in the effluent medium were detected by RIA and the glucose oxidase method, respectively.

In vitro pancreatic hormone release. Insulin release in vitro was measured in static incubations. Briefly, freshly isolated islets were preincubated for 30 minutes at 37°C in a Krebs-Ringer bicarbonate buffer (pH 7.4) consisting of 120 mM NaCl, 25 mM $NaHCO_3$, 4.7 mM KCl, 1.2 mM $MgSO_4$, 2.5 mM $CaCl_2$, 1.2 mM KH_2PO, 1 mM glucose, and 10 mM HEPES (pH 7.4). The medium was gassed with 95% O_2 and 5% CO_2 to obtain constant pH and oxygenation. Groups of 10 islets were then incubated in 1 ml for 60 minutes at 37°C in Krebs-Ringer buffered solution supplemented with either glucose, the L-type Ca^{2+} channel blocker isradipine, the R-type Ca^{2+} channel inhibitor SNX482, tolbutamide, or high K^+, as specified in the text and figures. Immediately after incubation, a 25-μl aliquot of the medium was removed for assay of insulin and glucagon radioimmunoassay as described previously (50).

Immunocytochemistry. Insulin and glucagon immunoreactivities were visualized in dissociated islet cells by indirect immunocytochemistry using a Carl Zeiss AG 510 LSM confocal microscope and a ×100 Plan-Apochromat ×100/1.4 oil objective. After fixation with 3% paraformaldehyde and permeabilization by 0.1% Triton-X, the cells were incubated with normal donkey serum to reduce unspecific staining. The primary insulin and glucagon Abs, raised in guinea pigs and sheep, respectively, were incubated at 1:1,000. To prevent cross-talk between the channels, the secondary Cy3-conjugated anti–guinea pig and the Cy5-conjugated anti-sheep Abs (1:600) were excited in the multitrack mode using the 543-nm and 633-nm lines of the HeNe lasers, and emitted light was collected using greater than 560-nm and greater than 650-nm long-pass filters, respectively.

Microfluorimetry. $[Ca^{2+}]_i$ in intact pancreatic islets was measured by dual-wavelength microfluorimetry using fura-2 and a D104 PTI microfluorimetry system. The temperature of the experimental chamber was +32°C to allow comparison with the electrophysiological data. Procedures for loading and calibration of the fluorescence signal were as described previously (52).

Statistical analysis. All data are given as means ± SEM. Statistical significance was evaluated using absolute values only. A paired Student's *t* test was used when comparing responses in the same cell. For comparisons between groups with independent observations we used independent Student's *t* tests or, when comparisons involved more than 2 groups, ANOVA.

Acknowledgments

We thank Kristina Borglid and Britt-Marie Nilsson for expert technical assistance. This work was supported by the Swedish Research Council (grant numbers 13509, 12239, and 6589), the European Foundation for the Study of Diabetes, European

Community network grant "Neuronal Ca^{2+} Channels," the Albert Påhlsson Foundation, the NovoNordisk Foundation, the Center of Molecular Medicine Cologne (BMBF 01 KS 9502), and the Deutsche Forschungsgemeinschaft (SCH 387/9-1). P. Rorsman is a recipient of the Göran Gustafsson Award for Research in the Natural Sciences and Medicine.

Received for publication June 24, 2004, and accepted in revised form October 24, 2004.

Address correspondence to: Erik Renström, Department of Physiological Sciences, BMC B11, SE-221 84 Lund, Sweden. Phone: 46-46-222-06-39; Fax: 46-46-222-77-63; E-mail: erik.renstrom@mphy.lu.se.

1. Catterall, W.A. 1998. Structure and function of neuronal Ca2+ channels and their role in neurotransmitter release. *Cell Calcium.* **24**:307–323.
2. D'Ascenzo, M., et al. 2004. Electrophysiological and molecular evidence of L-(Cav1), N- (Cav2.2), and R- (Cav2.3) type Ca2+ channels in rat cortical astrocytes. *Glia.* **45**:354–363.
3. Dolphin, A.C. 1999. L-type calcium channel modulation. *Adv. Second Messenger Phosphoprotein Res.* **33**:153–177.
4. Catterall, W.A. 2000. Structure and regulation of voltage-gated Ca2+ channels. *Annu. Rev. Cell Dev. Biol.* **16**:521–555.
5. Reid, C.A., Bekkers, J.M., and Clements, J.D. 2003. Presynaptic Ca2+ channels: a functional patchwork. *Trends Neurosci.* **26**:683–687.
6. Perez-Reyes, E. 2003. Molecular physiology of low-voltage-activated T-type calcium channels. *Physiol. Rev.* **83**:117–161.
7. Heady, T.N., Gomora, J.C., Macdonald, T.L., and Perez-Reyes, E. 2001. Molecular pharmacology of T-type Ca2+ channels. *Jpn. J. Pharmacol.* **85**:339–350.
8. Triggle, D.J. 1998. The physiological and pharmacological significance of cardiovascular T-type, voltage-gated calcium channels. *Am. J. Hypertens.* **11**:80S–87S.
9. Ashcroft, F.M., Proks, P., Smith, P.A., Ämmälä, C., Bokvist, K., and Rorsman, P. 1994. Stimulus-secretion coupling in pancreatic β cells. *J. Cell. Biochem.* **55**(Suppl.):54–65.
10. Del Prato, S., Marchetti, P., and Bonadonna, R.C. 2002. Phasic insulin release and metabolic regulation in type 2 diabetes. *Diabetes.* **51**(Suppl. 1):S109–S116.
11. Grodsky, G.M., and Bolaffi, J.L. 1992. Desensitization of the insulin-secreting β cell. *J. Cell. Biochem.* **48**:3–11.
12. Henquin, J.C., Ravier, M.A., Nenquin, M., Jonas, J.C., and Gilon, P. 2003. Hierarchy of the β cell signals controlling insulin secretion. *Eur. J. Clin. Invest.* **33**:742–750.
13. Schulla, V., et al. 2003. Impaired insulin secretion and glucose tolerance in β cell-selective Ca(v)1.2 Ca2+ channel null mice. *EMBO J.* **22**:3844–3854.
14. Sinnegger-Brauns, M.J., et al. 2004. Isoform-specific regulation of mood behavior and pancreatic β cell and cardiovascular function by L-type Ca^{2+} channels. *J. Clin. Invest.* **113**:1430–1439. doi:10.1172/JCI200420208.
15. Wiser, O., et al. 1999. The voltage sensitive Lc-type Ca2+ channel is functionally coupled to the exocytotic machinery. *Proc. Natl. Acad. Sci. U. S. A.* **96**:248–253.
16. Barg, S., Eliasson, L., Renström, E., and Rorsman, P. 2002. A subset of 50 secretory granules in close contact with L-type Ca2+ channels accounts for first-phase insulin secretion in mouse β cells. *Diabetes.* **51**(Suppl. 1):S74–S82.
17. Barg, S., et al. 2001. Fast exocytosis with few Ca(2+) channels in insulin-secreting mouse pancreatic B cells. *Biophys. J.* **81**:3308–3323.
18. Mochida, S., et al. 2003. Requirement for the synaptic protein interaction site for reconstitution of synaptic transmission by P/Q-type calcium channels. *Proc. Natl. Acad. Sci. U. S. A.* **100**:2819–2824.
19. Mochida, S., Sheng, Z.H., Baker, C., Kobayashi, H., and Catterall, W.A. 1996. Inhibition of neurotransmission by peptides containing the synaptic protein interaction site of N-type Ca2+ channels. *Neuron.* **17**:781–788.
20. Wu, L.G., Borst, J.G., and Sakmann, B. 1998. R-type Ca2+ currents evoke transmitter release at a rat central synapse. *Proc. Natl. Acad. Sci. U. S. A.* **95**:4720–4725.
21. Dietrich, D., et al. 2003. Functional specialization of presynaptic Cav2.3 Ca2+ channels. *Neuron.* **39**:483–496.
22. Saegusa, H., et al. 2000. Altered pain responses in mice lacking α 1E subunit of the voltage-dependent Ca2+ channel. *Proc. Natl. Acad. Sci. U. S. A.* **97**:6132–6137.
23. Kubota, M., et al. 2001. Intact LTP and fear memory but impaired spatial memory in mice lacking Ca(v)2.3 (α(IE)) channel. *Biochem. Biophys. Res. Commun.* **282**:242–248.
24. Lee, S.C., et al. 2002. Molecular basis of R-type calcium channels in central amygdala neurons of the mouse. *Proc. Natl. Acad. Sci. U. S. A.* **99**:3276–3281.
25. Vajna, R., et al. 1998. New isoform of the neuronal Ca2+ channel α1E subunit in islets of Langerhans and kidney—distribution of voltage-gated Ca2+ channel α1 subunits in cell lines and tissues. *Eur. J. Biochem.* **257**:274–285.
26. Pereverzev, A., et al. 2002. Disturbances in glucose-tolerance, insulin-release, and stress-induced hyperglycemia upon disruption of the Ca(v)2.3 (α 1E) subunit of voltage-gated Ca(2+) channels. *Mol. Endocrinol.* **16**:884–895.
27. Barg, S., Galvanovskis, J., Göpel, S.O., Rorsman, P., and Eliasson, L. 2000. Tight coupling between electrical activity and exocytosis in mouse glucagon-secreting α cells. *Diabetes.* **49**:1500–1510.
28. Rutter, G.A., Theler, J.M., Li, G., and Wollheim, C.B. 1994. Ca2+ stores in insulin-secreting cells: lack of effect of cADP ribose. *Cell Calcium.* **16**:71–80.
29. Bokvist, K., Eliasson, L., Ämmälä, C., Renström, E., and Rorsman, P. 1995. Co-localization of L-type Ca2+ channels and insulin-containing secretory granules and its significance for the initiation of exocytosis in mouse pancreatic B cells. *EMBO J.* **14**:50–57.
30. Nadal, A., Quesada, I., and Soria, B. 1999. Homologous and heterologous asynchronicity between identified α-, β- and delta cells within intact islets of Langerhans in the mouse. *J. Physiol.* **517**:85–93.
31. Satin, L.S. 2000. Localized calcium influx in pancreatic β cells: its significance for Ca2+-dependent insulin secretion from the islets of Langerhans. *Endocrine.* **13**:251–262.
32. Wilson, S.M., et al. 2000. The status of voltage-dependent calcium channels in α 1E knock-out mice. *J. Neurosci.* **20**:8566–8571.
33. Tottene, A., Volsen, S., and Pietrobon, D. 2000. α(1E) subunits form the pore of three cerebellar R-type calcium channels with different pharmacological and permeation properties. *J. Neurosci.* **20**:171–178.
34. Neher, E. 1998. Vesicle pools and Ca2+ microdomains: new tools for understanding their roles in neurotransmitter release. *Neuron.* **20**:389–399.
35. Rorsman, P., and Renström, E. 2003. Insulin granule dynamics in pancreatic β cells. *Diabetologia.* **46**:1029–1045.
36. Gromada, J., et al. 1999. CaM kinase II-dependent mobilization of secretory granules underlies acetylcholine-induced stimulation of exocytosis in mouse pancreatic B cells. *J. Physiol.* **518**:745–759.
37. Nandi, J., et al. 2002. Central mechanisms involved with catabolism. *Curr. Opin. Clin. Nutr. Metab. Care.* **5**:407–418.
38. Gromada, J., Ding, W.G., Barg, S., Renström, E., and Rorsman, P. 1997. Multisite regulation of insulin secretion by cAMP-increasing agonists: evidence that glucagon-like peptide 1 and glucagon act via distinct receptors. *Pflugers Arch.* **434**:515–524.
39. Ishihara, H., Maechler, P., Gjinovci, A., Herrera, P.L., and Wollheim, C.B. 2003. Islet β cell secretion determines glucagon release from neighbouring α cells. *Nat. Cell Biol.* **5**:330–335.
40. Wendt, A., et al. 2004. Glucose inhibition of glucagon secretion from rat α cells is mediated by GABA released from neighboring β cells. *Diabetes.* **53**:1038–1045.
41. Chen, S., Ren, Y.Q., Bing, R., and Hillman, D.E. 2000. A 1E subunit of the R-type calcium channel is associated with myelinogenesis. *J. Neurocytol.* **29**:719–728.
42. Hanson, R.L., et al. 1998. An autosomal genomic scan for loci linked to type II diabetes mellitus and body-mass index in Pima Indians. *Am. J. Hum. Genet.* **63**:1130–1138.
43. Elbein, S.C., Hoffman, M.D., Teng, K., Leppert, M.F., and Hasstedt, S.J. 1999. A genome-wide search for type 2 diabetes susceptibility genes in Utah Caucasians. *Diabetes.* **48**:1175–1182.
44. Wiltshire, S., et al. 2001. A genomewide scan for loci predisposing to type 2 diabetes in a U.K. population (the Diabetes UK Warren 2 Repository): analysis of 573 pedigrees provides independent replication of a susceptibility locus on chromosome 1q. *Am. J. Hum. Genet.* **69**:553–569.
45. Jun, G., Song, Y., Stein, C.M., and Iyengar, S.K. 2003. An autosome-wide search using longitudinal data for loci linked to type 2 diabetes progression. *BMC Genet.* **4**(Suppl. 1):S8.
46. Hanson, R.L., et al. 2001. Family and genetic studies of indices of insulin sensitivity and insulin secretion in Pima Indians. *Diabetes Metab. Res. Rev.* **17**:296–303.
47. Renström, E., Eliasson, L., Bokvist, K., and Rorsman, P. 1996. Cooling inhibits exocytosis in single mouse pancreatic B cells by suppression of granule mobilization. *J. Physiol.* **494**:41–52.
48. Martell, A.E., and Smith, R.M. 1971. *Amino acids.* Volume 1 of *Critical stability constants.* Plenum Press. New York, New York, USA.
49. Martell, A.E., and Smith, R.M. 1971. *Amines.* Volume 2 of *Critical stability constants.* Plenum Press. New York, New York, USA.
50. Salehi, A., et al. 1999. Dysfunction of the islet lysosomal system conveys impairment of glucose-induced insulin release in the diabetic GK rat. *Endocrinology.* **140**:3045–3053.
51. Bonnevie-Nielsen, V., Steffes, M.W., and Lernmark, A. 1981. A major loss in islet mass and B cell function precedes hyperglycemia in mice given multiple low doses of streptozotocin. *Diabetes.* **30**:424–429.
52. Olofsson, C.S., et al. 2002. Fast insulin secretion reflects exocytosis of docked granules in mouse pancreatic B cells. *Pflugers Arch.* **444**:43–51.

III

Supression of sulfonylurea- and glucose-induced insulin secretion in vitro and in vivo in mice lacking the chloride transport protein ClC-3

Erik Renström[1]*, Dai-Qing Li[1], Tanja Maritzen[2], Albert Salehi[1], Tilman Breiderhoff[2], Lena Eliasson[1], Xingjun Jing[1], Ingmar Lundquist[1], Charlotta S. Olofsson[1], Anselm A. Zdebik[2], Thomas J. Jentsch[2], Patrik Rorsman[3]

[1]Lund University Diabetes Center, Malmo University Hospital, SE-205 02 Malmö, Sweden
[2]Zentrum für Molekulare Neurobiologie Hamburg, ZMNH, Universität Hamburg, Falkenried 94, D-20252 Hamburg, Germany
[3] Oxford Centre for Diabetes, Endocrinology and Metabolism, University of Oxford, Oxford OX3 7LJ, UK

*To whom correspondence should be addressed:

Erik Renström:
Phone: +46-40-39 11 57
Fax: +46-40-39 12 22
e-mail: erik.renstrom@med.lu.se

Nonstandard abbreviations used:

KO, knock-out; WT, wildtype; RRP, readily releasable pool; LDCV, large dense-core vesicle; SLMV, synaptic-like microvesicle

OBJECTIVE – Priming of insulin secretory granules for release requires intragranular acidification and depends on vesicular Cl^--fluxes. The molecular identity of the mechanism mediating transgranular Cl^- flux remains uncertain. Here we have tested the hypothesis that the chloride transport protein ClC-3 provides the granular shunt conductance required for β-cell granule acidification.

RESEARCH DESIGN AND METHODS - Insulin secretion was analyzed *in vivo* and *in vitro* in wildtype and ClC-$3^{-/-}$ mice. The whole-islet secretion measurements were complemented by single-cell capacitance recordings of exocytosis, fluorimetric measurements of granular pH, subcellular fractionation and fluorescence-based granule purification to establish the localization of ClC-3 and electron microscopy to determine granule number, distribution and appearance.

RESULTS – Insulin secretion evoked by membrane depolarization (high extracellular K^+, sulfonylureas) and glucose was reduced by ~60% and 80% in ClC-$3^{-/-}$ islets/isolated cells. The effect was selective for insulin secretion and glucagon release was not affected. Single-cell exocytosis (monitored as increases in cell capacitance) evoked by a train of ten 500-ms depolarization to zero mV was also strongly reduced (~80%). Proton transport across the granule membrane (assayed by LysoSensor™Green DND-189®) was reduced by 44%. Subcellular fractionation and immunocytochemistry indicated that most of the β-cell ClC-3 located to endosomes/SLMVs. However, the presence of ClC-3 in insulin granules was detected in a high-purification fraction of LDCVs obtained by phogrin-GFP labelling.

CONCLUSIONS - The data confirm the importance of granular Cl^- fluxes in granule priming and provide direct evidence for the involvement of ClC-3 in the process.

A low intragranular pH is crucial for prohormone cleavage in pancreatic β-cells (1). In addition, the acidification of secretory vesicles may play a role in making them release-competent, an ATP-dependent process referred to as priming (2; 3). Substances that collapse vesicular pH gradients reduce exocytosis by impairing the replenishment of the readily releasable pool (RRP) of insulin-containing large dense core vesicles (LDCVs) in β-cells (2). Based on this observation, granular acidification has been proposed to be essential for the priming of β-cell LDCVs (2). Acidification is carried out by a V-type H^+-ATPase that pumps H^+ into the vesicular lumen. Without charge compensation, this electrogenic process leads to a lumen-positive voltage across the granular membrane that would prevent further proton pumping. Acidic organelles of the endosomal pathway principally depend on Cl^- fluxes for charge neutralization (4-6). Consistent with such a mechanism, procedures aimed at inhibiting Cl^- fluxes across membranes of β-cell granules impaired their luminal acidification and their priming for exocytosis (2).

Various members of the CLC family of Cl^- transport proteins facilitate the acidification of intracellular vesicles, most likely by limiting the generation of a transmembrane voltage by the H^+-ATPase (7-10). ClC-3 is present on endosomes and synaptic vesicles (9; 11). Acidification rates of both types of vesicles were reduced in ClC-$3^{-/-}$ mice (9; 12; 13). In addition, ClC-3 has been reported to also reside on secretory granules of β-cells (2). Functional experiments based on the intracellular application of an antibody directed against ClC-3 suggested that ClC-3 facilitates insulin secretion by enhancing the acidification of insulin-containing granules (2; 14-16). Here we have addressed this possibility using constitutive ClC-3 knock-out (KO) mice.

RESEARCH DESIGN AND METHODS

ClC-$3^{-/-}$ and ClC-$3^{+/+}$ littermates were used in these experiments. Details of the generation of the mice and their other characteristics have been summarized elsewhere (9). The experiments were generated in Hamburg and transported to Lund at least 2 weeks prior to the experiments.

Paraffin-embedded pancreatic sections were exposed to an in-house ClC-3-specific antibody (1035) at 1:300 dilution. The antibody was raised in rabbits by injecting a mixture of two peptides (C3/03A: SSTHLLDLLDEPIPGC; C3/03B: KDRERHRRINSKKKEC) that represent parts of the ClC-3 amino terminus. Carboxy-terminal cysteines were added to both peptides to facilitate their crosslinking to the carrier protein bovine serum albumin (BSA). The antibody was affinity-purified against peptide A. Immunoreactivity was visualized using Alexa-conjugated secondary anti-rabbit antibodies (Molecular Probes) and analyzed by confocal microscopy.

Blood sampling in the in vivo experiments were conducted as described previously (17). The surgical procedures used in the *in vitro* and *in vivo* studies were approved by the ethical committee at Lund University.

For the static hormone release measurements, adult mice were killed by cervical dislocation, the pancreas quickly excised and pancreatic islets isolated by standard collagenase digestion. Insulin and glucagon secretion were measured in a KRB-buffer as described previously (17). Total insulin islet content was determined after extraction with acidic ethanol.

$[Ca^{2+}]_i$ was measured in intact pancreatic islets using fura-2 as described previously (18).

For the capacitance measurements of exocytosis, single islet cells were obtained by shaking in Ca^{2+}-free medium. Exocytosis of β-cells was monitored by measurements of cell capacitance as described previously (2) using the standard whole-cell technique. The extracellular medium consisted of (in mM) 118 NaCl, 20 TEA-Cl, 5.6 KCl, 1.2 $MgCl_2$, 2.6 $CaCl_2$, 5 D-glucose and 5 HEPES (pH 7.4 with NaOH). The standard electrode (intracellular) solution contained (in mM) 125 Cs-glutamate, 10 KCl, 10 NaCl, 1$MgCl_2$, 5 HEPES, 0.05 EGTA, 3 Mg-ATP and 0.1 cAMP (pH 7.15 with KOH). In the experiments in Fig. 6A, glutamate was added as monopotassium salt and $[Ca^{2+}]_I$ was buffered to ~1.5 μM (cf. (19)) by inclusion of 10 EGTA and 9 $CaCl_2$. For rescue experiments (Fig. 4 E-F), ClC-$3^{-/-}$ islets were infected with a ClC-3-encoding recombinant Semliki Forest Virus prior to dispersion into single cells and then cultured for 00 h..

Granular pH was monitored semi-quantitatively as outlined elsewhere (19) by supplementing the extracellular solution with 5 μM of the fluorescent probe LysoSensor™Green DND-189® (Molecular Probes), which is fluorescent only in acidic compartments, and that in β-cells principally localises to the secretory granules (3).

For the subcellular fractionation experiments, islets from 12 WT animals were pooled and homogenized. Subcellular factions were obtained by continuous sucrose density gradient centrifugation. Fractions were collected and the protein and insulin contents

as well β-hexosaminidase activity were determined and analyzed by Western blotting for the distribution of ClC-3 (obtained as described above) subcellular markers. The latter were carboxypeptidase E (CPE, 1:500, Research Diagnostics), synaptophysin (1:500, Synaptic Systems) and rab4 (1:200, Santa Cruz).

A highly enriched LDCV fraction was obtained by using a recombinant phogrin-EGFP adenovirus made using the BD Adeno-X expression system 1 (Clontech, CA, U.S.A). INS-1 cells were infected for 1 h and homogenized after 36 h culture. The post-nuclear supernatant was pelleted (15 000 × *g* for 15 min, 4^{o}C) and resuspended in a sorting buffer containing (in mM) 135 KCl, 10 NaCl, 1 $MgCl_2$, 5 Hepes, 2 EGTA (pH 7.15 with KOH). EGFP-positive particles were collected using a Becton Dickinson Cell Sorter and tested for insulin and protein content (Fig. 7H).

ClC-3 silencing was accomplished using the EGFP-containing $P^{RNA\text{-}H1.1}$ vector (GenScript Corp, Piscataway, NJ, U.S.A) with 76 basepair shRNA inserts. EGFP-expressing cells were collected 72 h-post-infection using a Cell Sorter (Becton Dickinson, San Jose, CA). Efficency of silencing was estimated by blotting onto PVDF membrane (Pierce biotechnology Inc, Rockford. IL, U.S.A) and using the anti-ClC-3 antibody. The most efficient silencer construct (S3) contained the CTCCGGAATTCCAGAGATTAA target sequence in rat ClC-3 and was used for all functional assays.

For the secretion assay following silencing, INS-1 cells were plated in a 24-well dish (3×10^5 cells/well) and co-transfected using Effectene (Qiagen, Hilden, Germany) with 0.2 µg of the S3 silencer or scrambled control oligo inserted into the $P^{RNA\text{-}H1.1}$ vector,

and 0.2 µg human GH-expressing vector. Hormone secretion was quantified as the ratio of secreted hGH over total hGH content/well, as previously described (20).

Electron microscopy was performed as previously reported (21).

Data are quoted as mean values ± S.E.M. of indicated number of experiments. Statistical significance was evaluated using Student's *t*-test.

RESULTS

Pancreatic sections were immunostained using antibodies against insulin, glucagon and ClC-3. ClC-3 is strongly expressed in endocrine pancreas (Fig. 1). Co-staining for insulin and glucagon showed that the protein is expressed in both β- and α-cells (Fig. 1A). ClC-3 staining was absent in $ClC^{-/-}$ islets (Fig. 1B), confirming the specificity of the antibody.

Insulin secretion was measured from wildtype and ClC-$3^{-/-}$ islets (Fig. 2A). In wildtype islets, glibenclamide (2 µM) and high extracellular K^+ (50 mM) stimulated insulin secretion 3.1- and 3.4-fold over basal. Glucose (20 mM) was a much stronger stimulus and resulted in a ~10-fold stimulation; the latter effect being enhanced 1.8-fold by GLP-1 (100 nM). In ClC-3-deficient islets, the stimulatory effects of glibenclamide and high K^+ were largely abolished whereas the stimulatory effect of glucose was reduced by 67% and 57% in the absence or presence of GLP-1, respectively. The secretion defect of the ClC-$3^{-/-}$ islets cannot be accounted for by reduced insulin content, which was reduced by only ~10% (Fig. 2C), much less than the reduction of secretion. Although pancreatic α-cells also express ClC-3 (Fig. 1),

glucagon secretion at both 1 and 20 mM glucose was unaffected by ablation of ClC-3 (Fig. 2B).

Glucose stimulates insulin secretion by induction of Ca^{2+}-dependent electrical activity and the associated increase in $[Ca^{2+}]_i$ triggers exocytosis of the insulin granules (22). We monitored $[Ca^{2+}]_i$ in wildtype and ClC-$3^{-/-}$ islets (Fig. 3). Basal $[Ca^{2+}]_i$ levels were 88±6 nM and 106±15 nM in wildtype (n=7) and and ClC-$3^{-/-}$ (n=10) islets, respectively. Following stimulation with 15 mM glucose, $[Ca^{2+}]_i$ rose to a peak value of 419±52 nM and 452±29 nM in wildtype and $ClC^{-/-}$ islets. In both cases, this peak was followed by $[Ca^{2+}]$i oscillations (that are due to bursts of Ca^{2+}-dependent action potentials) with average $[Ca^{2+}]_i$ of 331±36 nM and 260±39 nM, respectively (P~0.05). The addition of the sulfonylurea tolbutamide (0.1 mM) increased $[Ca^{2+}]_i$ similarly in wildtype and knockout islets and peak $[Ca^{2+}]_i$ averaged 414±47 nM and 458±39 nM, respectively. Thus, if anything $[Ca^{2+}]_i$ is higher in ClC-3-deficient than in wildtype islets and we conclude that the suppression of glucose- and tolbutamide-induced insulin secretion must involve processes downstream of metabolic sensing, electrical activity and $[Ca^{2+}]_i$-signaling.

High-resolution capacitance measurements were next applied to isolated β-cells from wildtype and ClC-3 KO animals to compare the exocytotic capacity of wildtype and $ClC3^{-/-}$ β-cells. The b-cell identity was established by the presence of a voltage-gated Na^+-current that inactivated with a $V_{0.5}$ of ~ -100 mV. Exocytosis was elicited by trains of ten 500-ms depolarizations from -70 mV to 0 mV. In control β-cells, exocytosis proceeded throughout the stimulus train (Fig. 4A). The capacitance increase per pulse decreased from an average of ~75 fF in response to the initial depolarization to a final value of 10 fF/pulse (Fig. 4B). The total capacitance increase of control cells

averaged 381±36 fF (n=14). In ClC-3 KO β-cells, the capacitance increases per pulse were much smaller throughout the train (Fig. 4C-D), reaching a maximum rate of 20 fF/pulse with the total capacitance increase elicited by the train being a mere 70±12 fF ($P<0.001$ vs. control; n=14). The secretory response of β-cells lacking ClC-3 was almost normalized by infecting the cells with a recombinant Semliki Forest Virus (SFV) encoding ClC-3 (Fig. 4E-F); the total capacitance increase averaging 259±18 fF (n=5; $P<0.00$ vs. ClC-$3^{-/-}$). These findings (obtained in single cells maintained in tissue culture for >24) corroborate the insulin release data (Fig. 2). They further suggest that the secretion defect is a cell-intrinsic consequence of the lack of ClC-3 and not due to systemic/paracrine effects. The latter conclusion is supported by the finding that downregulation of ClC-3 in INS1 cells by si-RNA inhibited exocytosis (Fig. 5). Western blotting revealed that ClC-3 was reduced by ~70% within 72 h (Fig. 5A). This correlated with 27% ($P<0.01$ silencer vs. scramble oligo) inhibition of stimulated GH release (GH used as an insulin proxy to detect secretion in transfected cells (20) (Fig. 5B) and a marked decrease (65%; $P<0.05$ vs. control) in exocytosis elicited by trains of depolarization (Fig. 5C).

The data of Fig. 4 indicate that ClC-3 might be important for granule mobilization/priming. We addressed this aspect further by using an intracellular $[Ca^{2+}]_i$ dialysis protcol (1.5 μM free $[Ca^{2+}]_i$ with 3 mM Mg-ATP and 0.1 mM cAMP) (Fig. 6A). In wildtype β-cells, cell capacitance increased by 1.2±0.15 pF over 60 s under these conditions. This is equivalent to the fusion of ~400 secretory granules. For comparison, exocytosis of RRP results in a capacitance increase of only 0.1 pF. Thus, RRP must have turned over >10 times during the period of observation indicating that the increase involves mobilization/priming of “new“ granules that did not initially belong to RRP. The steady-state rate of capacitance increase thus

provides an estimate of the rate of mobilization. In a series of 15 experiments, the average rate of capacitace increase averaged 20±2 fF/s. In ClC-3-deficient β-cells, the total increase in cell capacitance averaged 0.70±0.05 pF (n=19; $p < 0.01$ vs wildtype) and the rate of capacitance increase was limited to 12±1 fF/s (n=19; $p < 0.01$). Thus, mobilization was reduced by ~40% in β-cells lacking ClC-3.

ClC-3 has been proposed to promote mobilization by providing a shunt conductance that allows the granule interior to acidify; the latter leading to an increased release competence of granules by mechanisms that remain unestablished (3; 19). In Fig. 6B we have tested whether ablation of ClC-3 affects intragranular pH by using the fluorescent probe LysoSensor Green DND-189. The protonophore CCCP (0.1 mM) was introduced to the cytosol to allow transmembrane proton flux. Addition of CCCP at t=0 led to a prompt reduction of fluorescence as the intragranular pH increased and fluorescent probe moved out of the cell. Previous experiments have established that this effect of CCCP is blocked by the Cl^--channel blocker DIDS (19). CCCP-mediated H^+-efflux from the granule is electrogenic. In the absence of a counterion conductance a large electrical potential will rapidly develop when the H^+ permeability is increased that would prevent pH equilibration across the granule membrane. If ClC-3 Cl^- channel activity is required for proton translocation over the granule membrane, then loss of these channels should reduce H^+-efflux via the protonophore leading to a reduced loss of fluorescence. Indeed, the CCCP-induced fluorescence decrease at steady-state (90 s after addition of CCCP) was reduced from 41±9% in wildtype cells to 18±5% in ClC-$3^{-/-}$ β-cells (*P <0.05).

It was ascertained that ablating ClC-3 did not interfere with granule biogenesis and structure. Ultrastructural analyses revealed that the number of granules (total as well

as docked) remained unchanged in ClC-3$^{-/-}$ islets. Moreover, their appearance and diameter were unaltered (Supplementary Fig. 1). This argues that insulin processing proceeds well in the absence of ClC-3 (23). These findings are in agreement with the finding that insulin content was unaffected (Fig. 2C).

ClC-3 has been reported to be present in membranes of insulin-containing secretory granules in the β-cells (2). Sucrose density centrifugation was used for the subcellular fractionation of vesicles from primary β-cells (Fig. 7A-G). The distribution of secretory granules in the different fractions was determined by measuring their insulin content. Endosomes and SLMVs were identified by antibodies against specific markers like rab4 and synaptophysin, respectively. ClC-3 was enriched in these lighter (endosome/SLMV) fractions, but not in the SG fractions. Similar data were obtained in INS1 cells (not shown). However, these data do not allow us to conclude that ClC-3 is absent from the insulin granules.

Phogrin is a specific marker of SGs (24). Expression of a GFP-phogrin in insulinoma cells followed by immunoprecipitation using an antibody directed against GFP has been shown to obtain an highly purified granule fraction (25). In our hands, granules isolated by GFP-labelling was enriched for insulin by a factor of ~20 over the homogenate when normalized to protein content. Granules thus obtained did contain detectable levels of ClC-3 immunoreactivity and was highly enriched above the level found in the homogenate (Fig. 7H). Thus, it appears that insulinoma granules are equipped with ClC-3. However, we acknowledge that most of the ClC-3 proteins locate to other membrane compartments.

To determine the systemic consequences of the ClC-3 deficiency on glucose homeostasis and insulin release, serum insulin and glucose concentrations were finally measured in wildtype and ClC-$3^{-/-}$ mice after an intraperitoneal glucose challenge (2g/kg body weight). Control mice responded to the glucose challenge with an increase in plasma insulin levels both at 3 and 8 min but no such response was detected in ClC-3 KO mice (Fig. 8A). Likewise, glibenclamide (500 µg/kg body weight), which in wildtype mice evoked a transient stimulation of insulin secretion, failed to enhance insulin secretion in ClC-3-deficient mice (Fig. 8B).

DISCUSSION

Secretory granules must undergo a priming reaction to gain release competence. We have previously proposed that priming of insulin granules requires the acidification of their lumen (2) and subsequent studies have provided further support in favor of this hypothesis. Processes interfering with the acidification have thus been found to reduced the secretory capacity of β-cells and impair the refilling of their readily releasable pool of vesicles (RRP) and late phase insulin secretion (2; 3). As Cl^- channel blockers as well as the replacement of cytosolic Cl^- with larger anions suppressed secretion (2), Cl^- fluxes seemed to be necessary for the priming of insulin granules. By analogy to what has been described in other systems (5), this Cl^- requirement was attributed to the need of a shunt conductance to neutralize the granular membrane potential (positive inside) that develops during the operation of the vesicular H^+-ATPase.

In the endosomal/lysosomal system, as well as in synaptic vesicles, such a shunt conductance is provided by various members of the CLC family of Cl^- channels and

transporters (26). For instance, renal proximal tubular cells need ClC5 to efficiently acidify their apical endosomes (7; 8; 10), while hepatic endosomes (12) and synaptic vesicles (9) rely on its close relative ClC-3. The strong expression of ClC-3 in pancreatic β-cells (Fig. 1A) raised the interesting possibility that it might mediate the Cl^- conductance involved in the priming of the secretory granules.

Previous evidence suggestive of a role of ClC-3 in insulin secretion involved the use of an antibody directed against ClC-3 (2) and antisense oligonucleotides (15; 16) to inhibit or knock-down ClC-3. However, there are always concerns about the specificity of such procedures. Here we have re-visited the role of ClC-3 in insulin secretion by analyzing mice in which these channels had been genetically removed. The new data presented here provide additional evidence that ClC-3 plays a role in insulin secretion.

Although glucose- and sulfonylurea-induced insulin secretion was strongly reduced both *in vitro* and *in vivo* in ClC-$3^{-/-}$ mice, the knockout mice nevertheless had normal basal plasma glucose (~10 mM) and insulin levels. Thus, the β-cell is clearly capable of maintaining an adequate supply of insulin even in the absence of ClC-3 channels. Our previous data suggest that granular Cl^--fluxes play an important role in the priming of secretory granules for release and the present data support this scenario. The reduced capacity of ClC-$3^{-/-}$ β-cells to replenish the releasable pool of granules is also evident from the Ca^{2+}-infusion experiments. In accordance with the notion that ClC-3 provides a shunt conductance required for granule acidification and priming, we demonstrate here that H^+-fluxes and priming were reduced by ~50% in ClC-$3^{-/-}$ β-cells. However, the fact that these processes were not abolished argues that there exist additional mechanisms for granule priming/acidification in the β-cell. It is likely

that these processes account for the normality of basal plasma insulin and glucose levels in the knockout animals. It is only when insulin secretion must increase much beyond basal that the demand of secretory granules exceeds that which can be met by the ClC-3-independent mechanisms.

It may seem surprising that the ClC-$3^{-/-}$ mouse is not overtly diabetic despite and exhibit marked glucose intolerance given the strong suppression of glucose-evoked insulin secretion. However, it should be noted that in the mouse, only ~30% of the glucose tolerance in mice is mediated by insulin and that non-insulin-dependent mechanisms, like the suppression of hepatic glucose production, play a major role (27). Furthermore, in both man (28) and mice (27), a reduction of insulin secretion often correlates with an increased insulin sensitivity and if this also occurs in the ClC-$3^{-/-}$ mouse it may obscure the influence of hypoinsulinemia. Finally, we cannot entirely exclude the possibility that systemic effects due to the global knockout of ClC-3 contributes to the effect. Unfortunately, our attempts to generate a β-cell specific ClC-3 knockout failed since insulin secretion in Rip-Cre mice was strongly suppressed. This is similar to what has previously been observed with a different Rip-Cre construct (29). However, we believe that systemic effects, even if they occur, are unlikely to explain the *in vitro* findings. It is reassuring that the inhibition of exocytosis seen in the capacitance measurements echoes the inhibition of insulin secretion in isolated islets. The finding that the consequences of ablating ClC-3 on exocytosis can be reversed by infection of ClC-$3^{-/-}$ β-cells with ClC-3 likewise provides evidence for a direct β-cell defect in favor of indirect/systemic effects. This conclusion is underpinned by the finding that siRNA-mediated downregulation of ClC-3 in INS1 cells is associated with a statistically significant reduction of secretion. The fact that the effect was milder than that seen in the ClC-$3^{-/-}$ β-cells and islets we attribute to

the fact that 30% of the channel protein remained within the cells. Finally, we point out that glucagon secretion was unperturbed in ClC-3$^{-/-}$ mice although α-cells express high levels of ClC-3 (Fig. 1). Thus, ClC-3 plays a particularly prominent role in β-cell insulin secretion, whereas a K^+ conductance rather than a Cl^- conductance is important for priming of glucagon-containing granules in rat α-cells (30).

The finding that most of the β-cell ClC-3 associates with endosomes/ SLMVs is in agreement with its reported localization to hepatic endosomes (9; 12), neuronal synaptic vesicles (SVs) (9), and endosomes and SLMVs of neuroendocrine PC12 cells (11). However, the presence of detectable levels of ClC-3 in insulin granules isolated using the highly specific LDCV marker phogrin indicates that some ClC-3 is present in insulin granules. The density of the ClC-3 channels in the granular membrane might be very low and still mediate sufficient Cl^- flux to allow granule acidification. Recently, Henquin and colleagues demonstrated that granule acidification plays a key role in insulin secretion (especially 2nd phase release) and identified Cl^- fluxes in the process (3). The data presented here strongly reinforce previous data implicating ClC-3 channels in the process.

Previous work has suggested that insulin secretion evoked by high-K^+ stimulation in the absence of glucose reflects exocytosis of the readily releasable pool of granules and that release of these granules underlie 1st phase insulin secretion. Insulin secretion evoked by high extracellular K^+ was abolished in ClC-3 mice. These findings are consistent with the concept that ClC-3-dependent processes have a strong impact on the size of the RRP. This would be in agreement with the marked reduction in the exocytotic responses elicited by a train of membrane depolarization (-82%). In addition there was a ~50% suppression of granule mobilization, which has

been argued to underlie 2nd phase release (31). Type-2 diabetes is characteristically associated with the complete loss of 1st phase insulin secretion (hypothesized to result from release of RRP granules) and a ~50% reduction of 2nd phase release (possibly reflecting mobilization) (32). These features are indeed reminiscent of those we now report for the ClC-3$^{-/-}$ mice. We emphasize that this should not be interpreted in terms of loss-of-function mutations in ClC-3 being part of the aetiology of type-2 diabetes. Rather, our data underscore the significance granule mobilization in the maintenance of the secretory capacity of the β-cell illustrate that any process that compromises granule priming may impair insulin secretion sufficiently to result in glucose intolerance and even manifest type-2 diabetes. Nevertheless, it is intriguing that interest that there is some evidence that the chromosomal region harboring ClC-3 (4q33) in some studies show an association with type-2 diabetes (33).

Acknowledgements

Supported by the European Foundation for the Study of Diabetes, the Swedish Research Council, Deutsche Forschungsgemeinschaft (SFB444) and the Wellcome Trust. E.R. is a Senior Researcher at the SRC.

References

1. Hutton JC: The insulin secretory granule. *Diabetologia* 32:271-281, 1989
2. Barg S, Huang P, Eliasson L, Nelson DJ, Obermuller S, Rorsman P, Thevenod F, Renstrom E: Priming of insulin granules for exocytosis by granular Cl(-) uptake and acidification. *J Cell Sci* 114:2145-2154, 2001
3. Stiernet P, Guiot Y, Gilon P, Henquin JC: Glucose acutely decreases pH of secretory granules in mouse pancreatic islets. Mechanisms and influence on insulin secretion. *The Journal of biological chemistry* 281:22142-22151, 2006
4. al-Awqati Q: Regulation of ion channels by ABC transporters that secrete ATP. *Science* 269:805-806, 1995
5. al-Awqati Q: Chloride channels of intracellular organelles. *Curr Opin Cell Biol* 7:504-508, 1995
6. Sonawane ND, Verkman AS: Determinants of [Cl-] in recycling and late endosomes and Golgi complex measured using fluorescent ligands. *J Cell Biol* 160:1129-1138, 2003
7. Piwon N, Gunther W, Schwake M, Bosl MR, Jentsch TJ: ClC-5 Cl- -channel disruption impairs endocytosis in a mouse model for Dent's disease. *Nature* 408:369-373, 2000
8. Gunther W, Piwon N, Jentsch TJ: The ClC-5 chloride channel knock-out mouse - an animal model for Dent's disease. *Pflugers Arch* 445:456-462, 2003
9. Stobrawa SM, Breiderhoff T, Takamori S, Engel D, Schweizer M, Zdebik AA, Bosl MR, Ruether K, Jahn H, Draguhn A, Jahn R, Jentsch TJ: Disruption of ClC-3, a chloride channel expressed on synaptic vesicles, leads to a loss of the hippocampus. *Neuron* 29:185-196, 2001
10. Hara-Chikuma M, Yang B, Sonawane ND, Sasaki S, Uchida S, Verkman AS: ClC-3 chloride channels facilitate endosomal acidification and chloride accumulation. *J Biol Chem* 280:1241-1247, 2005
11. Salazar G, Love R, Styers ML, Werner E, Peden A, Rodriguez S, Gearing M, Wainer BH, Faundez V: AP-3-dependent mechanisms control the targeting of a chloride channel (ClC-3) in neuronal and non-neuronal cells. *J Biol Chem* 279:25430-25439, 2004
12. Hara-Chikuma M, Takeda J, Tarutani M, Uchida Y, Holleran WM, Endo Y, Elias PM, Inoue S: Epidermal-specific defect of GPI anchor in Pig-a null mice results in Harlequin ichthyosis-like features. *J Invest Dermatol* 123:464-469, 2004
13. Yoshikawa M, Uchida S, Ezaki J, Rai T, Hayama A, Kobayashi K, Kida Y, Noda M, Koike M, Uchiyama Y, Marumo F, Kominami E, Sasaki S: CLC-3 deficiency leads to phenotypes similar to human neuronal ceroid lipofuscinosis. *Genes Cells* 7:597-605, 2002
14. Barg S, Olofsson CS, Schriever-Abeln J, Wendt A, Gebre-Medhin S, Renstrom E, Rorsman P: Delay between fusion pore opening and peptide release from large dense-core vesicles in neuroendocrine cells. *Neuron* 33:287-299, 2002
15. Juhl K, Hoy M, Olsen HL, Bokvist K, Efanov AM, Hoffmann EK, Gromada J: cPLA2alpha-evoked formation of arachidonic acid and lysophospholipids is required for exocytosis in mouse pancreatic beta-cells. *Am J Physiol Endocrinol Metab* 285:E73-81, 2003
16. Hoy M, Olsen HL, Bokvist K, Petersen JS, Gromada J: The imidazoline NNC77-0020 affects glucose-dependent insulin, glucagon and somatostatin secretion in mouse pancreatic islets. *Naunyn Schmiedebergs Arch Pharmacol* 368:284-293, 2003
17. Salehi A, Chen D, Hakanson R, Nordin G, Lundquist I: Gastrectomy induces impaired insulin and glucagon secretion: evidence for a gastro-insular axis in mice. *J Physiol* 514 (Pt 2):579-591, 1999
18. Olofsson CS, Gopel SO, Barg S, Galvanovskis J, Ma X, Salehi A, Rorsman P, Eliasson L: Fast insulin secretion reflects exocytosis of docked granules in mouse pancreatic B-cells. *Pflugers Arch* 444:43-51, 2002

19. Barg S, Huang P, Eliasson L, Nelson DJ, Obermuller S, Rorsman P, Thevenod F, Renstrom E: Priming of insulin granules for exocytosis by granular Cl(-) uptake and acidification. *Journal of cell science* 114:2145-2154, 2001
20. Ivarsson R, Jing X, Waselle L, Regazzi R, Renstrom E: Myosin 5a controls insulin granule recruitment during late-phase secretion. *Traffic* 6:1027-1035, 2005
21. Olofsson CS, Gopel SO, Barg S, Galvanovskis J, Ma X, Salehi A, Rorsman P, Eliasson L: Fast insulin secretion reflects exocytosis of docked granules in mouse pancreatic B-cells. *Pflugers Archiv* 444:43-51, 2002
22. Ashcroft F, Rorsman P: Type 2 diabetes mellitus: not quite exciting enough? *Hum Mol Genet* 13 Spec No 1:R21-31, 2004
23. Furuta M, Yano H, Zhou A, Rouille Y, Holst JJ, Carroll R, Ravazzola M, Orci L, Furuta H, Steiner DF: Defective prohormone processing and altered pancreatic islet morphology in mice lacking active SPC2. *Proceedings of the National Academy of Sciences of the United States of America* 94:6646-6651, 1997
24. Wasmeier C, Hutton JC: Molecular cloning of phogrin, a protein-tyrosine phosphatase homologue localized to insulin secretory granule membranes. *The Journal of biological chemistry* 271:18161-18170, 1996
25. Varadi A, Tsuboi T, Rutter GA: Myosin Va transports dense core secretory vesicles in pancreatic MIN6 beta-cells. *Molecular biology of the cell* 16:2670-2680, 2005
26. Jentsch TJ, Maritzen T, Zdebik AA: Chloride channel diseases resulting from impaired transepithelial transport or vesicular function. *J Clin Invest* 115:2039-2046, 2005
27. Pacini G, Thomaseth K, Ahren B: Contribution to glucose tolerance of insulin-independent vs. insulin-dependent mechanisms in mice. *Am J Physiol Endocrinol Metab* 281:E693-703, 2001
28. Kahn SE, Prigeon RL, McCulloch DK, Boyko EJ, Bergman RN, Schwartz MW, Neifing JL, Ward WK, Beard JC, Palmer JP, et al.: Quantification of the relationship between insulin sensitivity and beta-cell function in human subjects. Evidence for a hyperbolic function. *Diabetes* 42:1663-1672, 1993
29. Lee JY, Ristow M, Lin X, White MF, Magnuson MA, Hennighausen L: RIP-Cre revisited, evidence for impairments of pancreatic beta-cell function. *The Journal of biological chemistry* 281:2649-2653, 2006
30. Hoy M, Olsen HL, Bokvist K, Buschard K, Barg S, Rorsman P, Gromada J: Tolbutamide stimulates exocytosis of glucagon by inhibition of a mitochondrial-like ATP-sensitive K+ (KATP) conductance in rat pancreatic A-cells. *J Physiol* 527 Pt 1:109-120, 2000
31. Rorsman P, Renstrom E: Insulin granule dynamics in pancreatic beta cells. *Diabetologia* 46:1029-1045, 2003
32. Porte D, Jr., Kahn SE: beta-cell dysfunction and failure in type 2 diabetes: potential mechanisms. *Diabetes* 50 Suppl 1:S160-163, 2001
33. Permutt MA, Wasson JC, Suarez BK, Lin J, Thomas J, Meyer J, Lewitzky S, Rennich JS, Parker A, DuPrat L, Maruti S, Chayen S, Glaser B: A genome scan for type 2 diabetes susceptibility loci in a genetically isolated population. *Diabetes* 50:681-685, 2001
34. Gopel SO, Kanno T, Barg S, Rorsman P: Patch-clamp characterisation of somatostatin-secreting -cells in intact mouse pancreatic islets. *The Journal of physiology* 528:497-507, 2000

Figure Legends

Figure 1. Immunofluorescence revealed a strong ClC-3 expression in WT pancreatic islets (**A**), whereas no signal was detected in ClC-3$^{-/-}$ sections. (**B**). Co-staining with antibodies directed against insulin and glucagon indicated that ClC-3 is expressed in both α- and β-cells as well as a third cell type that was insulin- and glucagon-negative (δ-cell?). Scale bar: 15 µm.

Figure 2. Effect of ClC-3 ablation on *in vitro* insulin and glucagon release. (**A**) Insulin secretion measured from wildtype (black) and ClC-3$^{-/-}$ islets (grey) in vitro during 1-h static incubations in the presence of 1 mM glucose, 1 mM glucose + 1 μM glibenclamide (G), 1 mM glucose at 50 mM extracellular K^+, 20 mM glucose and 20 mM glucose + 100 nM GLP-1 as indicated. (**B**) As in (A) but glucagon was measured at 1 and 20 mM glucose. (**C**) Islet insulin content from wildtype (black) and knockout (grey) islets. Data are mean values ± S.E.M. of 9-23, 6-8 and 4 experiments (=animals) under the different conditions in A, B and C, respectively. *** P<0.001.

Figure 3. Mild effects of ClC-3 ablation on intracellular Ca^{2+}. Intracellular $[Ca^{2+}]_i$ recordings in WT (**A**) and ClC-3$^{-/-}$ islets (**B**). Glucose was increased from 5 mM to 15 mM and tolbutamide included in the medium as indicated. Data are representative for 7 (A) and 10 experiments (B).

Figure 4. (**A**) Increases in membrane capacitance (ΔC), evoked by a train of ten 500-ms voltage-clamp depolarisations from -70 mV to 0 mV (V) in a wildtype β-cell (identified by Na^+ current inactivation properties; cf. (34); inset). (**B**) Increases in membrane capacitance elicited by the individual pulses of the train stimulus (ΔC_n-

ΔC_{n-1}). (C-D) Same as in (A-B) but using cells from ClC-3$^{-/-}$ mice. (E-F) Same as in C-D but ClC-3 had been reintroduced by Semliki Forest Virus. Data represent mean values ± S.E.M. obtained from 14, 14 and 5 cells in B, D and F, respectively. ***P < 0.001 **P < 0.01.

Figure 5. Silencing of ClC-3 in INS1 cells reduces secretion and exocytosis. (A) Western blots of INS1 cells treated with vector-based RNAi against ClC-3 with either a scrambled control oligo (C) or silencing oligos S1-3. (B) Stimulated hGH secretion from control INS1 cells and cells in which ClC-3 had been downregulated using S3. Data are mean values ± S.E.M. of 6 experiments. (C) Increases in membrane capacitance in ClC-3-silenced cells (gray bars) elicited by the individual pulses of the train stimulus (ΔC_n-ΔC_{n-1}). The black line shows data from control cells. Data are mean values ±S.E.M. of 11 and 6 experiments, respectively. ** P < 0.01.

Figure 6. Reduced granule mobilization and granular proton permeability in ClC-3$^{-/-}$ β-cells. (**A**) Exocytosis measured in wildtype (WT) and ClC-3$^{-/-}$ β-cells during intracellular dialysis with 1.5 μM $[Ca^{2+}]_i$. (**B**) Changes in granular pH following establishment of whole-cell configuration and wash-in of 0.1 mM CCCP in wildtype and ClC-3$^{-/-}$ β-cells. The whole-cell configuration was established at t=0. Data are given as mean fluorescence values normalized to fluorescence intensity at t=0 of 5 control cells and 9 ClC-3$^{-/-}$ cells. *P < 0.05.

Figure 7. Subcellular localization of ClC-3 in islet cells. (A-G) Sucrose density gradient centrifugations of an islet homogenates. Eighteen fractions were collected starting from the top and analyzed by Western blotting with antibodies against carboxypeptidase E (secretory granule marker) (A), rab4 (endosomal marker) (B),

synaptophysin (SLMV marker) (C) and ClC-3 (D). The distribution of secretory granules was also ascertained by determining the insulin concentration of the fractions (E). Lysosomes were identified by measuring the enzymatic activity of β-hexosaminidase (F) and protein content (G). (H) Presence of ClC-3 in INS1 post-nuclear cell homogenates (HM), as well as insulin granules (IG) purified by fluorescence activated "cell" sorting after tagging the vesicles with phogrin-GFP.

Figure 8. Reduced insulin secretion in ClC-3$^{-/-}$ mice in vivo. **(A)** Changes in plasma glucose (upper) and plasma insulin concentration (lower) following an intraperitoneal glucose challenge. 2 g glucose/kg body weight was administered at t=0. Serum insulin and glucose concentrations were measured before, and 3 and 8 min after injection. (B) Same as in (A) but insulin secretion was stimulated with glibenclamide (500 μg/kg body weight). Data represent mean values ± S.E.M. from 12 wildtype and 13 ClC-3$^{-/-}$ mice in A and 7 wildtype and 8 ClC-3$^{-/-}$ mice in B. **P<0.01.

On-line supplementary material (Renstrom et al.)

Figure S1. Normal ulstrastuctural appearance of ClC-3$^{-/-}$ β-cells. (A-B) Typical electron micrographs of WT and ClC-3$^{-/-}$ β-cells. (B-C) Total number (B) and number of granules docked with the plasma membrane (C) in wildtype and ClC-3-/-mice as indicated. Data represent mean values ± S.E.M calculated from 3 and 4 animals per genotype. Scale bar: 0.5 μm.

Figure 1

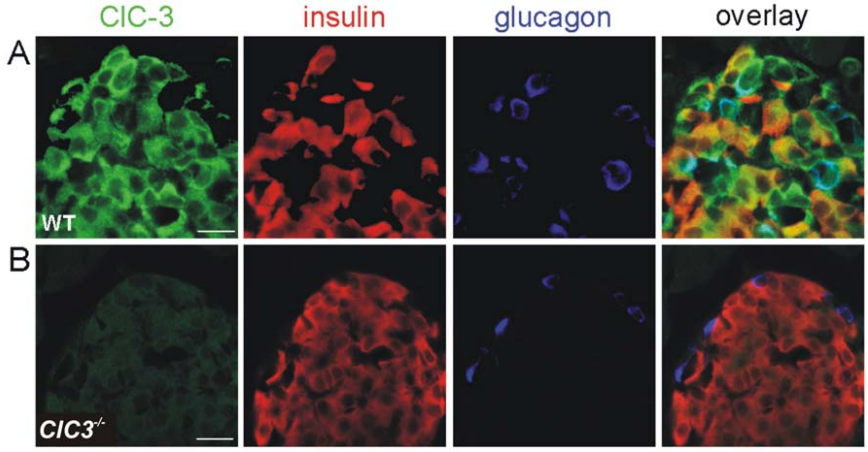

Figure 2

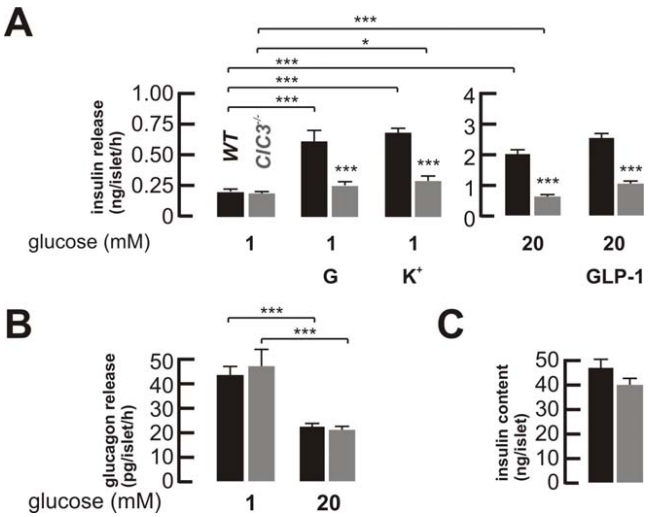
A
B
C
insulin release (ng/islet/h)
WT
Clc3-/-
glucose (mM)
1
1
G
1
K+
20
20
GLP-1
glucagon release (pg/islet/h)
insulin content (ng/islet)
***
*

Figure 3

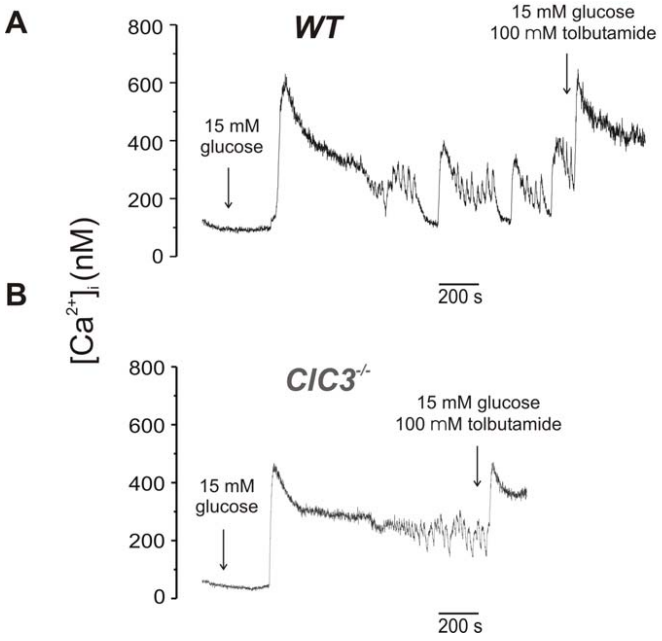
A
WT
15 mM glucose
100 mM tolbutamide
15 mM glucose
800
600
400
200
0
200 s
B
[Ca2+]i (nM)
CIC3-/-
15 mM glucose
100 mM tolbutamide
15 mM glucose
800
600
400
200
0
200 s

Figure 4

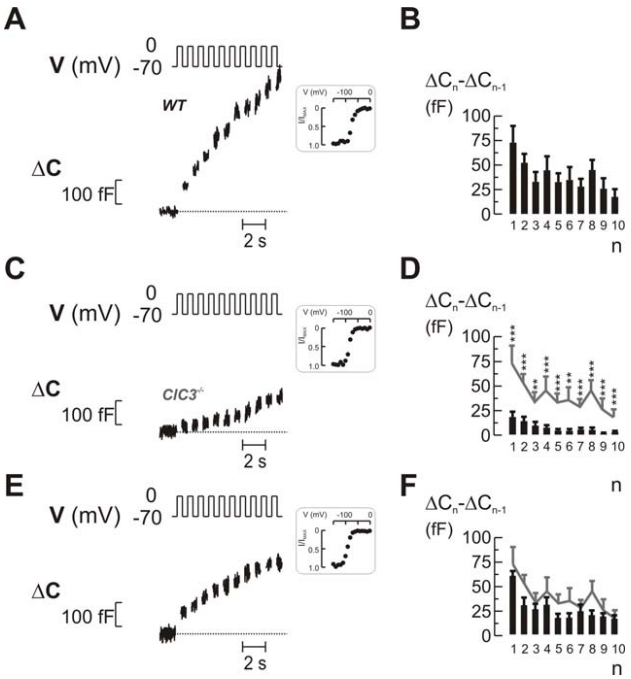
A
V (mV)
0
-70
WT
ΔC
100 fF
2 s
B
ΔCn-ΔCn-1
(fF)
100
75
50
25
0
1 2 3 4 5 6 7 8 9 10
n
C
V (mV)
0
-70
ClC3-/-
ΔC
100 fF
2 s
D
ΔCn-ΔCn-1
(fF)
100
75
50
25
0
1 2 3 4 5 6 7 8 9 10
E
V (mV)
0
-70
ΔC
100 fF
2 s
F
n
ΔCn-ΔCn-1
(fF)
100
75
50
25
0
1 2 3 4 5 6 7 8 9 10
n

Figure 5

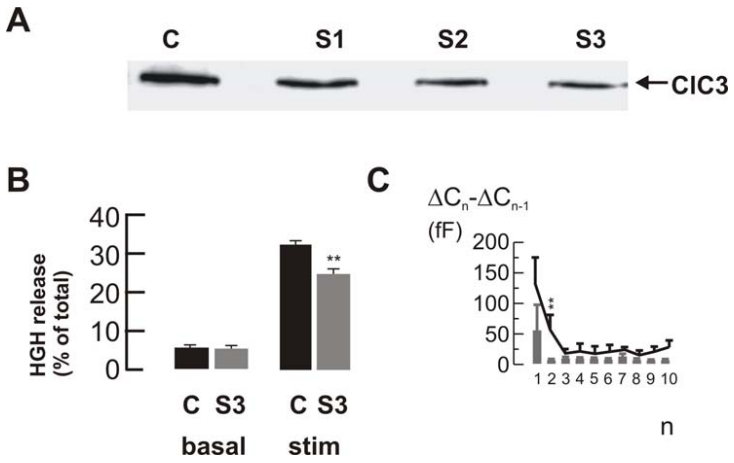
A
C
S1
S2
S3
ClC3
B
HGH release
(% of total)
40
30
20
10
0
**
C S3
basal
C S3
stim
C
ΔCn-ΔCn-1
(fF)
200
150
100
50
0
**
1 2 3 4 5 6 7 8 9 10
n

Figure 6

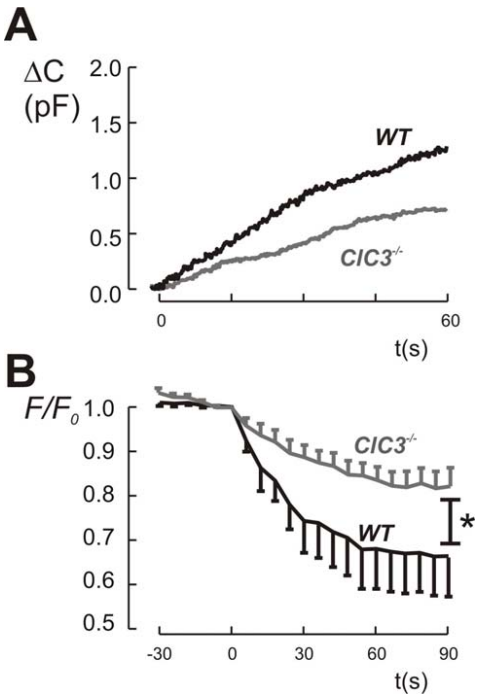
A
ΔC
(pF)
2.0
1.5
1.0
0.5
0.0
WT
ClC3-/-
0
60
t(s)
B
F/F0
1.0
0.9
0.8
0.7
0.6
0.5
ClC3-/-
WT
*
-30
0
30
60
90
t(s)

Figure 7

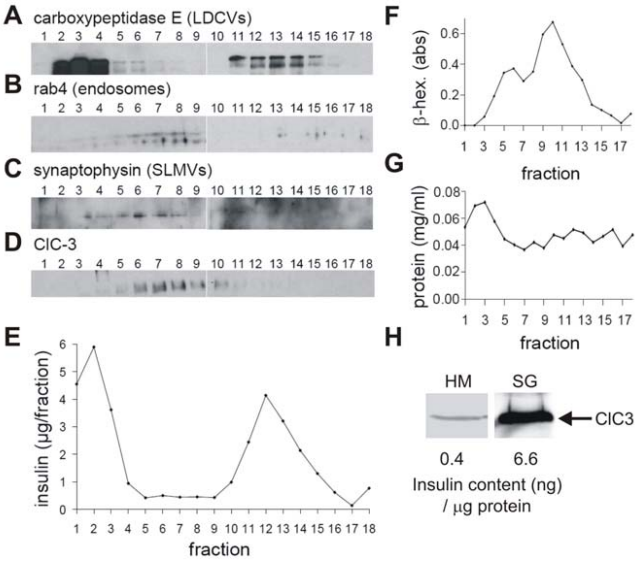
A
carboxypeptidase E (LDCVs)
1 2 3 4 5 6 7 8 9 10 11 12 13 14 15 16 17 18
B
rab4 (endosomes)
1 2 3 4 5 6 7 8 9 10 11 12 13 14 15 16 17 18
C
synaptophysin (SLMVs)
1 2 3 4 5 6 7 8 9 10 11 12 13 14 15 16 17 18
D
ClC-3
1 2 3 4 5 6 7 8 9 10 11 12 13 14 15 16 17 18
E
insulin (µg/fraction)
0 1 2 3 4 5 6
1 2 3 4 5 6 7 8 9 10 11 12 13 14 15 16 17 18
fraction
F
β-hex. (abs)
0.0 0.2 0.4 0.6
1 3 5 7 9 11 13 15 17
fraction
G
protein (mg/ml)
0.00 0.02 0.04 0.06 0.08
1 3 5 7 9 11 13 15 17
fraction
H
HM
SG
ClC3
0.4
6.6
Insulin content (ng)
/ µg protein

Figure 8

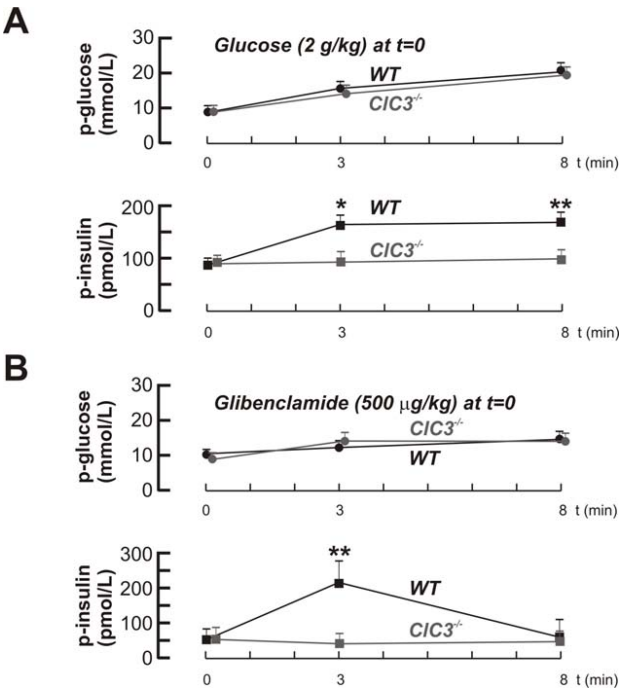
A
p-glucose (mmol/L)
30
20
10
0
Glucose (2 g/kg) at t=0
WT
ClC3-/-
0
3
8 t (min)
p-insulin (pmol/L)
200
100
0
*
WT
**
ClC3-/-
0
3
8 t (min)
B
p-glucose (mmol/L)
30
20
10
0
Glibenclamide (500 μg/kg) at t=0
ClC3-/-
WT
0
3
8 t (min)
p-insulin (pmol/L)
300
200
100
0
**
WT
ClC3-/-
0
3
8 t (min)

Figure S1

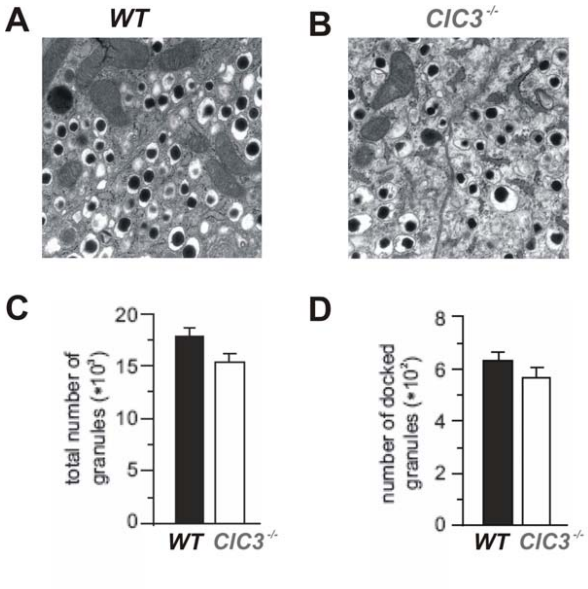
A
WT
B
ClC3-/-
C
total number of granules (*10³)
20
15
10
5
0
WT
ClC3-/-
D
number of docked granules (*10²)
8
6
4
2
0
WT
ClC3-/-